K-1896

THE DESUBLIMATION OF KRYPTON FROM A NONCONDENSABLE CARRIER GAS

R. S. Eby

Systems and Equipment Technology Department
Enrichment Technology Division

September 1978

UNION CARBIDE

OAK RIDGE GASEOUS DIFFUSION PLANT
OAK RIDGE, TENNESSEE

prepared for the U.S. DEPARTMENT OF ENERGY *under*
U.S. GOVERNMENT *Contract W-7405 eng 26*

(Sponsor: J. R. Merriman)

DISCLAIMER

Printed in the United States of America. Available from
National Technical Information Service
U.S. Department of Commerce
5285 Port Royal Road, Springfield, Virginia 22161
Price: Printed Copy $7.25 ; Microfiche $ 3.00

Date of Issue: August 1978 Report Number: K-1896

SUBJECT CATEGORY: UC-79c

THE DESUBLIMATION OF KRYPTON FROM A NONCONDENSABLE CARRIER GAS*

R. S. Eby

Systems and Equipment Technology Department
Enrichment Technology Division

Oak Ridge Gaseous Diffusion Plant
Union Carbide Corporation
Oak Ridge, Tennessee

Prepared for the Department of Energy
Under U.S. Government Contract W-7405 eng 26

*This report was prepared as a thesis presented for the Master of Science Degree at the University of Tennessee, Knoxville, Tennessee in August 1978.

Blank Page

Missing Pages 3 and 4
from
Original Document

ABSTRACT

The purpose of this study was to obtain column concentration profiles and point buildup rates for a cold trap freezing out krypton from a nitrogen carrier gas stream and to compare those experimentally obtained profiles with profiles generated from a theoretical model. Profiles were obtained over a range of flow conditions from 0.14 to 1.06 standard cubic feet per minute, krypton feed gas concentrations varied from 5.2 to 13.5%, and cold trap operating temperatures from -281°F to -312°F. Gamma scintillation techniques using tracer amounts of krypton-85 provided the major analytical tool employed in the investigation.

Data obtained from the experiments indicate that if values for the density and thermal conductivity of the krypton frost are known, the model can accurately predict krypton loading profiles in the cold trap. The frost density and frost thermal conductivity appear to be functions of the freeze-out temperature and condensable krypton concentration. Presented in this thesis is a discussion of cold trapping theory, a description of the experimental apparatus and tests performed, and an explanation of the usefulness of the model as a design tool for engineering use.

Blank Page

TABLE OF CONTENTS

LIST OF TABLES

LIST OF FIGURES

LIST OF SYMBOLS

a	parameter combination equivalent to $\frac{M_l C_l N}{M_m C_m} \ln[(1 - p_w/p_T)/(1 - x)]$
b	deposit thickness, ft
b_{max}	maximum deposit thickness, ft
$B(\kappa t)$	buildup factor
C_m	mean specific heat of gas in stream, Btu/lb-°F
C_P	specific heat of gas, Btu/lb-mole-°F
C_l	specific heat of condensable, Btu/lb-°F
D_{AB}	diffusivity, ft^2/hr
D_e	equivalent diameter, ft
f(Re)	Reynolds number function
F(X)	function in Newton-Raphson iteration evaluated at X
F'(X)	first derivative of the function F evaluated at X
G	mass velocity of gas mixture, $lb/hr\text{-}ft^2$
h	heat transfer coefficient, $Btu/hr\text{-}ft^2\text{-}°F$
h_{con}	scaling constant determined experimentally
j_h	heat transfer "j" factor
j_m	mass transfer "j" factor
k	thermal conductivity of gas, Btu/hr-ft-°F
k_B	Boltzmann constant, ergs/°K
k_s	frost thermal conductivity, Btu/hr-ft-°F
K	mass transfer coefficient, $lb\text{-}mole/hr\text{-}ft^2\text{-}atm$
L	the total rate of condensation per unit area, $ha/[M_l C_l (1 - \alpha)]$

m	mass of condensable materials reaching a unit area of cooling wall surface, lb/ft^2
M_m	mean molecular weight of gas in stream, lb/lb-mole
M_l	molecular weight of condensable component, lb/lb-mole
N	$(Pr/Sc)^{2/3}$
p	partial pressure of condensable in bulk gas stream, atm
p_i	partial pressure of noncondensable in gas stream, atm
p_{iw}	partial pressure of noncondensable at wall, atm
p_T	total pressure, atm
p_w	partial pressure of condensable at wall, atm
P_{gf}	log mean partial pressure, atm
P	perimeter of flow channel, ft
Pr	Prandtl number, $C_p\mu/k$, dimensionless
Q	heat flow, $Btu/hr\text{-}ft^2$
Q_T	total heat flow, $Btu/hr\text{-}ft^2$
Q_{frost}	heat due to sublimation, $Btu/hr\text{-}ft^2$
r_h	hydraulic radius, ft
r_o	collision diameter for low velocity head-on collision, angstroms
R	universal gas constant, 1.986 Btu/lb-mole-°R
Sc	Schmidt number, $\mu/\rho D_{AB}$, dimensionless
t	thickness, in.
T	bulk gas temperature, °R
T_c	coolant (trap wall surface) temperature, °R
T_s	saturation temperature, °R
T_w	wall surface temperature, °R

U	parameter combination equivalent to $\ell n(b_{max} - b)$
V	flow of noncondensable gas, lb-mole/hr
V	volume, ft^3
x	bulk average mole fraction of condensable in gas stream
X	independent variable used in Runge-Kutta numerical method
y	moles of condensable per mole of inert gas
Y	dependent variable used in Runge-Kutta numerical method
z	distance along length of trap, ft
α	mist fraction
β	(p_w/p)
ε	energy difference between separated molecules and the molecules in the configuration in which they have the maximum energy of attraction
ε_{AB}	Lennard-Jones force constant for a binary mixture
θ	time, hr
κ	linear attenuation coefficient
μ	viscosity of component, lb/ft-hr
μ_{mix}	viscosity of gaseous mixture, lb/ft-hr, except where noted
η	fin efficiency
λ	latent heat of sublimation of condensable component, Btu/lb-mole
$\psi(t)$	radiation flux through lead of thickness t
ρ	density of component, lb/ft^3
ρ_s	frost density of condensable component, lb/ft^3

σ_{AB} Lennard-Jones force constant for a binary mixture

ϕ_{12} functional term equivalent to $\dfrac{[1 + (\frac{\mu_1}{\mu_2})^{1/2} (\frac{M_2}{M_1})^{1/4}]^2}{\sqrt{\frac{4}{2}} [1 + \frac{M_1}{M_2}]^{1/2}}$

Ω_D collision integral, $f(\frac{k_B T}{\varepsilon_{AB}})$

Blank Page

CHAPTER I

INTRODUCTION

Stringent emission standards are being formulated to limit release of various volatile fission products from nuclear fuel reprocessing facilities. These fission products include the long-lived isotopes krypton-85 and carbon-14 and the short-lived isotopes of xenon. The Oak Ridge Gaseous Diffusion Plant has been actively engaged in developing a process for the removal of these contaminants from the off-gas of fuel reprocessing plants. The method of contaminant removal, selective absorption in the solvent dichlorodifluoromethane[1,2], has reached the advanced stages of development, but the method of contaminant concentration prior to final product storage has not yet been decided.

One proposed contaminant concentration method employs a series of Molecular Sieve traps to produce a final product containing argon, krypton, and xenon. The Molecular Sieve traps remove any refrigerant-12 vapors, carbon dioxide, and nitrous oxide that might be present in the off-gas stream. Two heated beds, one of copper turnings and one of calcium, to react with the oxygen and nitrogen, respectively, are also required. The effluent of the calcium trap is the final Ar-Kr-Xe product ready for storage.

An alternative method of product concentration and isolation is to collect the xenon and krypton fractions in

a batch-type cold trap and then allow the frozen solids to warm and be collected in a gas cylinder. The cold trap would be located downstream of the refrigerant-12 and carbon dioxide removal steps. The obvious advantage of this collection method is the removal of the diluent gas argon, making higher krypton product concentrations possible. The ultimate result then would be a greatly reduced storage volume required for the radioactive contaminant. Another advantage of this collection method is the elimination of the heated chemical metal reactive beds of copper and calcium required for oxygen and nitrogen removal. Instead, the cold trap effluent, which could contain some untrapped krypton in its essentially all-diluent gas stream, could be recycled to the primary krypton removal facility.

Very little work has been performed on separation of materials by cold trapping or desublimation. However, a mathematical model of a desublimer, a pseudo term for cold trap, has been written by D. I. Dunthorn which predicts solid build-up of the desublimed component along the length of the trap[3]. Specifically, the work performed by Dunthorn studied the desublimation and collection of uranium and plutonium hexafluorides in the volatility processing of spent power reactor fuel elements[4]. This model, patterned after the method of Thompson[5], is written generally enough, though, to incorporate the desublimation of any component in any noncondensable carrier gas.

To acquire necessary design data for a commercial product purification cold trap, the experimental work of this thesis utilized gamma scintillation tracer techniques to obtain solids buildup profiles for the single component krypton freezing out of a nitrogen carrier gas stream. These experimentally obtained profiles were then compared to profiles generated by the theoretical model.

CHAPTER II

THEORY

Presented in this chapter is a brief summary of the concepts and theory behind desublimation. Solutions of the differential equations to yield the theoretical profiles were performed by standard numerical techniques, while the correlating form used to describe the governing heat transfer coefficient is of a standard chemical engineering form recommended by the manufacturer of the heat exchanger finned tube used in the studies.

I. DERIVATION OF DESUBLIMER EQUATIONS

This derivation follows closely that presented by Dunthorn[3]. Since this reference has become somewhat difficult to obtain, it was thought desirable to include in detail those portions of that reference which are directly applicable to the present study.

Generally, when a gas stream enters a desublimer, the gaseous influent is superheated; i.e., it contains less than a saturated amount of condensable component. As the gas contacts the refrigerated walls, it is cooled to saturation which causes solid to condense on the walls and to set up a driving force for mass transfer between the bulk gas and the wall. Simultaneously, the gas stream is cooled by convective heat transfer. Since diffusive mass transfer might not remove

condensables fast enough to keep the stream below saturated conditions, the bulk gas tends to approach saturation. As saturation is reached and as the gas is further cooled along the trap, then theoretically, enough condensable material must be removed from the bulk stream to prevent supersaturation. Therefore, material other than that traveling to the wall by normal mass transfer then freezes out in the stream itself as a mist or snow and settles to the surface by falling or other mechanical means. Because of this, it would be expected that the solid deposit thickness would vary along the length of the trap and that an increase in deposit thickness should occur where the bulk gas becomes saturated.

At any point in the desublimer, the base rate of mass transfer to the cooling walls may be expressed as

$$\left(\frac{\partial m}{\partial \theta}\right)_z^o = M_1 K(p - p_w) = M_1 K p(1 - \beta), \qquad (1)$$

where

$\left(\frac{\partial m}{\partial \theta}\right)_z^o$ = diffusive mass transfer rate,

m = mass of condensable material reaching a unit area of cooling wall surface, lb/ft^2,

θ = time, hr,

M_1 = molecular weight of condensable,

z = distance along length of trap, ft,

K = mass transfer coefficient, lb mole/hr-ft^2-atm,

p = partial pressure of condensable in the gas stream, atm,

p_w = partial pressure of condensable at the cooling wall, atm, and

$\beta = p_w/p$.

The point buildup of the solid deposit due to mass transfer to the wall may be expressed as

$$\left(\frac{\partial b}{\partial \theta}\right)_z^o = \frac{M_1 K p}{\rho_s} (1 - \beta), \tag{2}$$

where

b = deposit thickness, ft, and

ρ_s = deposit bulk density, lb/ft^3.

The mass transfer coefficient is not easily obtainable; however, by using the Chilton-Colburn analogy[6] which relates mass and heat transfer, an expression for K may be reasonably approximated for many engineering applications. This analogy is:

$$j_m = \frac{KP_{gf}}{G/M_m} Sc^{2/3} = \frac{h}{C_m G} Pr^{2/3} = j_h, \tag{3}$$

where

j_m = mass transfer "j" factor,

j_h = heat transfer "j" factor,

P_{gf} = logarithmic mean partial pressure difference of non-condensable gas, atm,

G = mass velocity of gas mixture, $lb/hr\text{-}ft^2$,

M_m = mean molecular weight of gas in stream, lb/lb-mole,

C_m = mean specific heat of gas in stream, Btu/lb-°F,

h = heat transfer coefficient, Btu/hr-ft^2-°F,

Sc = Schmidt number, $\mu/\rho D_{AB}$, dimensionless,

ρ = viscosity of gas, lb/ft-hr,

D_{AB} = diffusivity, ft^2/hr,

Pr = Prandtl number, $C_m\mu/k$, dimensionless, and

k = thermal conductivity of gas, Btu/hr-ft-°F.

Using the heat transfer coefficient to estimate the mass transfer coefficient via the Chilton-Colburn analogy, the heat transfer coefficient used must be that for heat transfer from a warm gas to a chilled wall and not an overall coefficient or one which considers the transfer of latent heat. For a heat exchange medium having finned cooling surfaces, the manufacturer of the finned tube used in the experimental apparatus, Brown Fin-Tube Company, recommends the following semiempirical relationship[7]:

$$\frac{h}{C_m G} = (h_{con})(Pr^{-2/3})\ f(Re), \qquad (4)$$

where

h_{con} = scaling constant determined experimentally, and

f(Re) = function of Reynolds number.

Used in the above form, the Reynolds number is defined as the equivalent diameter multiplied by the gas flow

rate and divided by the gas viscosity (Appendix A). A least squares fit to data supplied by the finned tube manufacturer[7] indicated the following Reynolds number dependency:

$$f(Re) = \exp[-1.2587 - 0.62828 \ln (\frac{D_e G}{\mu})], \quad (5)$$

where

D_e = equivalent diameter, ft,

$\frac{D_e G}{\mu}$ = Reynolds number, dimensionless.

The logarithmic term in the Chilton-Colburn analogy may be expressed as

$$p_{gf} = \frac{p_i - p_{iw}}{\ln(p_i/p_w)}, \quad (6)$$

where

p_i = partial pressure of noncondensable in gas stream, atm, and

p_{iw} = partial pressure of noncondensable at wall, atm.

More specifically, by Dalton's law,

$$p_i = p_T - p = p_T - xp_T, \quad (7)$$

$$p_{iw} = p_T - p_w, \quad (8)$$

where

p_T = total pressure, atm,

x = bulk average mole fraction of condensable in gas stream,

p = partial pressure of condensable in bulk gas stream, atm, and

p_w = partial pressure of condensable at wall, atm.

Therefore,

$$P_{gf} = \frac{p_w - p}{\ell n\left(\frac{p_T - xp_T}{p_T - p_w}\right)} = \frac{p(1 - \beta)}{\ell n\left(\frac{1 - p_w/p_T}{1 - x}\right)} . \tag{9}$$

Combining equations (2), (3), and (9) yields

$$\left(\frac{\partial b}{\partial \theta}\right)_z^o = \frac{M_l h}{\rho_s M_m C_m} N \ \ell n\left(\frac{1 - p_w/p_T}{1 - x}\right), \tag{10}$$

where

$N = (Pr/Sc)^{2/3}$.

In a strict sense of the word, this equation applies only for a superheated gas. In the case of a saturated gas, though, it also represents the buildup due to the diffusive mass transfer phenomena. The relationship between the actual buildup, $\left(\frac{\partial b}{\partial \theta}\right)_z$ and $\left(\frac{\partial b}{\partial \theta}\right)_z^o$, can be defined as

$$\left(\frac{\partial b}{\partial \theta}\right)_z = \frac{1}{1-\alpha}\left(\frac{\partial b}{\partial \theta}\right)^o_z = \frac{M_1 hN}{\rho_s M_m C_m (1-\alpha)} \ln\left(\frac{1 - p_w/p_T}{1 - x}\right), \quad (11)$$

where

α = fraction of solid buildup due to frosting or misting.

Under superheated conditions, this mist fraction, α, is zero, and the equation reduces back to the previous form, representing only normal mass transfer. Under saturated conditions, however, the mist fraction will represent that portion of condensable which reaches the wall by means other than diffusive mass transfer. If a differential material balance for a section of desublimer is made in terms of bulk average concentration, then assuming plug flow and assuming that the gas concentration change with time at a point is negligible,

$$Vy - V(y + \Delta y) = P\frac{\rho_s}{M_1}\frac{db}{d\theta}\Delta z \quad (12)$$

where

y = moles of condensable per mole of inert gas,

V = flow of noncondensable gas, lb mole/hr,

M_1 = molecular weight of condensable component, lb/lb mole,

P = perimeter of flow channel, ft, and

ρ_s = density of solid deposit, lb/ft^3.

Rearranging and taking the limit as Δy and Δz become infinitely small gives,

$$-V\frac{dy}{dz} = P\frac{\rho_s}{M_1}\frac{db}{d\theta}, \tag{13}$$

In terms of the mole fraction, x,

$$\frac{dy}{dz} = \frac{1}{(1 - x)^2}\frac{dx}{dz}. \tag{14}$$

Substituting into (13) yields the following expression for the concentration profile along the trap:

$$\frac{dx}{dz} = \frac{-(1 - x)^2}{V}\frac{\rho_s P}{M_1}\left(\frac{db}{d\theta}\right), \tag{15}$$

which, when combined with (11), becomes

$$\frac{dx}{dz} = \frac{-(1 - x)^2}{V}\frac{hPN}{M_m C_m(1 - \alpha)}\ln\left(\frac{1 - P_w/P_T}{1 - x}\right). \tag{16}$$

The derivation of the heat transfer equation can be handled similarly to obtain theoretical temperature profiles along the length of the trap[8]. If it is assumed that there is a film through which heat is being transferred, then it can be treated like conduction through a slab. Figure 1 graphically depicts this type of conduction. At $t = t_1$, the temperature of the stream is T, and at $t = 0$, the temperature at the wall is T_w. Allowing conduction in only one direction, Q is constant and at any point can be represented by $Q = k\frac{dT}{dt}$. When there is material being transferred through

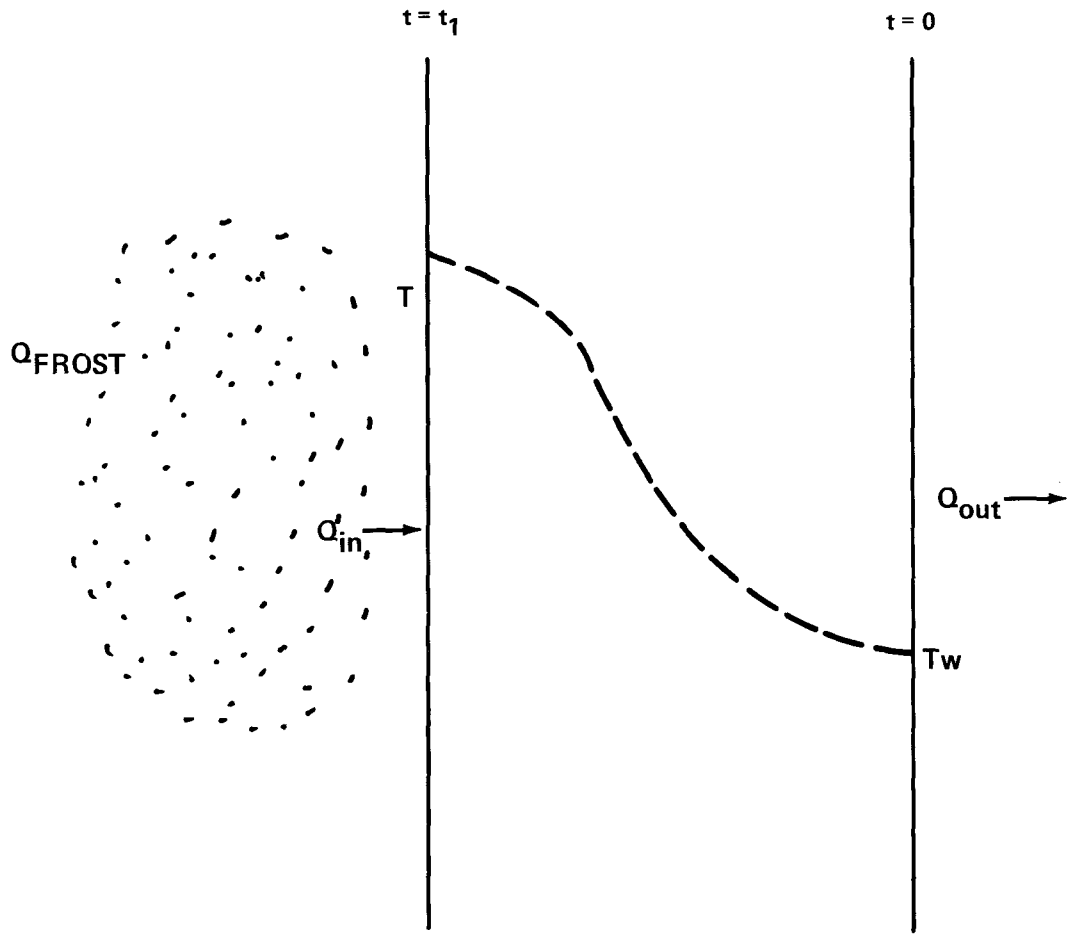

Figure 1

HEAT CONDUCTION THROUGH A SLAB

the film, then the material must be cooled as it passes through and the heat transferred must also be carried by $k\frac{dT}{dt}$. The total heat flow into the film at $t = t_1$ must equal that reaching $t = 0$. At $t = 0$, however, the heat carried by mass flow will equal zero, since the mass temperature will be identical to the wall temperature. Therefore, at any point within the film,

$$Q_T = \text{Constant} = \underbrace{-k\frac{dT}{dt}}_{\text{Conduction}} + \underbrace{C_l \rho_s \frac{\partial b}{\partial \theta}(T - T_w)}_{\substack{\text{Heat Carried} \\ \text{By Mass Flow}}}. \qquad (17)$$

where

Q_T = total heat transferred, Btu/hr-ft^2,

T = bulk gas temperature, °R,

T_w = wall surface temperature, °R, and

C_l = specific heat of condensable component, Btu/lb-°F.

Now from equation (11),

$$\rho_s C_l \left(\frac{\partial b}{\partial \theta}\right) = \frac{hM_l N C_l}{M_m C_m} \ln\left[\frac{(1 - p_w/p_T)}{(1 - x)}\right], \qquad (18)$$

let

$$a = \frac{M_l C_l N}{M_m C_m} \ln\left(\frac{1 - P_w/P_T}{1 - x}\right). \qquad (19)$$

Then,

$$\rho_s C_l \left(\frac{\partial b}{\partial \theta}\right) = ha. \tag{20}$$

Substituting back into equation (17), the following relationship is obtained:

$$Q_T + k\frac{dT}{dt} - ha(T - T_w) = 0. \tag{21}$$

Separating variables and integrating yields,

$$\int_T^{T_w} \frac{k\,dT}{-Q_T + ha(T - T_w)} = -\int_o^t dt, \tag{22}$$

$$\frac{k}{ha} \ln\left[\frac{-Q_T + ha(T - T_w)}{-Q_T}\right] = -t, \tag{23}$$

$$-Q_T + ha(T - T_w) = -Q_T e^{-tha/k}. \tag{24}$$

Since k/t corresponds to the usual definition of the heat transfer coefficient, h,

$$Q_T = \frac{ha(T - T_w)}{(1 - e^{-a})}, \tag{25}$$

which is the total heat across the film.

The term, $a/(1 - e^{-a})$, is called the Ackerman correction factor and includes the heat transfer to the wall

through mass flow[8-11]. Another way to express the total heat equation is by summing the individual heat flux components. These components are due to the heat of desublimation, change of convective heat in the flowing liquid, and the heat due to the mass transfer from the flowing fluid to the wall.

The heat due to desublimation, Q_{frost}, may be expressed as:

$$Q_{frost} = \lambda L \alpha, \tag{26}$$

where

λ = latent heat of sublimation of condensable, Btu/lb-mole,

$L = \frac{ha}{M_l C_l (1 - \alpha)}$, the total rate of condensation per unit area, lb-mole/hr-ft^2, and

α = mist fraction; i.e., that fraction of solid removed from the gas stream by condensation in the gas stream rather than directly on the trap walls.

The total change in heat content of the flowing fluid through the element dz can be written as:

$$Q_{\text{Flow Change}} = \frac{V}{P(1 - x)} M_m C_m \frac{dT}{dz}, \tag{27}$$

where

V = flow of noncondensable gas, lb-mole/hr, and

P = perimeter of flow channel, ft.

Finally, the heat due to the mass transfer to the wall through the film may be expressed as:

$$Q_{\text{Mass Flow}} = h(T - T_w)a. \tag{28}$$

By equating the two total heat fluxes and rearranging the equation, an expression for the temperature profile, dT/dz, may be obtained. This yields

$$\frac{dT}{dz} = \frac{ha(1 - x)P}{VM_mC_m}\left[\frac{\lambda\alpha}{M_lC_l(1 - \alpha)} - \frac{(T - T_w)}{(e^a - 1)}\right]. \tag{29}$$

As long as the gas stream remains superheated, then α will remain zero; and this equation may be solved numerically to obtain the temperature profile, and equation (16) can be solved to yield the concentration profile. Solid buildup rates may also be obtained by using the information in equation (11).

Since some condensing material will not be carried to the wall by normal mass transfer at saturated conditions, α is no longer zero and the equations are no longer easily solved. It is assumed that the condensable desubliming from the vapor stream settles out at the point of formation. Also, it is assumed that, after saturation, the bulk concentration and temperature of the gas stream follow the Clausius-Clapeyron equation:

$$\frac{dx}{dT} = \frac{x\lambda}{RT^2} \quad . \tag{30}$$

where

R = universal gas constant, 1.986 Btu/lb-mole-°R.

By combining equations (16), (29), and (30), an expression may be obtained for the mist fraction, α.

$$\alpha = 1 - \frac{\frac{\lambda}{C_m M_m} + \frac{RT^2(1 - x)}{\lambda x}}{\frac{\lambda}{C_m M_m} + \frac{C_l M_l (T - T_w)}{C_m M_m (e^a - 1)}} \quad . \tag{31}$$

The mist fraction may now be calculated. By using this calculated α, it is possible to determine the temperature and concentration profiles from the mass transfer and Clausius-Clapeyron or vapor pressure equations, equations (16) and (30).

The effect of the solid deposit on the gas-solid interface temperature, T_W, must be considered in the above treatment. Initially, this temperature can be assumed to be nearly equal to the coolant temperature, but as the solids build up, the conduction of heat through the solid layer must be considered in determining the interfacial temperature. This is especially so, since the thermal conductivity of the frost layer is quite low. The interfacial temperature may

be determined by equating the heat flux through the deposit to the heat flux at the deposit surface:

$$\frac{k_s}{b}(T_w - T_c) = \frac{ha}{(1 - e^{-a})}(T - T_w) + \frac{\lambda ha}{M_1 C_1} \qquad (32)$$

where

k_s = thermal conductivity of solid deposit, Btu/hr-ft-°F, and

T_c = coolant temperature, °R.

The interfacial temperature may then be found which, in turn, establishes the driving force required to effect the solids buildup along the trap length.

Since the interfacial temperature may be considered as a separate system variable, solution of the above equation for T_w may be obtained by a trial and error technique and poses no problem for most of the numerical solution. However, if the calculated T_w exceeds its physical limit, significant errors may propogate in the solution.

The limiting or maximum value of T_w may be found by first finding the maximum deposit thickness and then calculating the interfacial temperature which coincides with this maximum deposit thickness. By equating the differential equation for the deposit buildup with respect to time,

$$\frac{db}{d\theta} = \frac{M_l h N}{\rho_s M_m C_m (1 - \alpha)} \ln\left[\frac{(1 - p_w/p_T)}{1 - x}\right] = 0, \qquad (33)$$

to zero, the maximum thickness may be obtained. Since all of the terms outside the logarithmic term are non-zero, the logarithmic term then must be zero for the equality to hold true. Since the antilogarithm of zero is one,

$$\frac{1 - p_w/p_T}{1 - x} = 1, \qquad (34)$$

or

$$\frac{p_w}{p_T} = x. \qquad (35)$$

Since p_w is the vapor pressure of the condensable at the solid surface temperature T_w, p_w/p_T will equal x when T_w reaches the saturation temperature of the gas stream.

If more solid were to deposit at that point, T_w would rise above the gas stream saturation temperature and the deposited solid would sublime back into the gas stream. The condition described cannot occur in the saturated portion of the trap since the gas is already at saturated conditions; and for any heat transfer to take place, some temperature differential must be maintained between the gas stream and solid surface temperatures. For a superheated gas, however, this sets an upper bound on both the solids surface temperature and maximum deposit thickness. If the maximum thickness

is insufficient to plug the trap, the trap then cannot plug in the superheated region.

Not only can equation (32) be used to obtain the interfacial temperature, but it may also be used to determine either the maximum surface temperature, i.e., the saturation temperature, or the maximum deposit thickness, b_{max}.

Recall from equations (10) and (19) that

$$a = \frac{\rho_s(1 - \alpha)}{h} C_l \frac{db}{d\theta} . \tag{36}$$

As $\frac{db}{d\theta}$ goes to zero, a also goes to zero, and

$$\lim_{a \to 0} \frac{a}{(1 - e^{-a})} = 1. \tag{37}$$

At the maximum deposit thickness, the surface temperature, T_w, will be at its maximum, T_s, and from equations (32) and (37),

$$T_s = \frac{k_s T_c + h b_{max} T}{k_s + h b_{max}}, \tag{38}$$

or

$$b_{max} = \frac{k_s}{h} \frac{(T_s - T_c)}{(T - T_s)} . \tag{39}$$

II. COMPUTER PROGRAM AND NUMERICAL TECHNIQUES FOR SOLVING DIFFERENTIAL EQUATIONS

To solve the equations derived in the preceding section for a theoretical concentration profile (equation 16), temperature profile (equation 29), deposit height (equation 11), and solids surface temperature (equation 32), the computer program published by Dunthorn[3] was adapted to the specific system being studied. The program was written specifically for cold trapping uranium and plutonium hexafluorides in the volatility processing of spent power reactor fuel elements; however, it was written generally enough to incorporate the desublimation of any component in any noncondensable carrier gas. Solutions to the governing useful differential equations were obtained by common numerical method techniques. Prior to obtaining these solutions, however, certain physical properties, i.e., vapor pressure, viscosity, density, diffusivity, thermal conductivity, and heat capacity, had to be correlated into a usable form. Equations used in the program for each of these required parameters may be found in Appendix A.

Solutions of the concentration and temperature profile equations were obtained using a four-step Runge-Kutta[12] numerical method. Only the gas temperature and concentration were allowed to vary while the surface temperature and deposit thickness were assumed to be constant at the values in effect at the beginning of the step.

To calculate the integral curve of the equation, $\frac{dY}{dX} = f(X,Y)$, through the point X_o,Y_o, the following formulae are used in the four-step method:

$$k_1 = f(X_o,Y_o)\Delta X, \tag{40}$$

$$k_2 = f(X_o + \frac{\Delta X}{2}, Y_o + \frac{k_1}{2})\Delta X, \tag{41}$$

$$k_3 = f(X_o + \frac{\Delta X}{2}, Y_o + \frac{k_2}{2})\Delta X, \tag{42}$$

$$k_4 = f(X_o + \Delta X, Y_o + k_3)\Delta X, \tag{43}$$

$$\Delta Y = 1/6(k_1 + 2k_2 + 2k_3 + k4), \tag{44}$$

$$X_1 = X_o + \Delta X, \tag{45}$$

$$Y_1 = Y_o + \Delta Y. \tag{46}$$

The four individual steps as outlined above are written as a subroutine of the main program and accessed by appropriate programming call statements. Between successive calls, a check is made to determine if numerical errors have caused the intermediate bulk gas temperature to be less than the surface temperature. If this physically impossible situation occurs, it is corrected by equating the solid surface temperature with the bulk gas temperature. At the beginning of each distance integration, it is assumed that the gas

stream is superheated. At each step, this assumption is tested. When the temperature drops below the saturation temperature, the program transfers to saturated conditions. To prevent any unnecessary propogation of errors, the gas concentration is calculated using the vapor pressure equation instead of the Clausius-Clapeyron differential form. If an excess of heat transfer area exists, the gas and trap wall temperatures are so nearly equal that the fraction of solids condensing out in the gas stream is zero. In this instance, the program changes back to the superheat calculation mode.

Time integrations are calculated following the first of the four steps in the Runge-Kutta method. At this point in the program, distance derivatives, and physical and flow properties have correct point values and may be employed directly. A simple Euler's[13] method is used to calculate the change in deposit height with respect to time. If the temperature and composition, as well as all physical properties and flows, are assumed to be constant with respect to time at the point in question and if the condensable concentration in the gas stream is small, then equation (11) may be integrated to give

$$\int_0^b \frac{db}{\ln\left(\frac{1 - p_w/p_T}{1 - x}\right)} = \frac{M_l h N}{\rho_s M_m C_m}\,\theta \qquad (47)$$

Recall that the partial pressure of the condensable at the cooling wall, p_w, is a function of the wall temperature which, in turn, is a function of the deposit height (equation 32). Figure 2 is a curve generated by solving the above equation (47) using typical values for the parameters. As seen in the curve, it is important to note that the rate of solids buildup is essentially constant until better than 50% of the solids have accumulated. Since there is no maximum buildup thickness in the saturated region, the implication here is that solids buildup should be relatively constant in that region. A maximum deposit height does exist, however, in the superheated region of the trap; and as can be seen in Figure 2, this buildup rate is no longer constant with time. To obtain an accurate solution to the differential equation using a simplified method such as Euler's method, very small step intervals would have to be employed. If intervals too large are chosen, calculated deposit heights may be greater than the maximum possible deposit thickness causing computational difficulties.

From Figure 3, it is seen that if the solution is replotted as $\ell n[(b_{max} - b)/b_{max}]$ versus time, a nearly linear relationship is found. Therefore, if

$$U = \ell n(b_{max} - b), \tag{48}$$

by the chain rule of differentiation,

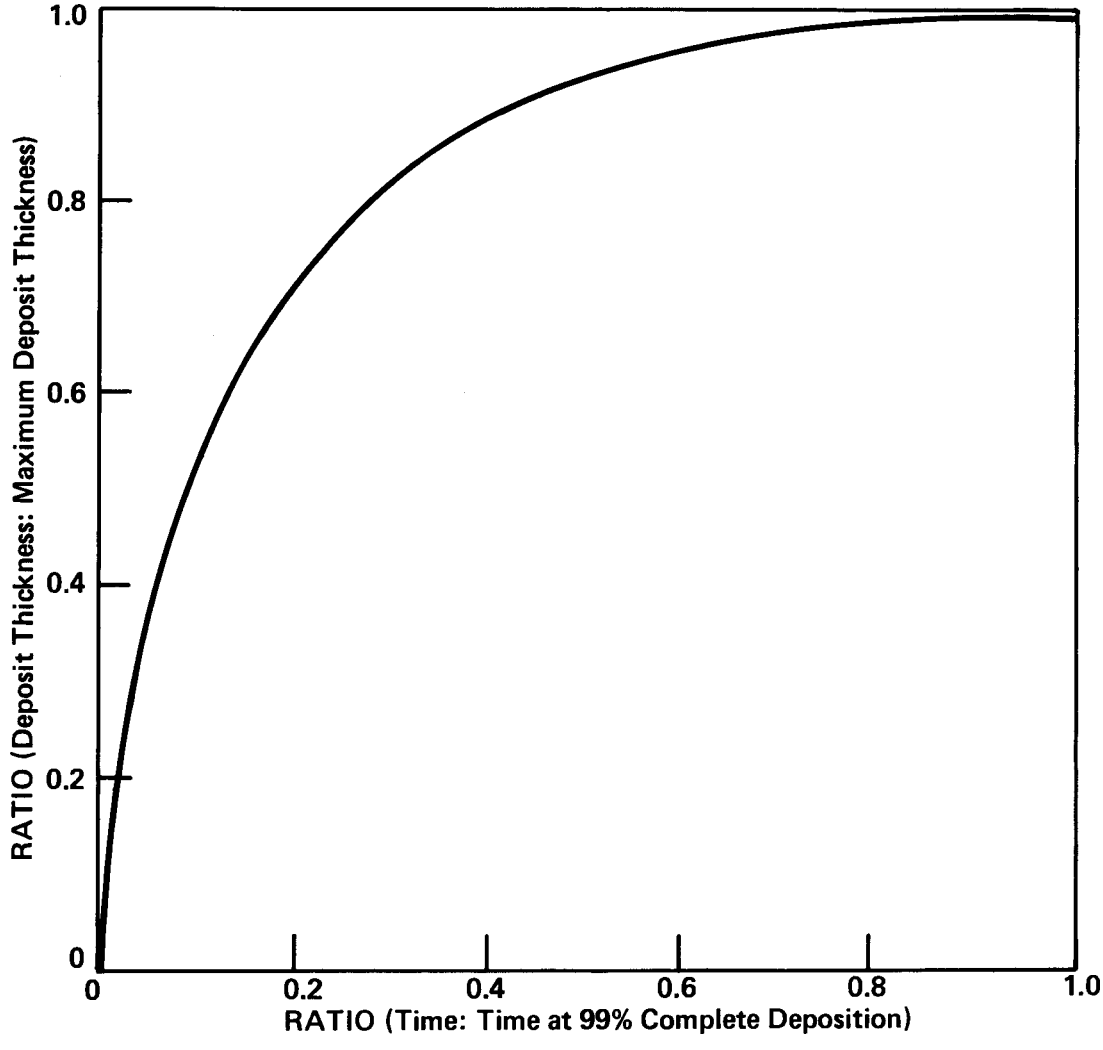

Figure 2

TYPICAL DEPOSIT THICKNESS RELATIONSHIP WITH TIME

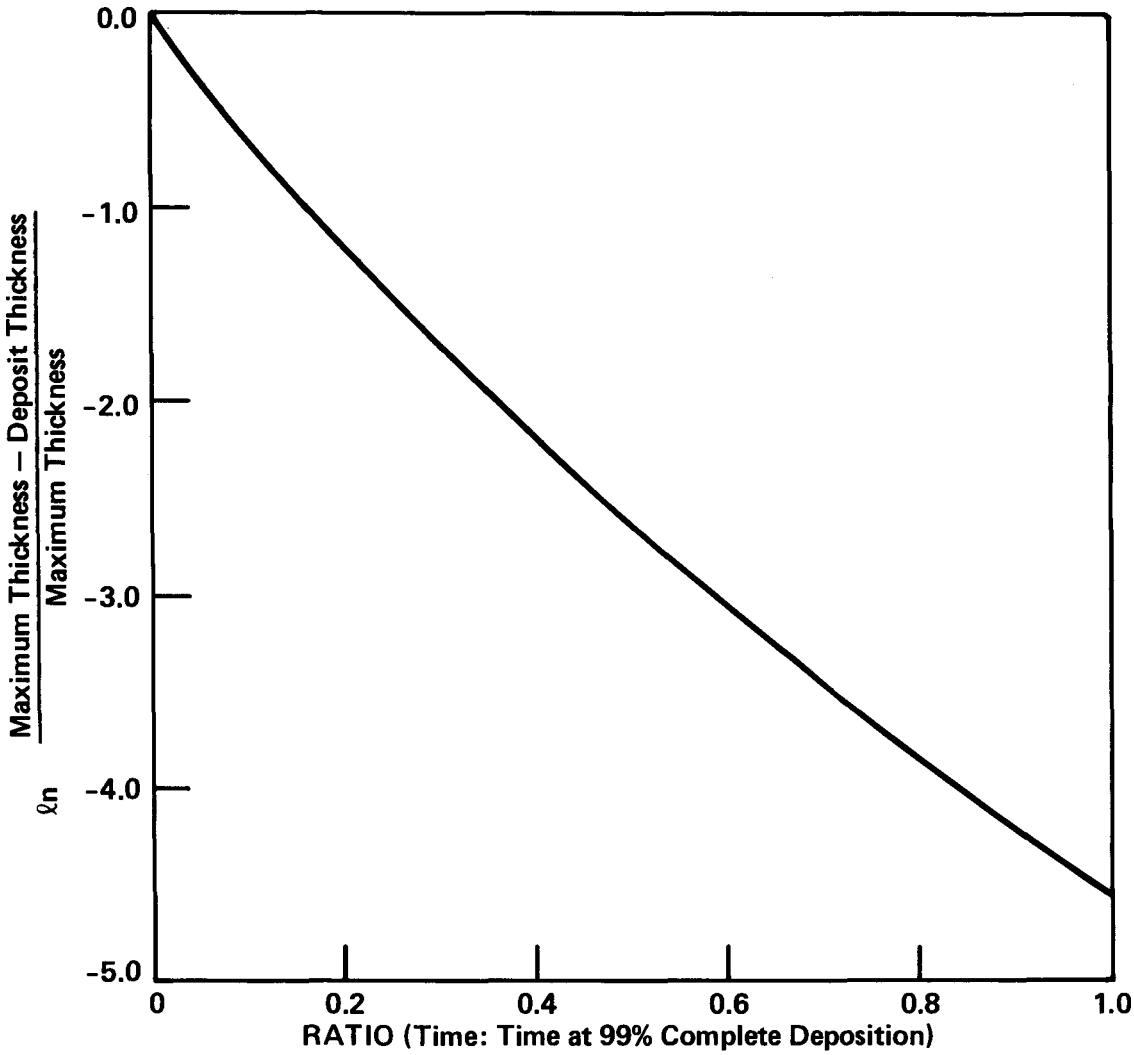

Figure 3

LINEARIZED DEPOSIT THICKNESS RELATIONSHIP WITH TIME

$$\frac{dU}{d\theta} = \frac{dU}{db}\frac{db}{d\theta} , \tag{49}$$

and

$$\frac{dU}{d\theta} = \frac{1}{(b - b_{max})}\frac{db}{d\theta} . \tag{50}$$

Since $\frac{dU}{d\theta}$ is relatively constant, this equation can be more easily solved using numerical methods than can the equation for $\frac{db}{d\theta}$. To obtain the desired deposit thickness on the superheat region, Euler's method is employed in the computer program using the following calculations:

$$U_1 = \ell n(b_{max} - b_1), \tag{51}$$

$$U_2 = \ell n(b_{max} - b_2), \tag{52}$$

$$U_2 - U_1 = \ell n(\frac{b_{max} - b_2}{b_{max} - b_1}), \tag{53}$$

$$(b_{max} - b_1)e^{\Delta U} = b_{max} - b_2, \tag{54}$$

$$b_2 = b_{max} - (b_{max} - b_1)e^{\Delta U}, \tag{55}$$

$$b_2 - b_1 = (b_{max} - b_1) - (b_{max} - b_1)e^{\Delta U}. \tag{56}$$

Finally,

$$\Delta b = (b_{max} - b_1)(1 - e^{\Delta U}), \tag{57}$$

where Δb is the change in deposit thickness over a unit change in time.

Because of the nearly linear relationship of this equation, Euler's method for numerical integration offers good accuracy for reasonably large time steps. Since the deposit buildup is constant in the saturated region of the trap, this is calculated by simple use of the derivative instead of the above method described.

Following calculation of the deposit height, the solid surface temperature is then calculated using the familiar Newton-Raphson[14] numerical method with end point corrections on a balance of heat flux. The primary form of the Newton-Raphson method is

$$X_n = X_{n-1} - \frac{F(X_{n-1})}{F'(X_{n-1})}$$

with

$$F(X) = 0,$$

where

X_n = newly calculated value of X,

X_{n-1} = previous calculated value of X,

$F(X_{n-1})$ = the function evaluated at X_{n-1}, and

$F'(X_{n-1})$ = the first derivative of the function evaluated at X_{n-1}.

This method is said to converge when the absolute value of the difference between two successive values for x is less than some predetermined convergence criteria. The Newton-Raphson method is excellent for finding the root of an equation because of its ability to converge rapidly, within 3 to 6 iterations. This method is not without fault, however. To converge, the initial guess must be sufficiently close to the root. Also, it is obvious that as the first derivative approaches zero, $[F(X_{n-1})]/[F'(X_{n-1})]$ goes to infinity. If either of these two conditions exist, or if the second derivative of F(X) at X_{n-1} is excessively large, the Newton-Raphson method will probably not converge. For this reason, an escape is incorporated in the program if convergence is not reached within twenty iterations. If the convergence criteria are not met within the twenty passes, the solid surface temperature is determined by successively halving twenty times the interval where the temperature lies. Using this method ensures convergence and is equivalent in accuracy to the Newton-Raphson method; however, this method is normally a great deal slower than the Newton-Raphson method and is only used if the preferred method fails.

The program also calculates the total amount of solids collected in the trap by carrying an integration of deposit height with distance and by integrating a material balance over the trap with time. Theoretically, these two values should be equal; however, satisfactory accuracy is said to have been achieved if the numbers vary no more than

10%. These two values, then, are a good indication of how reliable a particular calculation is.

Appendix B presents a full listing of the computer program, including a description of the program input. Initially, the program was written for an IBM 7090 machine and some of the symbols may seem archaic. The IBM 360 compiler will translate these outdated symbols to modern interpretations. All computer runs made for this work were made on an IBM Model 360 computer.

CHAPTER III

EXPERIMENTAL APPARATUS

This chapter presents a brief description of the experimental apparatus used to collect the data. Included is a summary of not only the mechanical equipment employed, but also the analytical instruments used to obtain stream compositions. Figure 4 is a photograph of the completed facility.

I. PROCESS PIPING AND FLOW EQUIPMENT

The primary piece of equipment is a 132-inch-long single-shell and tube-type heat exchanger or desublimer. The shell is fabricated from a nominal 2-inch, Schedule 80, 304L stainless steel pipe. A single 3/4-inch OD finned tube with sixteen 1/2-inch-high by 10-foot-long longitudinal exterior fins provided the surface area for cooling. The fins are cut and twisted every 6 inches to promote mixing and reduce channeling effects. Boiling liquid nitrogen tubeside yields the low temperatures necessary for the krypton to freeze. The trap is equipped with internal copper-constantan thermocouples equally spaced 6 inches apart along the length of the shell. Six inches of polyurethane foam insulates the desublimer, reducing heat inleakage into the trap. Figure 5 is an assembly, detail, and section drawing of the desublimer. In the drawing, it is of interest to

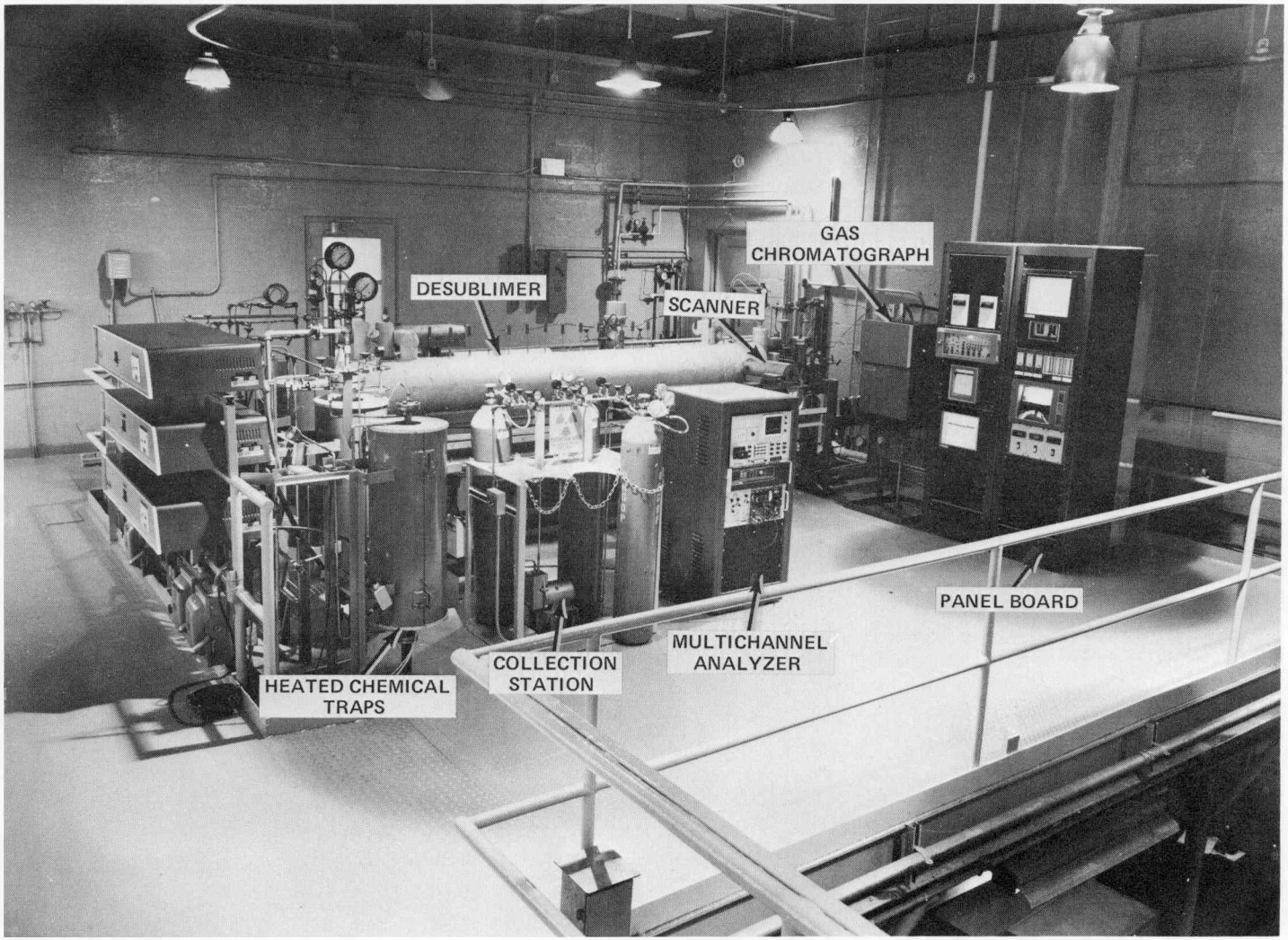

Figure 4
EXPERIMENTAL TEST FACILITY

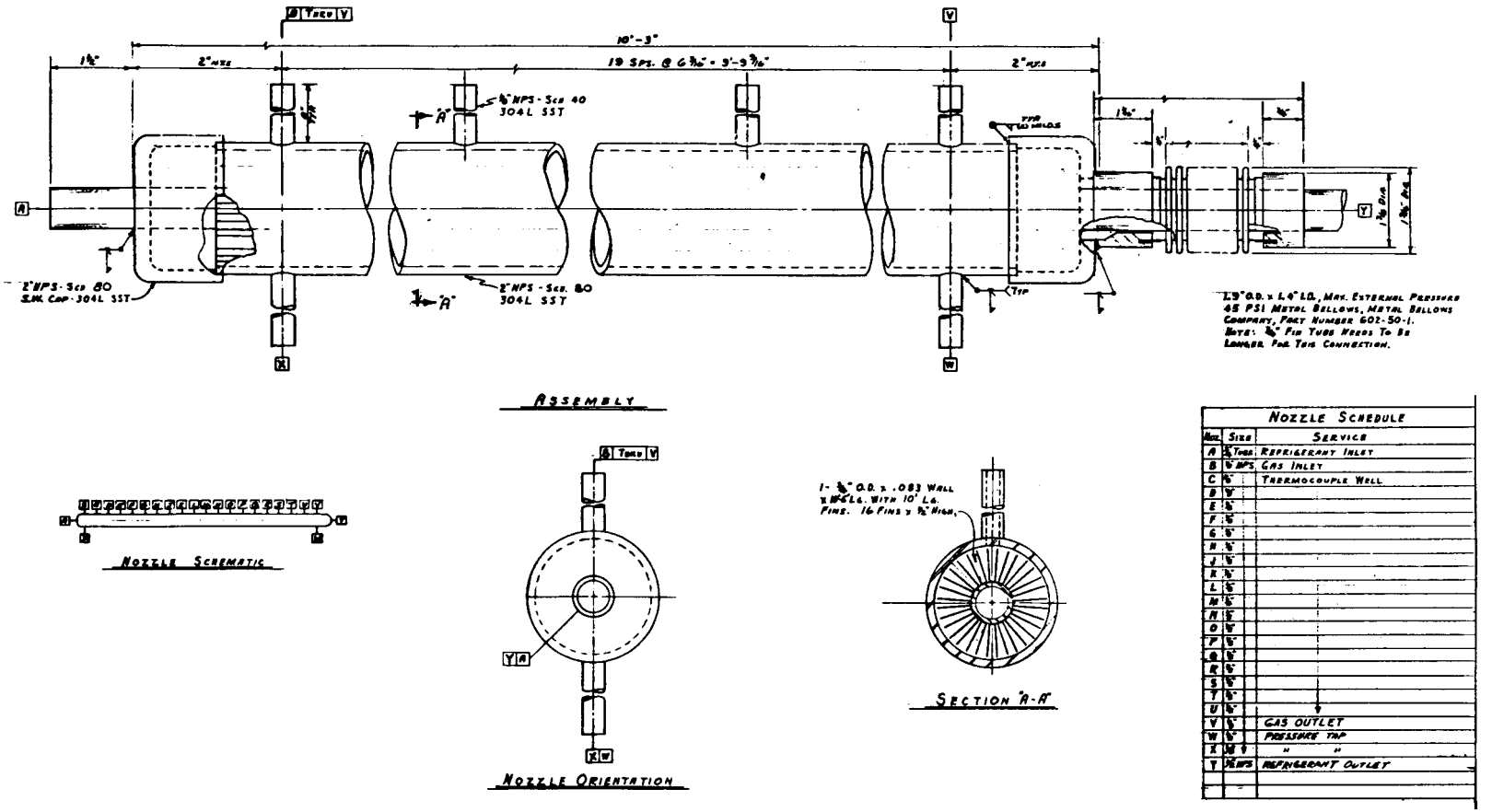

Figure 5

ASSEMBLY, DETAIL, AND SECTION DRAWING OF THE DESUBLIMER

note the metal bellows at the end of the heat exchanger. This bellows provides the needed flexibility for joining the finned tube with the cold trap. A thermal expansion stress analysis calculation (Appendix C) indicated that over the operating temperatures, the 400°F temperature change would result in up to a 1/2-inch contraction in the stainless steel tube and pipe heat exchanger.

Process instrumentation was designed to provide all process parameters required for adequate data analysis. Linear thermal mass flow meters were installed on the desublimer inlet and outlet streams. A differential pressure transmitter, calibrated between zero and 7 inches of water, was used to monitor the pressure drop across the trap and indicate plugging in the pipe flow channels. Shell side pressure was controlled by means of an absolute pressure transmitter, an automatic electronic controller, and an air-to-open control valve. The operating temperature was determined by the temperature of the boiling liquid nitrogen which was fixed by the liquid coolant pressure inside the finned tube. This coolant pressure was controlled by a system similar to the shell side pressure control loop; however, a feed forward system, instead of a feedback control loop, was used. Liquid nitrogen was fed from a Department of Transportation approved cylinder holding up to 5.6 ft^3 of coolant. During a test run, one cylinder lasted approximately 7 hours before there was a measurable change in the pressure of the coolant cylinder. Figure 6 is a flow and instrumentation schematic

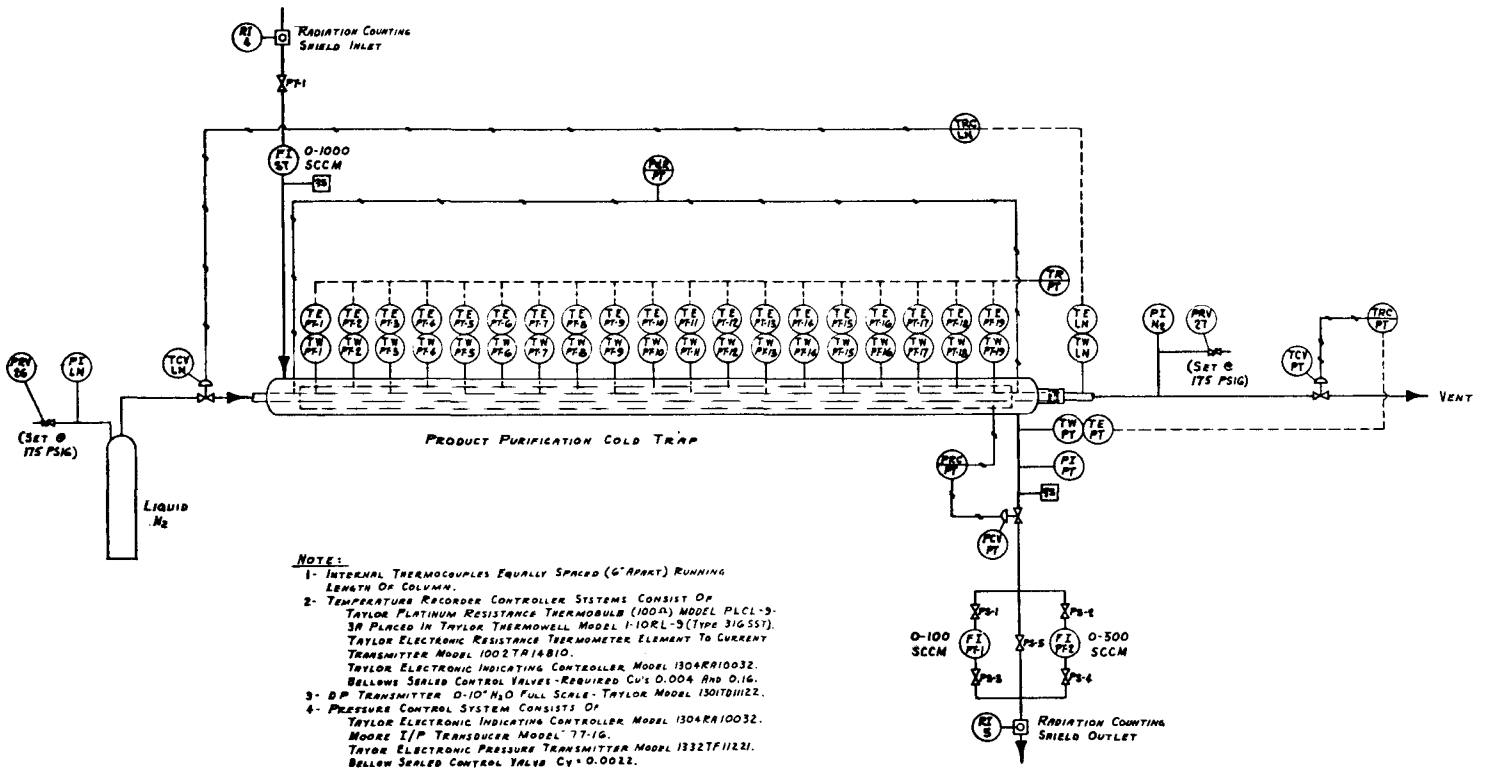

Figure 6

FLOW AND INSTRUMENTATION SCHEMATIC OF THE DESUBLIMER

of the physical apparatus. Table I describes in detail the necessary monitoring and control instrumentation employed in the process.

II. ANALYTICAL EQUIPMENT

The analytical equipment included a gas chromatograph and mass spectrometer, as well as a unique gamma ray spectroscopy tool developed by the author and his colleagues.

Gas samples were drawn from the cold trap inlet and outlet streams and either directed through an in-line process gas chromatograph or placed into cylinders for mass spectrometer or other laboratory analysis. The in-line chromatograph has ranges of 0-50% nitrogen, 0-50% krypton, 0-100% carbon dioxide, 0-100% xenon, 0-100% oxygen and argon combined, and 0-1000 ppm refrigerant-12. The refrigerant-12, carbon dioxide, and xenon detection capabilities are specific for the fluorocarbon development program and are not needed for the test performed for this thesis.

Radioisotope measurement has recently become a very useful tool in laboratory research and development activities to better define process behavior[15]. Although the method is well defined for laboratory and bench-scale equipment, very little work has been done using this technique in pilot plant-scale type work. In 1975, Canadians Fulham and Hulbert used gamma scanning to determine liquid levels, foam heights, plugging in sieve traps, and internal structural

TABLE I

INSTRUMENTATION KEY TO THE COLD TRAP

Symbol	Service	Description	Manufacturer	Model	Input Range	Output Range
PRC-PT	Product Purification Cold Trap Pressure Control	Pressure Transmitter	Taylor	1332TF11221	10-100 psi	4-20 mA
		Indicating Controller	Taylor	1304RA10002	0.25-1.25 v	4-20 mA
		Recorder	Taylor	1322JA14123	0.25-1.25 v	0-100 div
		I/P Transducer	Moore	77-16	4-20 mA	3-15 psi
PCV-PT	Product Purification Cold Trap Control	Control Valve	Precision Products	¼ in., 0.003 C_v	3-15 psi	Mechanical
PdR-PT	Product Purification Cold Trap Pressure Drop	ΔP Tramsmitter	Taylor	1301TD11122	0-10 in. H_2O	4-20 mA
		Recorder	Taylor	1322JA14123	0.25-1.25 v	0-100 div
TE-LN	Product Purification Liquid Nitrogen Temperature Control	Thermobulb/Thermowell	Taylor	PLCL-9-3A/ 1-10RL-9	-320 to +32°F	19-100 Ω
		Resistance to Current Transmitter	Taylor	1002TA14810	19-43 Ω	4-20 mA
		Indicating Controller	Taylor	1304RA10002	0.25-1.25 v	4-20 mA
		I/P Transducer	Moore	77-16	4-20	3-15 psi
TCV-LN	Product Purification Liquid Nitrogen Control	Control Valve	Precision Products	¼ in., 0.006 C_v	3-15 psi	Mechanical
TE-PT	Product Purification Cold Trap Temperature Control	Thermobulb/Thermowell	Taylor	PLCL-9-3A/ 1-10RL-9	-320 to +32°F	19-100 Ω
		Resistance to Current Transmitter	Taylor	1002TA14810	19-43 Ω	4-20 mA
		Indicating Controller	Taylor	1304RA10002	0.25-1.25 v	4-20 mA
		I/P Transducer	Moore	77-16	4-20 mA	3-15 psi
TCV-PT	Product Purification Cold Trap Temperature Control	Control Valve	Precision Product	¼ in., 0.02 C_v	3-15 psi	Mechanical
FIR-ST	Stripper Product Flow	Thermal Mass Flowmeter Transducer	Tylan	FM-360	0-1 slm	0-5 v
		Thermal Mass Flowmeter Indicator	Tylan	RO-751	0-5 v	0-1 slm
		Recorder	Taylor	1322JA14123	0.25-1.25 v	0-100 div
FIR-PT1	Product Purification Cold Trap Off-Gas Flow	Thermal Mass Flowmeter Transducer	Tylan	FM-360	0-100 sccm	0-5 v
		Thermal Mass Flowmeter Indicator	Tylan	RO-751	0-5 v	0-100 sccm
		Recorder	Taylor	1322JA14123	0.25-1.25 v	0-100 div
FIR-PT2	Product Purification Cold Trap Off-Gas Flow	Thermal Mass Flowmeter Transducer	Tylan	FM-360	0-500 sccm	0-5 v
		Thermal Mass Flowmeter Indicator	Tylan	RO-751	0-5 v	0-500 sccm
		Recorder	Taylor	1322JA14123	0.25-1.25 v	0-100 div

damage on large sieve trap towers[16]. These experiments, however, did not use tracer isotopes inside the process as an internal system component, but instead used a source and detector on opposite sides of the equipment, and plotted a density profile of the material inside the vessel to determine liquid levels, etc. In 1975, Stephenson, et al, began using gamma scanning techniques to determine packed column concentration profiles. Absorber and fractionator column profiles obtained yielded a greater understanding of the physical phenomena occurring in gas-liquid contacting[17-20]. From the experience gained about scintillation analysis techniques for these gas-liquid contactors, it could be seen that these same techniques could provide a unique method for solids buildup determination in a cold trap.

Two single-channel and one multichannel pulse height analysis systems were used to simultaneously determine the isotopic content of the entering and exiting flow streams, as well as the point deposit thickness and buildup rate. Each counting system consists of a sodium iodide detector, a photomultiplier tube, a tube base, a scintillation preamplifier, a spectroscopy amplifier, a pulse height analyzer, a timer, and a digital counter. The multichannel analyzer (MCA) also includes a 200 MHz analog-to-digital converter, a 1024 channel analyzer, a multiple input multiplexer, a cathode ray tube display, and a thermal printer. Sixteen thousand words of memory give the MCA a great deal of versatility for analyzing the data. The MCA also provided a

common counting base to individually calibrate each single channel system prior to each test run. A schematic of the counting network is presented in Figure 7.

Process gamma counting is performed directly through the pipe wall. For the inlet and outlet counting positions, the process pipe is encased in a 1-1/2- to 2-inch thick lead shield to reduce background radiation to acceptable levels. A hole was bored in one end of each of the shields to receive the cylindrical crystal detector which is positioned directly against the process pipe. Figure 8 is a schematic of the lead shields employed. They were constructed to block out more than 95% of the background radiation levels. Appendix D presents a sample calculation for determining the required shielding thickness. In addition to the two stationary shielded counting positions, a motor driven mobile shield was installed on a track to horizontally scan the cold trap and to obtain the experimental concentration profiles.

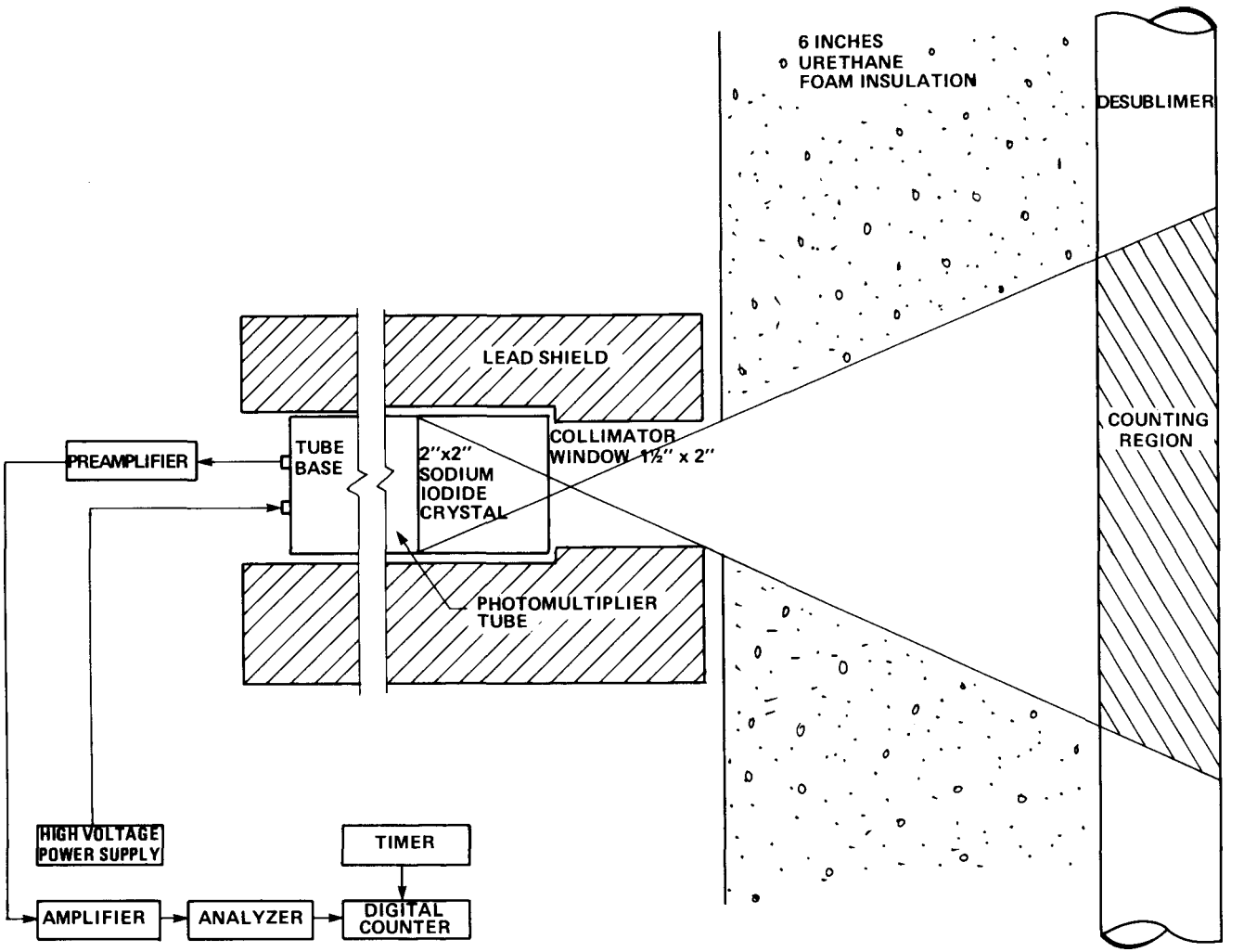

Figure 7

SCHEMATIC OF GAMMA COUNTING EQUIPMENT

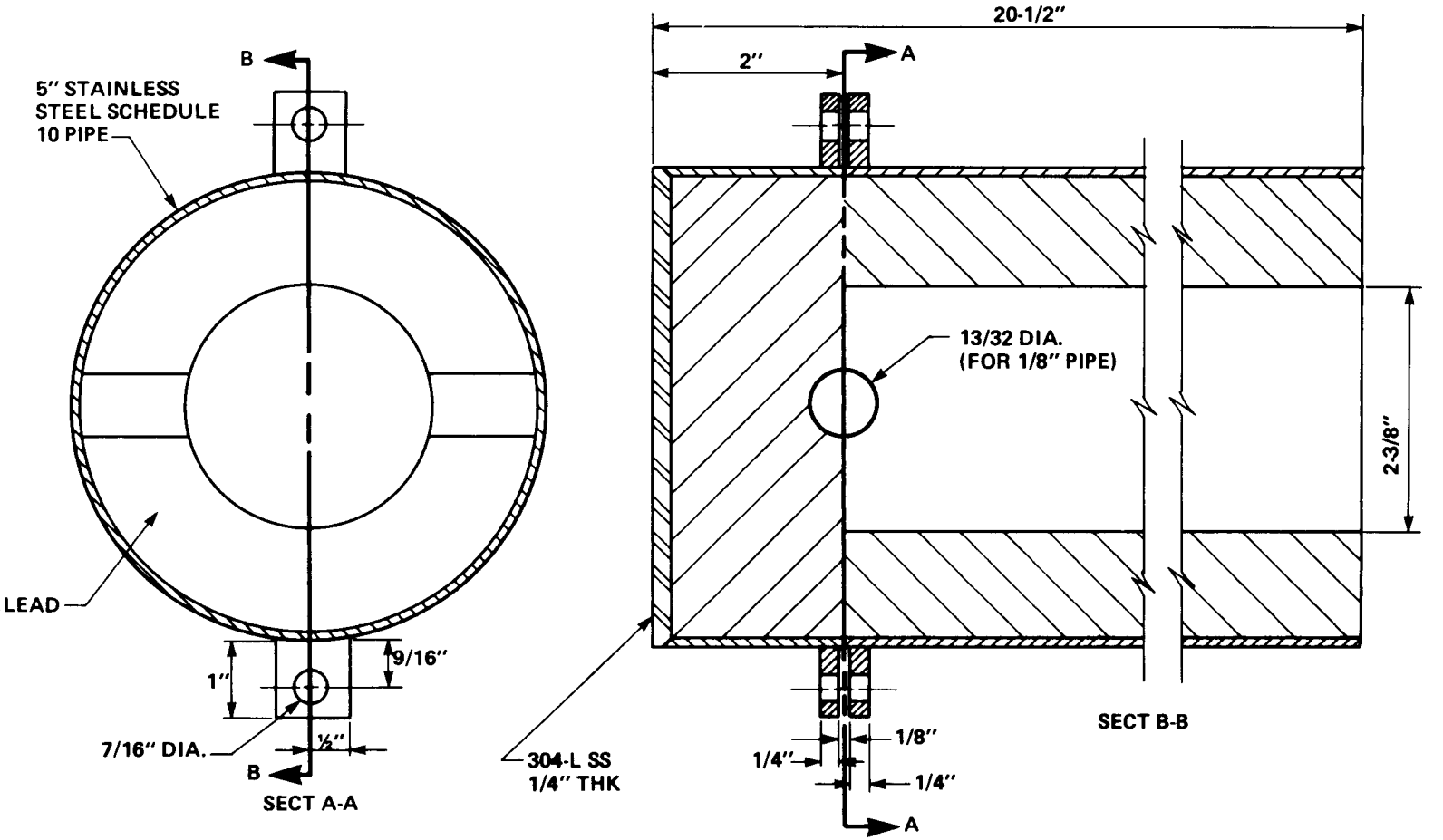

ASSEMBLY NOTES:
1. LEAD IS TO BE CAST INTO COMPLETED SHELL.
2. CUT AT PLANE A-A PRIOR TO DRILLING HOLES IN LEAD.

TOLERANCES: FRAC: ± 1/32

Figure 8
SCHEMATIC OF LEAD SHIELD

CHAPTER IV

EXPERIMENTAL PROCEDURE

The experimental procedure used in this study can be broken down into three major categories or steps: (1) pre-trapping setup; (2) cold trapping operations; and (3) post-trapping inventory analysis. Each category requires a series of specific functions.

I. PRETRAPPING SETUP

Prior to the actual cold trapping operation, the three primary steps performed were (1) preparation of the gas feed mixture, (2) preliminary cooldown of the trap, and (3) calibration of the counting equipment.

Feed Gas Preparation

The feed gas was prepared in a standard 1A (220 ft^3) nitrogen gas cylinder which had been evacuated to approximately 2 inches of mercury total pressure. One curie of tracer krypton-85 was added with a known quantitative amount of cold krypton to the cylinder. A nitrogen carrier gas was then added to dilute the krypton concentration to the desired feed concentration level. During the initial test, it was observed that this method of gas preparation did not result in a well-mixed gas. As the gas was fed from the cylinder, the krypton concentration started at a low value and steadily

rose to a value higher than the desired amount. To ensure better mixing, a heat lamp was directed toward the cylinder to promote convective currents. A steadier gas feed concentration was realized from this action.

Preliminary Cooldown Step

A time consuming step, preliminary cooldown was accomplished several hours prior to initiating the actual test run. This was to ensure that a thermal equilibrium had been reached in all process piping. Initially, a nitrogen gas flow was introduced into the trap at a rate equivalent to the desired cold trapping feed gas flow rate. The cold trap pressure controller was allowed to operate automatically, while the gas outlet temperature and liquid nitrogen pressure control valves were manually opened as were the block valves bypassing each of these two control valves. This permitted a maximum flow of liquid nitrogen through the tube side of the cold trap. As the coolant was fed from the 5.6 ft^3 cylinder, the coolant cylinder pressure had a tendency to drop. A blanket of gaseous nitrogen was introduced through a regulator on top of the liquid nitrogen to maintain a constant coolant feed pressure.

As the trap was cooled down, the shell side gas outlet temperature was monitored by means of a platinum resistance thermobulb and a resistance-to-current transmitter. This transmitter then sent a signal to a recorder for visual observation. As the trap temperature approached the set

point condition, the two manual valves were slowly closed, and the liquid nitrogen control valve automatically operated. The gas outlet temperature control valve was left on manual and slowly closed until the final temperature was reached. The operator manually adjusted the opening of this valve to give the desired gas outlet temperature. Should the temperature need to be lowered, the valve was opened to allow more coolant to pass, resulting in a temperature reduction. Similarly, should the temperature be too cold, the operator simply closed the valve, reducing the coolant flow, and hence warmed up the trap. The trap was allowed to run at a constant temperature for a minimum of 7 hours to achieve thermal equilibrium. As the liquid nitrogen was depleted in a feed cylinder, a new cylinder was valved in line. This momentarily disrupted the system; however, the trap temperature variation was usually less than ± 5°F during a cylinder change. New cylinders were placed on-stream just prior to feeding the prepared gas mixture, allowing most of the tests to be completed without changing coolant cylinders.

Calibration of Radioisotope Tracer Counting Systems

Prior to each test run, all three counting systems were calibrated to a common base using the multichannel analyzer. A krypton spectrum, similar to the one seen in Figure 9, was obtained using each counting system and displayed on the multichannel cathode ray tube screen. Each of the individual amplifiers was adjusted to force the primary

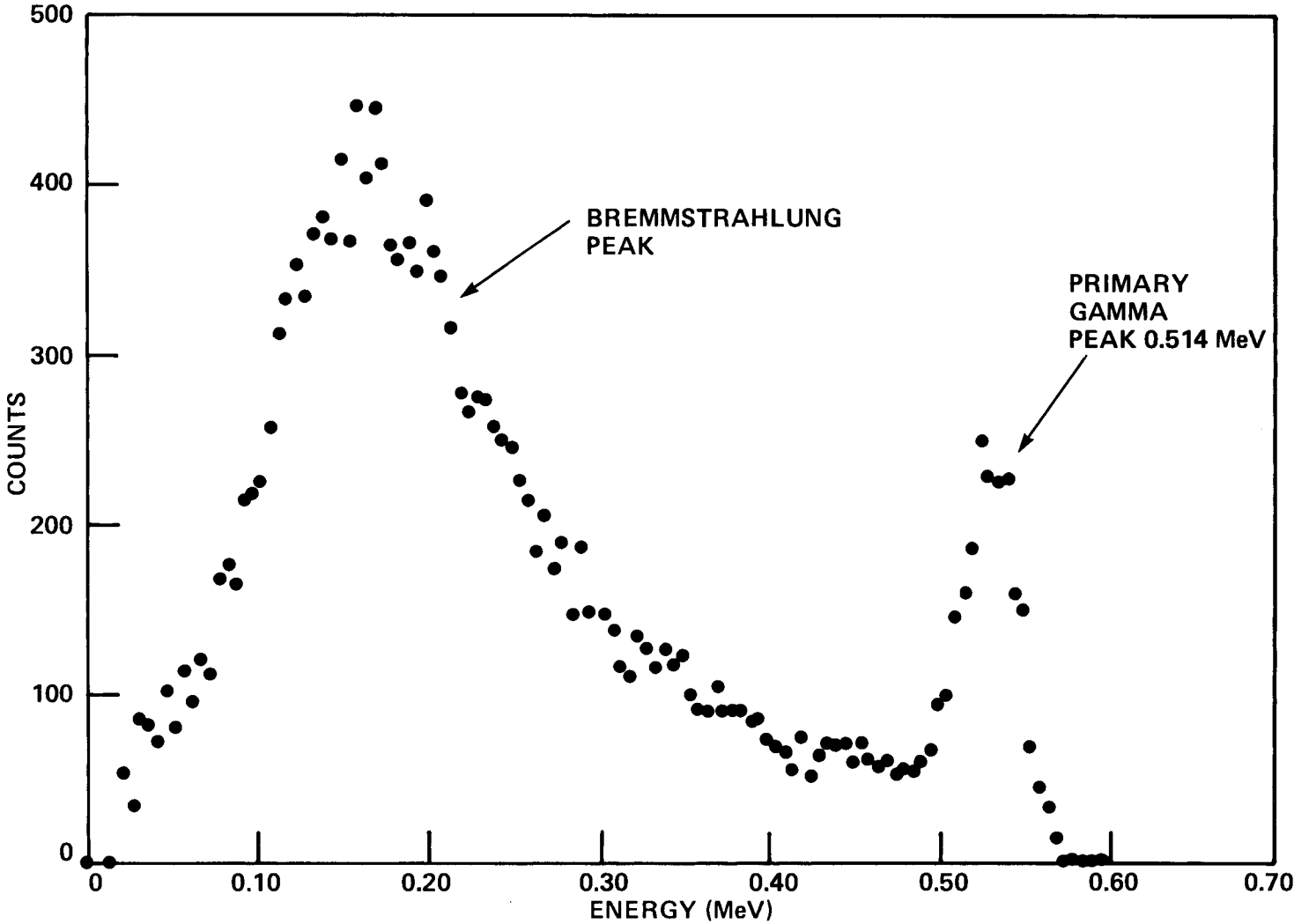

Figure 9
KRYPTON-85 ENERGY SPECTRUM

gamma peak to fall at channel number 514 on the screen, since the gamma energy level of krypton is 0.514 MeV. During operations, only the primary peak was counted, while the Bremmstrahlung or breaking radiation peak due to the energy release of the destroyed beta particles was excluded. With all amplifiers set, the calibration scheme was only a matter of adjusting the analyzer "windows" to produce an identical number of counts in each of the three systems for a given source. The counting systems were considered calibrated when all three individual systems were counting with one-half of one percent of each other.

Before the tracer krypton was fed into the cold trap, a preliminary scan of the desublimer was taken, as well as counts of the trap inlet and outlet flow streams. This provided a background count for later comparison to the actual running conditions.

II. COLD TRAPPING OPERATIONS

Following the pretrapping setup, the prepared feed gas was ready to be fed into the cold trap. The nitrogen purge gas flow was valved out, and subsequently, the mixed gas feed was valved into the trap. The sodium iodide scintillation detectors to monitor the krypton distribution were placed on the trap inlet, outlet, and at a position on the pipe wall 2 inches downstream of the trap inlet. The inlet trap concentration was monitored both by gamma spectroscopy and gas chromatography to assure that a constant

feed composition was being maintained. The outlet stream was monitored to arrive at an overall cold trap removal efficiency, while the position 2 inches from the trap inlet was recorded to produce a point deposit buildup versus time relationship. The gas was allowed to feed until either the feed gas mixture ran out or until a preset experimental run time had elapsed.

Operation of the cold trap during each test was similar to the preliminary cooldown step. The operator manually adjusted the gas outlet temperature control valve to maintain a constant trap temperature. Gas flow rates were also monitored to ensure that a steady flow rate was being maintained, while the cold trap pressure drop was observed to indicate if plugging was occurring in the pipe.

III. POSTTRAPPING INVENTORY ANALYSIS

After the feed gas mixture had been shut off and prior to any warming of the cold trap, a concentration profile scan was taken along the length of the horizontal column. This scan was taken at 2-inch intervals over the entire length. These scans were then corrected for position counting efficiencies, plotted, and compared to the theoretical model output. Following the gamma scan, the trap was warmed, and the krypton was collected as it sublimed back into a gaseous state.

CHAPTER V

RESULTS AND DISCUSSION OF RESULTS

Presented in this chapter are the experimental testing conditions and the subsequent test results. Also included in this chapter is a comparison of the experimental results with those predicted from the theoretical model.

I. RESULTS

Experimental Runs

The majority of the experimental effort was focused on determining the effect that gas flow rate has on the krypton deposit buildup profiles. Scoping tests were also conducted to indicate what other parametric dependencies, such as coolant temperature, cold trap pressure, and krypton concentration, the cold trapping phenomenon has.

Eight experimental runs were performed in the testing facility. Gas flow rates were varied from 0.035 to 1.06 scfm, while coolant temperature, cold trap pressure, and krypton concentration were held at the nominal values of -311°F, 2 atmospheres, and 6.3 mole percent, respectively. The test duration ranged from a minimum of 62 minutes to a maximum of 697 minutes. The scoping tests included one run with a krypton concentration of 13.5%, and the system pressure was lowered to 1.3 atmospheres for another experiment. Finally, the liquid nitrogen coolant temperature was raised

30°F to -281°F for still another test. Table II presents a listing of the parameters and the values used in each of the eight experimental runs.

Following each test, the trap was scanned to obtain the krypton deposit buildup profile along its length. An example of the raw data taken is given in Table III. After the raw counts were corrected for background and count position, the ratio of net counts at position Z to the net counts at the inlet was plotted for each test. The resulting plots are seen in Figures 10 through 17. Also included in these figures are the profiles generated by the computer model. The two curves, one theoretical and one experimental, seen in Figure 18, represent the ratio:deposit thickness to maximum deposit thickness as the ordinate, and the ratio:time to time at 99% complete deposition as the abscissa. These two curves are similar to the one seen in Figure 2, page 41 , and discussed in Chapter II.

Computer Simulation Runs

Prior to obtaining the profiles as predicted from the theoretical model and illustrated in Figures 10 through 17, several system variables simulating each experimental run had to be specified. The parameters required to run the program and simulate the test are stated in Table IV.

Some of these parameters, such as molecular weights and trap type, would not change from run to run; while as is seen in Table II, other parameters, such as flow rate,

TABLE II

OPERATING PARAMETERS USED IN THE EIGHT EXPERIMENTAL RUNS

Run Number	Inlet Gas Krypton (mole %)	Inlet Gas Temperature (°F)	Total Gas Flow Rate (scfm)	Cold Trap Pressure (atm)	Coolant Temperature (°F)	Run Time (min)
11/10/77	5.2	79.6	0.140	2.008	-310	179
11/15/77	6.2	84.5	0.035	2.022	-311	697
11/22/77	7.4	75.0	0.140	2.009	-281	163
12/1/77	7.4	75.0	0.140	2.001	-309	164
12/15/77	13.5	77.9	0.088	2.010	-311	251
1/5/78	7.0	84.3	0.710	2.034	-312	89
1/12/78	6.7	83.3	1.06	2.025	-312	62
1/19/78	6.9	78.8	0.140	1.311	-312	180

TABLE III

SAMPLE OF RAW DATA TAKEN FROM
RUN 1/12/78

Position (Inches from Inlet)	Counts/Min (Uncorrected)	Position (Inches from Inlet)	Counts/Min (Uncorrected)
0.0	48,400	6.4	42,754
0.2	87,719	6.6	35,750
0.4	103,105	6.8	22,494
0.6	110,000	7.0	19,146
0.8	110,578	7.2	20,620
1.0	116,795	7.4	32,056
1.2	127,883	7.6	41,124
1.4	133,385	7.8	32,502
1.6	137,908	8.0	24,241
1.8	144,356	8.2	26,559
2.0	153,196	8.4	23,289
2.2	161,469	8.6	19,886
2.4	167,925	8.8	24,262
2.6	165,290	9.0	22,266
2.8	168,172	9.2	16,202
3.0	168,957	9.4	16,867
3.2	164,486	9.6	18,132
3.4	162,674	9.8	13,196
3.6	161,509	10.0	11,073
3.8	153,698	10.2	10,865
4.0	147,808	10.4	13,131
4.2	141,600	10.6	19,564
4.4	129,085	10.8	15,353
4.6	129,076	11.0	8,877
4.8	124,650	11.2	8,825
5.0	103,454	11.4	6,425
5.2	84,471	11.6	4,090
5.4	72,755	11.8	2,077
5.6	66,427	12.0	1,707
5.8	60,948	12.15	1,311
6.0	64,431	0.1	71,802
6.2	54,700		

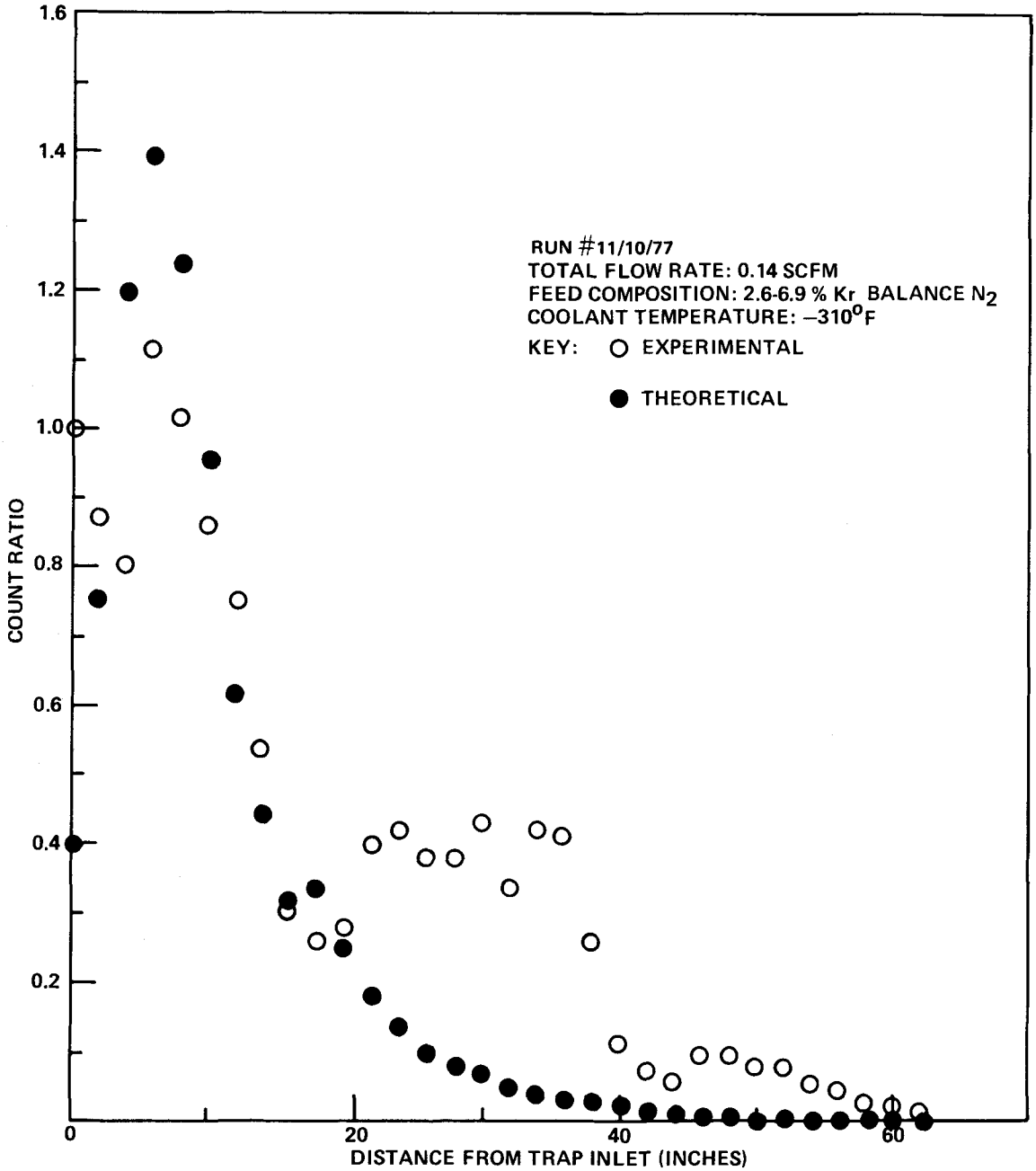

Figure 10

COMPARISON OF EXPERIMENTAL AND THEORETICAL PROFILES
FOR RUN 11/10/77

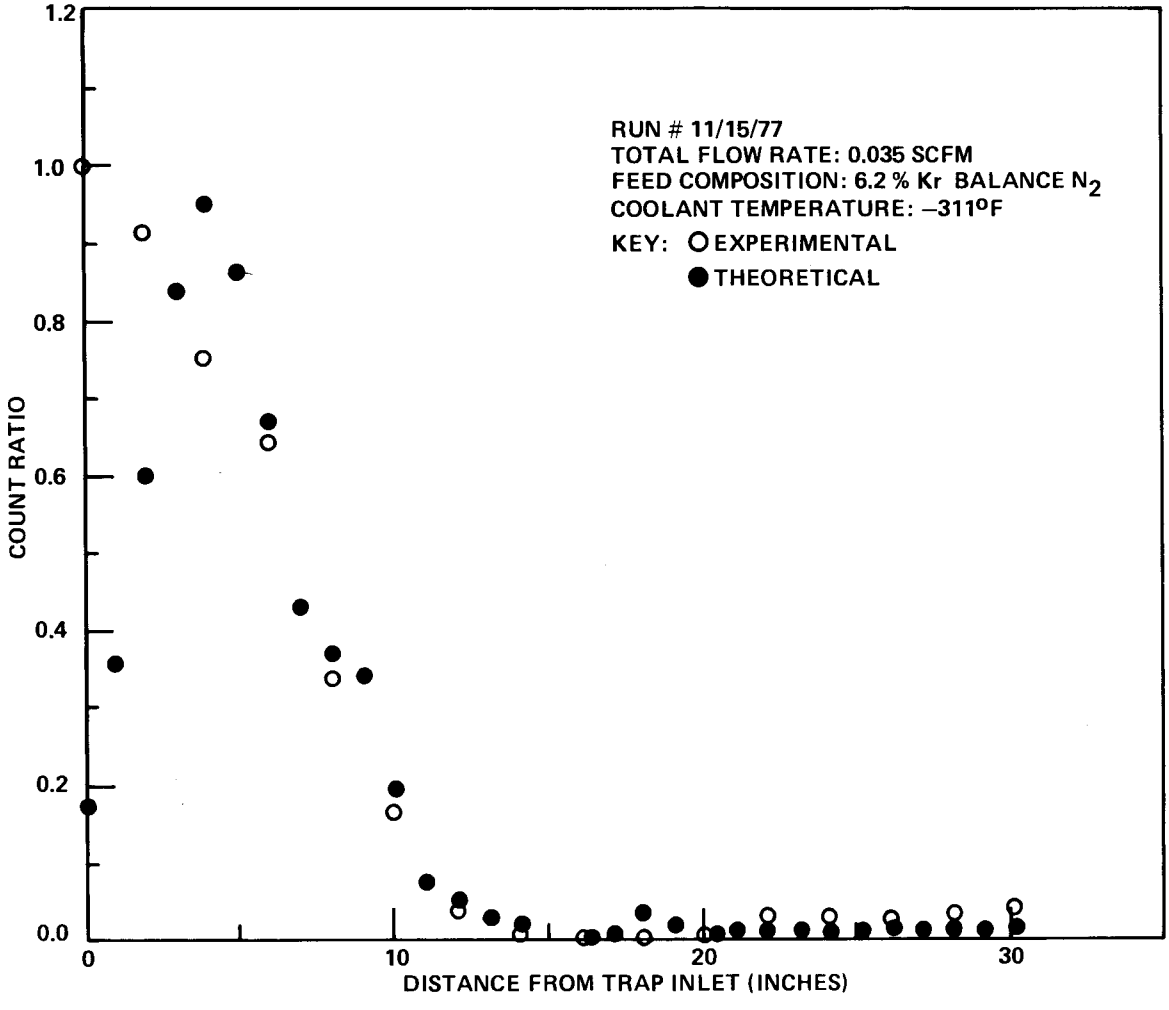

Figure 11

COMPARISON OF EXPERIMENTAL AND THEORETICAL PROFILES
FOR RUN 11/15/77

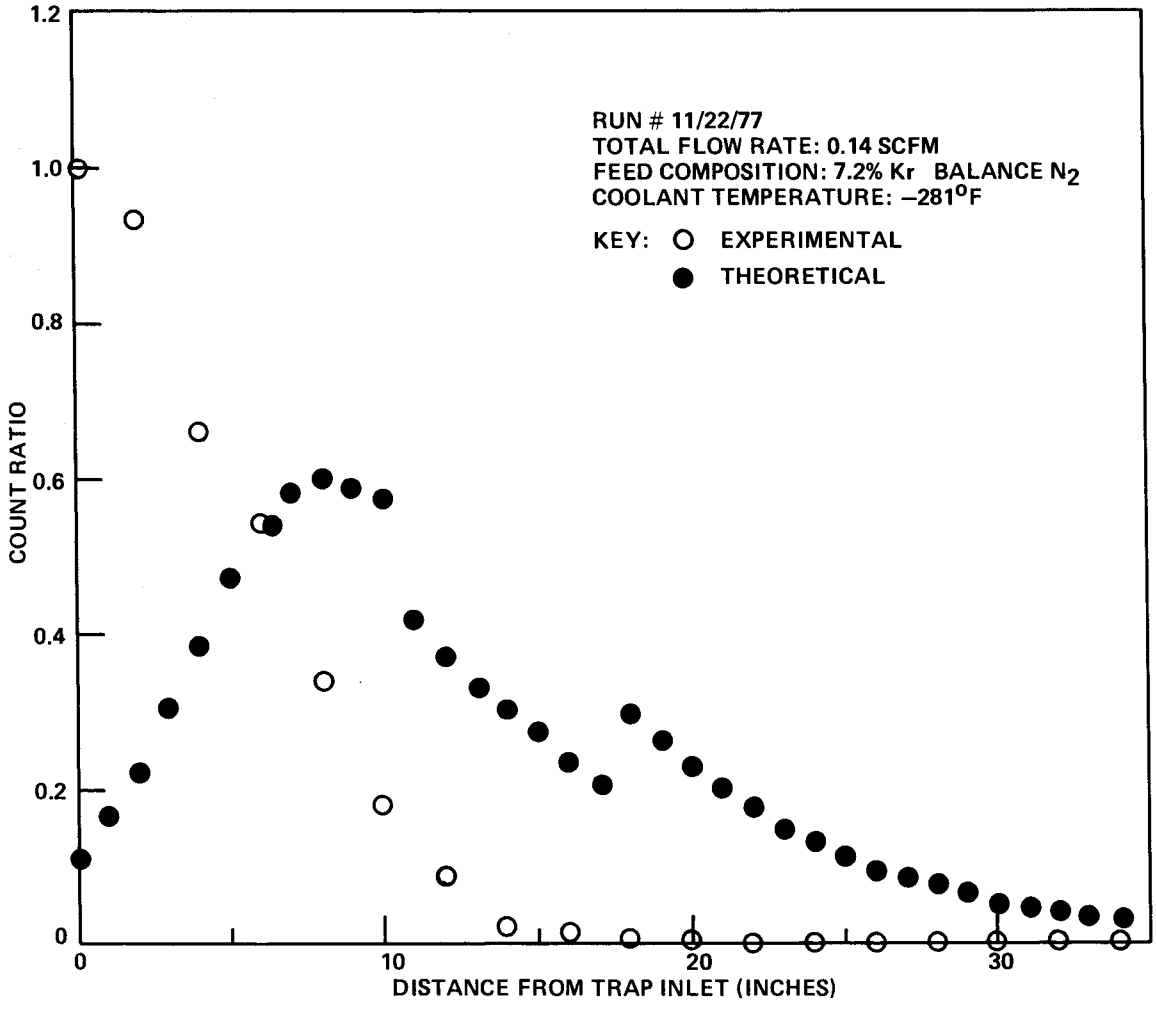

Figure 12

COMPARISON OF EXPERIMENTAL AND THEORETICAL PROFILES
FOR RUN 11/22/77

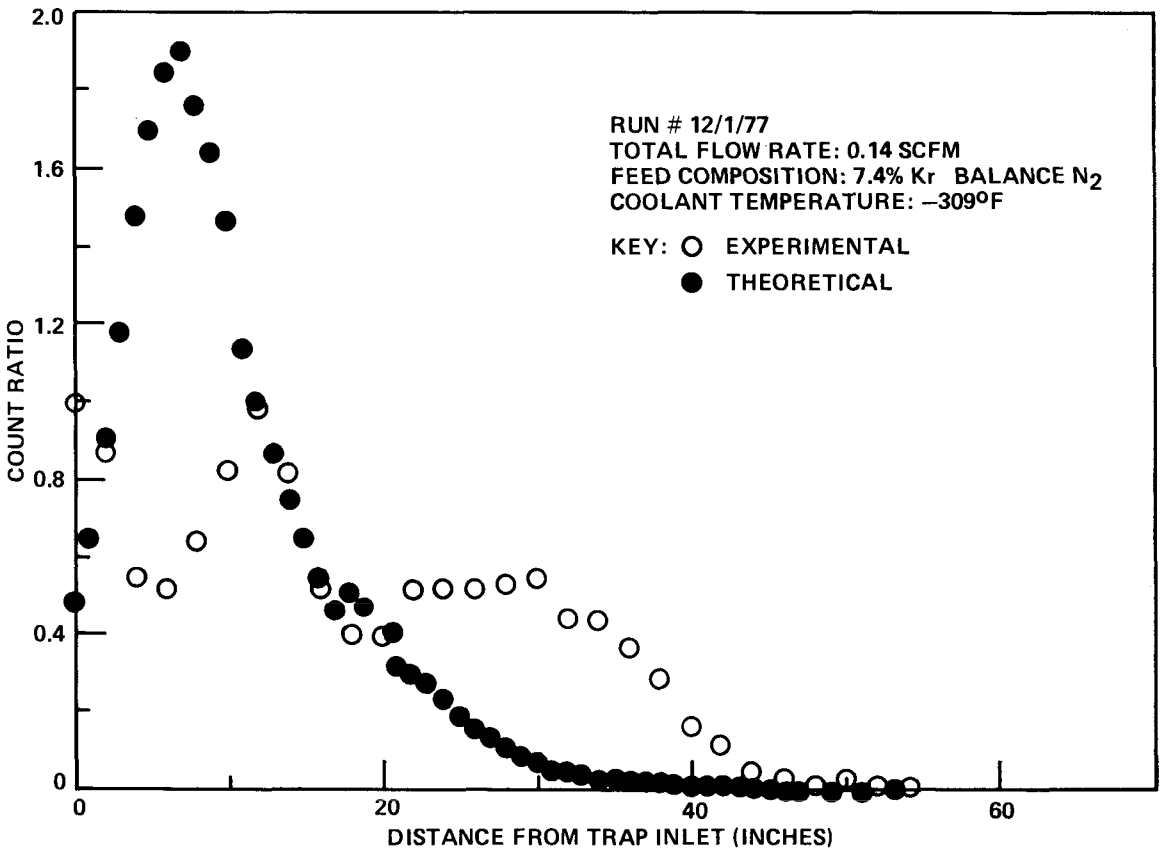

Figure 13

COMPARISON OF EXPERIMENTAL AND THEORETICAL PROFILES
FOR RUN 12/1/77

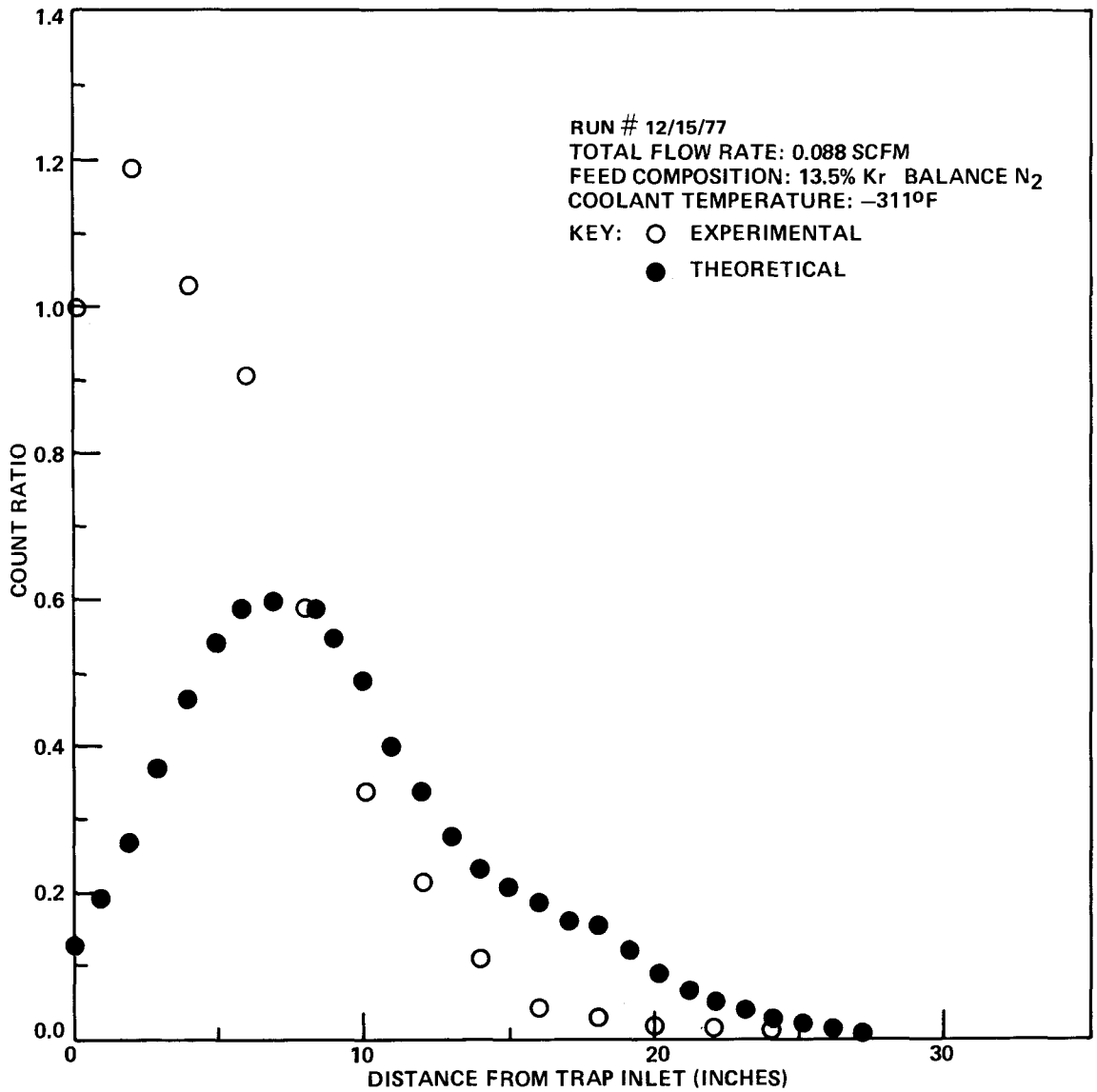

Figure 14

COMPARISON OF EXPERIMENTAL AND THEORETICAL PROFILES
FOR RUN 12/15/77

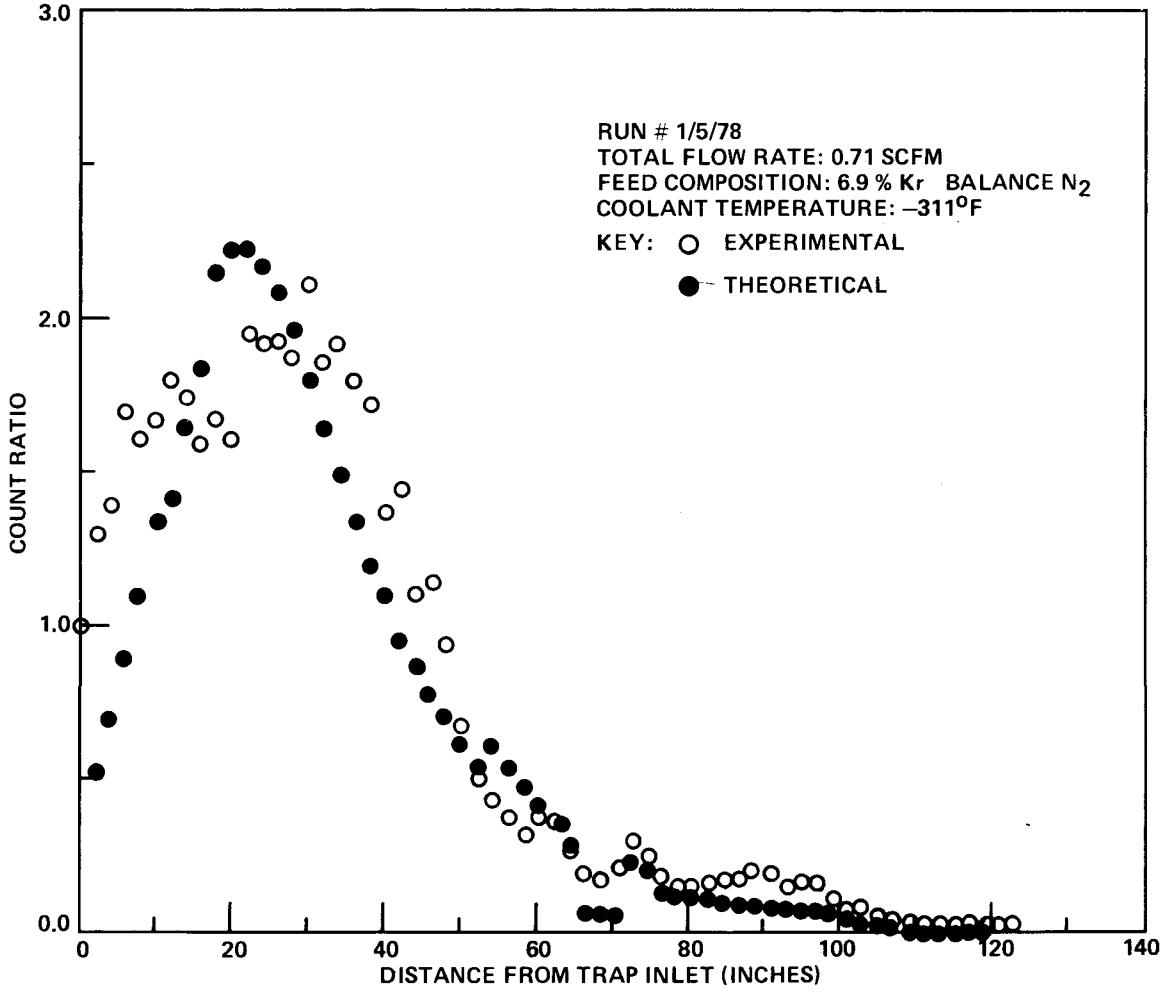

Figure 15

COMPARISON OF EXPERIMENTAL AND THEORETICAL PROFILES
FOR RUN 1/5/78

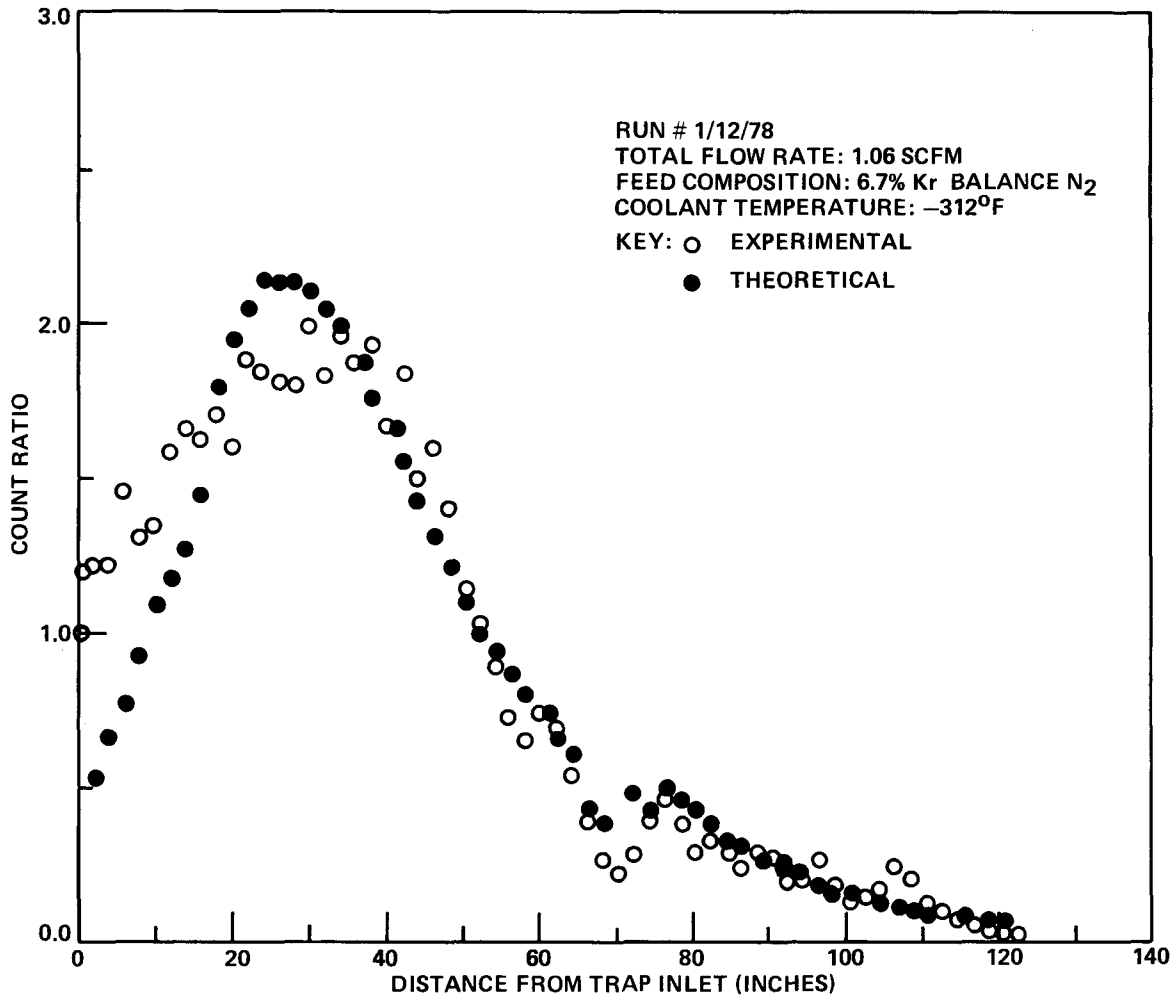

Figure 16

COMPARISON OF EXPERIMENTAL AND THEORETICAL PROFILES
FOR RUN 1/12/78

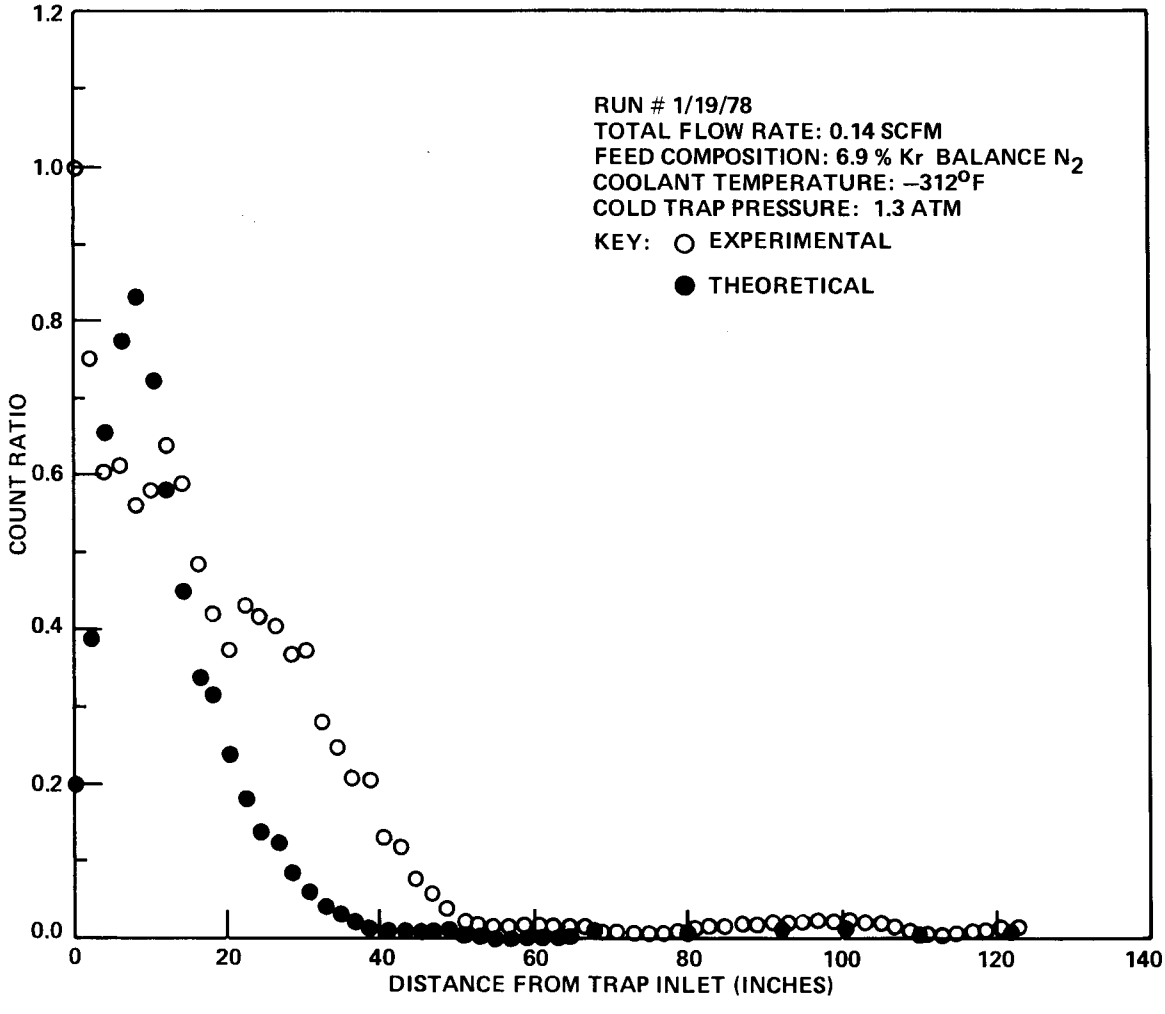

Figure 17

COMPARISON OF EXPERIMENTAL AND THEORETICAL PROFILES
FOR RUN 1/19/78

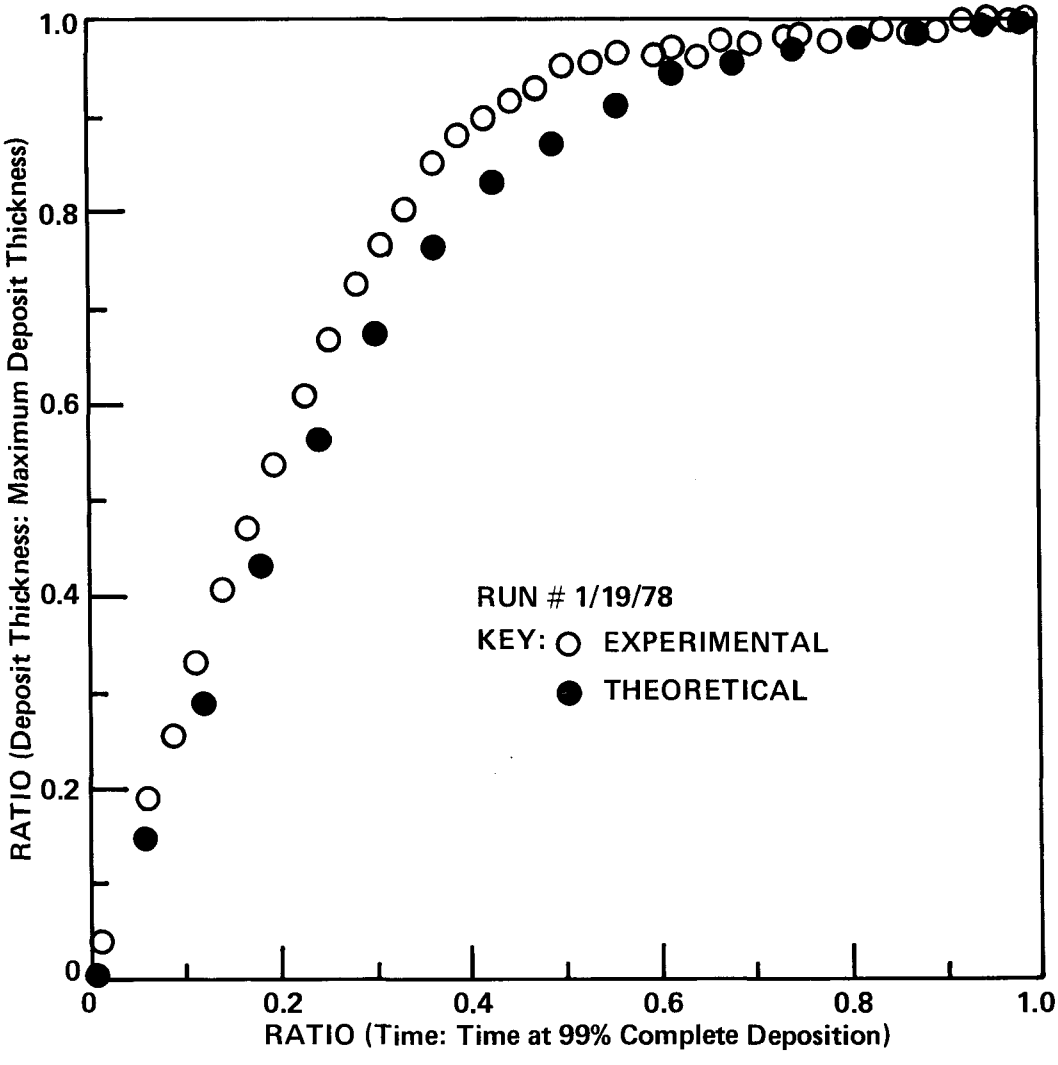

Figure 18

COMPARISON OF EXPERIMENTAL AND THEORETICAL
DEPOSIT THICKNESS RELATIONSHIP WITH TIME

TABLE IV

REQUIRED PARAMETERS TO SIMULATE TEST RUNS WITH COMPUTER PROGRAM

1.	Trap type and dimensions
2.	Flow rate of the gas stream
3.	Percentage of krypton in the gas stream
4.	Temperature of the gas stream
5.	Pressure of the gas stream
6.	Trapping time
7.	Molecular weight of the condensable gas (krypton)
8.	Molecular weight of the noncondensable gas (nitrogen)
9.	Frost density of the as-trapped solid
10.	Thermal conductivity of the as-trapped solid
11.	Temperature of the liquid nitrogen coolant
12.	Increase in temperature from heat inleakage due to trap supports

temperature, krypton concentration, and cold trap pressure, did change.

Simulation of the physical trap for the computer model was done by assuming the trap consisted of sixteen equal rectangles bounded by the finned tube, inner shell wall, and the extended longitudinal fins. The length of the flow channel was taken to be 6 inches, the length between cut and twist portions of the finned tube. Figure 19 is an illustration of the trap model configuration, as well as the dimensions of each rectangular flow channel used in the program.

A value for the frost density was patterned after known values for frost densities of other materials. For example, the generally accepted meteorological statement that one inch of rain equals about 10 inches of snow implies that the frost density-to-liquid density ratio for snow-to-water is 0.1. Similarly, Dunthorn reported a frost-to-liquid density ratio of uranium hexafluoride to be 0.69[3]. Since the cold trap was operated near the melting temperature of krypton, the solid product should be comparable to a "wet or heavy" snow. In other words, the frost-to-liquid density ratio for krypton should be closer to 1.0 than for snow and probably comparable to the value for uranium hexafluoride. A value of 68.0 lb/ft^3 was chosen to be used in the program. This corresponds to a frost-to-liquid density ratio of approximately 0.5 as the liquid density of krypton reported in the available literature is 134.4 lb/ft^3[21].

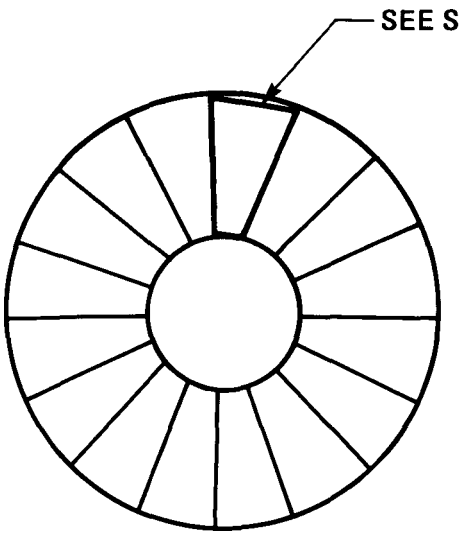

TOTAL NUMBER OF FLOW CHANNELS = 16

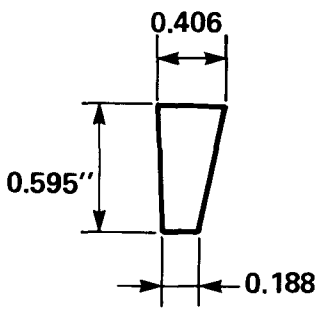

DIMENSION OF FLOW CHANNEL
HEIGHT = 0.595"
WIDTH = 1/2 (0.188 + 0.406) = 0.297"
LENGTH = 6"
FLOW AREA/CHANNEL = 0.177 in^2

Figure 19

COLD TRAP MODEL CONFIGURATION USED IN COMPUTER PROGRAM

A nominal value of 0.01 Btu/hr-ft-°F was chosen initially for the thermal conductivity of the frost deposit. This value was changed, however, to obtain the best match between the theoretical model and the experimental data. The best overall frost thermal conductivity value was found to be 0.0013 Btu/hr-ft-°F. Temperature correction factors to account for heat inleakage due to trap supports were experimentally found through internal thermocouples to be about 10°; however, a 4 to 5-degree temperature rise in the model gives a better match to the experimental deposit profile data.

Following a good definition of all the program parameters, the computer program was run to simulate each experimental test. Table V is a sample output from the program. Specifically, this output represents a simulation of the experimental Run 1/5/78. At the top of the page is given the run identification code, the time step being printed, and the length of real operating time at that time step. Also printed is the amount of trapped solids, calculated by the two methods discussed in Chapter II. Under the column headings, DISTANCE refers to the distance of the point from the trap inlet, and DEPOSIT THICKNESS describes the height of the solid buildup on the trap wall. CLEARANCE refers to the linear clearance remaining for flow in the trap and MOLE FRACTION represents the mole fraction of the krypton in the gas stream. TEMPERATURE and SURFACE TEMPERATURE stand for the bulk gas temperature and the temperature of the solid

TABLE V

SAMPLE OUTPUT FROM COMPUTER PROGRAM

DESUBLIMATION OF KRYPTON RUN 1/5/78 PAGE 1

TIMESTEP NO. 121

TIME 1.004300 HR. TIMESTEP 0.008300 HR.

HOLDUP, SOLID BASIS 0.59246 LB.

HOLDUP, GAS BASIS 0.57271 LB.

DISTANCE IN.	DEPOSITION THICKNESS IN.	CLEARANCE IN.	MOL FRACTION	TEMPERATURE DEG F	SURFACE TEMPERATURE DEG F	MIST FRACTION,	DIVISIONS	RATIO
0.0	0.41503D-02	0.28870D 00	0.069600	45.00	-275.78	0.0	16	1.00000
1.0000	0.48112D-02	0.28738D 00	0.069600	11.47	-275.78	0.0	16	1.15925
2.0000	0.55335D-02	0.28593D 00	0.069600	-17.48	-275.78	0.0	16	1.33330
3.0000	0.63197D-02	0.28436D 00	0.069600	-42.66	-275.78	0.0	16	1.52273
4.0000	0.71720D-02	0.28266D 00	0.069600	-64.68	-275.78	0.0	16	1.72809
5.0000	0.80913D-02	0.28082D 00	0.069599	-84.07	-275.79	0.0	16	1.94960
6.0000	0.90748D-02	0.27885D 00	0.069597	-101.21	-275.81	0.0	16	2.18657
7.0000	0.10112D-01	0.27678D 00	0.069586	-116.45	-275.86	0.0	16	2.43648
8.0000	0.11182D-01	0.27464D 00	0.069556	-130.05	-275.98	0.0	16	2.69416
9.0000	0.12251D-01	0.27250D 00	0.069486	-142.23	-276.18	0.0	16	2.95189
10.0000	0.13281D-01	0.27044D 00	0.069351	-153.20	-276.51	0.0	16	3.20001
11.0000	0.12770D-01	0.27146D 00	0.069117	-163.11	-276.80	0.0	16	3.07692
12.0000	0.13563D-01	0.26987D 00	0.068809	-172.10	-277.32	0.0	16	3.26602
13.0000	0.14235D-01	0.26853D 00	0.068366	-180.28	-277.96	0.0	16	3.42993
14.0000	0.14767D-01	0.26746D 00	0.067770	-187.77	-278.73	0.0	16	3.55821
15.0000	0.15150D-01	0.26670D 00	0.067009	-194.64	-279.62	0.0	16	3.65049
16.0000	0.15382D-01	0.26624D 00	0.066078	-200.98	-280.62	0.0	16	3.70633
17.0000	0.15468D-01	0.26606D 00	0.064978	-206.85	-281.72	0.0	16	3.72693
18.0000	0.16947D-01	0.26311D 00	0.063716	-212.30	-283.65	0.0	16	4.08325
19.0000	0.16689D-01	0.26362D 00	0.062159	-217.43	-285.09	0.0	16	4.02116
20.0000	0.16313D-01	0.26437D 00	0.060459	-222.25	-286.60	0.0	16	3.93069
21.0000	0.15841D-01	0.26532D 00	0.058638	-226.79	-288.17	0.0	16	3.81698
22.0000	0.15294D-01	0.26641D 00	0.056722	-231.08	-289.76	0.0	16	3.68516
23.0000	0.14692D-01	0.26762D 00	0.054735	-235.15	-291.35	0.0	16	3.54008
24.0000	0.14054D-01	0.26889D 00	0.052704	-239.02	-292.93	0.0	16	3.38618
25.0000	0.13394D-01	0.27021D 00	0.050651	-242.70	-294.46	0.0	16	3.22732
26.0000	0.12728D-01	0.27154D 00	0.048599	-246.21	-295.93	0.0	16	3.06673
27.0000	0.12065D-01	0.27287D 00	0.046565	-249.56	-297.33	0.0	16	2.90702
28.0000	0.11414D-01	0.27417D 00	0.044566	-252.76	-298.65	0.0	16	2.75022
29.0000	0.10782D-01	0.27544D 00	0.042613	-255.81	-299.87	0.0	16	2.59783
30.0000	0.10172D-01	0.27666D 00	0.040717	-258.72	-301.00	0.0	16	2.45093
31.0000	0.95879D-02	0.27782D 00	0.038884	-261.50	-302.04	0.0	16	2.31020
32.0000	0.90313D-02	0.27894D 00	0.037120	-264.15	-302.98	0.0	16	2.17607
33.0000	0.85028D-02	0.27999D 00	0.035426	-266.68	-303.84	0.0	16	2.04874
34.0000	0.80027D-02	0.28099D 00	0.033805	-269.08	-304.61	0.0	16	1.92823
35.0000	0.75304D-02	0.28194D 00	0.032257	-271.37	-305.30	0.0	16	1.81445
36.0000	0.70854D-02	0.28283D 00	0.030781	-273.54	-305.93	0.0	16	1.70722
37.0000	0.66656D-02	0.28367D 00	0.029377	-275.60	-306.49	0.0	16	1.60631
38.0000	0.62728D-02	0.28445D 00	0.028042	-277.56	-306.99	0.0	16	1.51144
39.0000	0.59029D-02	0.28519D 00	0.026774	-279.42	-307.43	0.0	16	1.42231
40.0000	0.55556D-02	0.28589D 00	0.025571	-281.18	-307.83	0.0	16	1.33862
41.0000	0.52296D-02	0.28654D 00	0.024430	-282.85	-308.18	0.0	16	1.26007
42.0000	0.49237D-02	0.28715D 00	0.023348	-284.43	-308.50	0.0	16	1.18636
43.0000	0.46365D-02	0.28773D 00	0.022324	-285.93	-308.78	0.0	16	1.11718
44.0000	0.43672D-02	0.28827D 00	0.021354	-287.34	-309.02	0.0	16	1.05227

TABLE V (Continued)

DESUBLIMATION OF KRYPTON RUN 1/5/78 PAGE 2

TIMESTEP NO. 121

DISTANCE IN.	DEPOSITION THICKNESS IN.	CLEARANCE IN.	MOL FRACTION	TEMPERATURE DEG F	SURFACE TEMPERATURE DEG F	MIST FRACTION.	DIVISIONS	RATIO
45.0000	0.41143D-02	0.28877D 00	0.020436	-288.68	-309.24	0.0	16	0.99135
46.0000	0.38770D-02	0.28925D 00	0.019567	-289.95	-309.44	0.0	16	0.93416
47.0000	0.36542D-02	0.28969D 00	0.018744	-291.15	-309.61	0.0	16	0.88047
48.0000	0.34450D-02	0.29011D 00	0.017966	-292.28	-309.77	0.0	16	0.83006
49.0000	0.32484D-02	0.29050D 00	0.017229	-293.34	-309.90	0.0	16	0.78270
50.0000	0.30637D-02	0.29087D 00	0.016533	-294.35	-310.02	0.0	16	0.73821
51.0000	0.28902D-02	0.29122D 00	0.015873	-295.30	-310.13	0.0	16	0.69639
52.0000	0.27270D-02	0.29155D 00	0.015250	-296.20	-310.23	0.0	16	0.65708
52.9999	0.25736D-02	0.29185D 00	0.014660	-297.05	-310.31	0.0	16	0.62011
53.9999	0.27856D-02	0.29143D 00	0.013919	-297.76	-310.30	0.2873	16	0.67120
54.9999	0.27292D-02	0.29154D 00	0.013206	-298.41	-310.36	0.2825	16	0.65760
55.9999	0.25933D-02	0.29181D 00	0.012549	-299.02	-310.42	0.2782	16	0.62485
56.9999	0.24373D-02	0.29213D 00	0.011945	-299.61	-310.49	0.2739	16	0.58727
57.9999	0.22817D-02	0.29244D 00	0.011387	-300.17	-310.55	0.2695	16	0.54977
58.9999	0.21334D-02	0.29273D 00	0.010873	-300.71	-310.60	0.2649	16	0.51405
59.9999	0.19863D-02	0.29303D 00	0.010399	-301.22	-310.65	0.2601	16	0.47859
60.9999	0.18490D-02	0.29330D 00	0.009961	-301.72	-310.69	0.2552	16	0.44552
61.9999	0.17186D-02	0.29356D 00	0.009556	-302.19	-310.73	0.2502	16	0.41409
62.9999	0.15977D-02	0.29380D 00	0.009183	-302.64	-310.76	0.2450	16	0.38496
63.9999	0.14857D-02	0.29403D 00	0.008838	-303.07	-310.79	0.2398	16	0.35797
64.9999	0.23374D-03	0.29653D 00	0.008519	-303.48	-305.99	0.1243	16	0.05632
65.9999	0.21949D-03	0.29656D 00	0.008412	-303.62	-305.99	0.1224	16	0.05289
66.9999	0.20594D-03	0.29659D 00	0.008312	-303.75	-305.99	0.1201	16	0.04962
67.9999	0.19320D-03	0.29661D 00	0.008219	-303.88	-305.99	0.1177	16	0.04655
68.9999	0.18126D-03	0.29664D 00	0.008131	-304.00	-305.99	0.1153	16	0.04367
69.9999	0.17009D-03	0.29666D 00	0.008049	-304.11	-305.99	0.1129	16	0.04098
70.9999	0.15964D-03	0.29668D 00	0.007972	-304.22	-305.99	0.1107	16	0.03847
71.9999	0.12785D-02	0.29444D 00	0.007900	-304.32	-310.85	0.2231	16	0.30806
72.9999	0.11907D-02	0.29462D 00	0.007651	-304.67	-310.87	0.2177	16	0.28691
73.9999	0.11082D-02	0.29478D 00	0.007421	-305.01	-310.89	0.2124	16	0.26702
74.9999	0.10319D-02	0.29494D 00	0.007207	-305.33	-310.90	0.2072	16	0.24864
75.9999	0.96246D-03	0.29507D 00	0.007009	-305.64	-310.91	0.2021	16	0.23190
76.9999	0.89704D-03	0.29521D 00	0.006825	-305.92	-310.92	0.1971	16	0.21614
77.9999	0.83648D-03	0.29533D 00	0.006654	-306.20	-310.93	0.1923	16	0.20155
78.9999	0.78038D-03	0.29544D 00	0.006496	-306.46	-310.94	0.1875	16	0.18803
79.9999	0.72767D-03	0.29554D 00	0.006348	-306.71	-310.95	0.1828	16	0.17533
80.9999	0.67952D-03	0.29564D 00	0.006211	-306.94	-310.95	0.1783	16	0.16373
81.9999	0.63483D-03	0.29573D 00	0.006083	-307.16	-310.96	0.1739	16	0.15296
82.9999	0.59334D-03	0.29581D 00	0.005964	-307.37	-310.96	0.1696	16	0.14297
83.9999	0.55433D-03	0.29589D 00	0.005853	-307.57	-310.97	0.1655	16	0.13357
84.9999	0.51855D-03	0.29596D 00	0.005750	-307.76	-310.97	0.1615	16	0.12494
85.9999	0.48528D-03	0.29603D 00	0.005653	-307.94	-310.98	0.1576	16	0.11693
86.9999	0.45395D-03	0.29609D 00	0.005563	-308.11	-310.98	0.1539	16	0.10938
87.9999	0.42515D-03	0.29615D 00	0.005479	-308.27	-310.98	0.1503	16	0.10244
88.9999	0.39802D-03	0.29620D 00	0.005400	-308.42	-310.98	0.1468	16	0.09590
89.9999	0.37303D-03	0.29625D 00	0.005327	-308.57	-310.98	0.1435	16	0.08988
90.9999	0.34948D-03	0.29630D 00	0.005258	-308.70	-310.99	0.1403	16	0.08421
91.9999	0.32775D-03	0.29634D 00	0.005194	-308.83	-310.99	0.1372	16	0.07897
92.9999	0.30726D-03	0.29639D 00	0.005134	-308.95	-310.99	0.1343	16	0.07403
93.9999	0.28834D-03	0.29642D 00	0.005078	-309.07	-310.99	0.1315	16	0.06948
94.9999	0.27048D-03	0.29646D 00	0.005025	-309.17	-310.99	0.1288	16	0.06517

deposit surface at the solids-gas interface, respectively. MIST FRACTION is that fraction of solid removed from the gas stream that condenses out of the gas stream directly rather than on the trap walls. Naturally, this fraction is zero in the superheated region of the trap. The number of parallel groups being analyzed is stated under the column headed DIVISIONS, and the RATIO column represents the ratio of solids buildup at a distance, Z, to the buildup at the distance 0.0, or inlet position.

By changing the base position from the inlet to determine the ratio, the theoretical curves, as seen in Figures 10 through 17, pages 68 through 75, were adjusted to make the integral under the theoretical curve equal to the integral under the experimental profile to a reasonable degree.

A single set of parameters, i.e., frost density, temperature correction factors, and frost thermal conductivity, was used to obtain the theoretical profiles. Because, however, the profiles representing the run made with a warmer coolant temperature and the run made with a higher krypton concentration were so different from their respective experimental profile, theoretical profiles using different frost thermal conductivities were generated and are plotted with the appropriate experimental data in Figures 20 and 21.

Finally, a simulation run was performed to show the effect operating time has on the solids buildup profile. The results of this run are plotted in Figure 22.

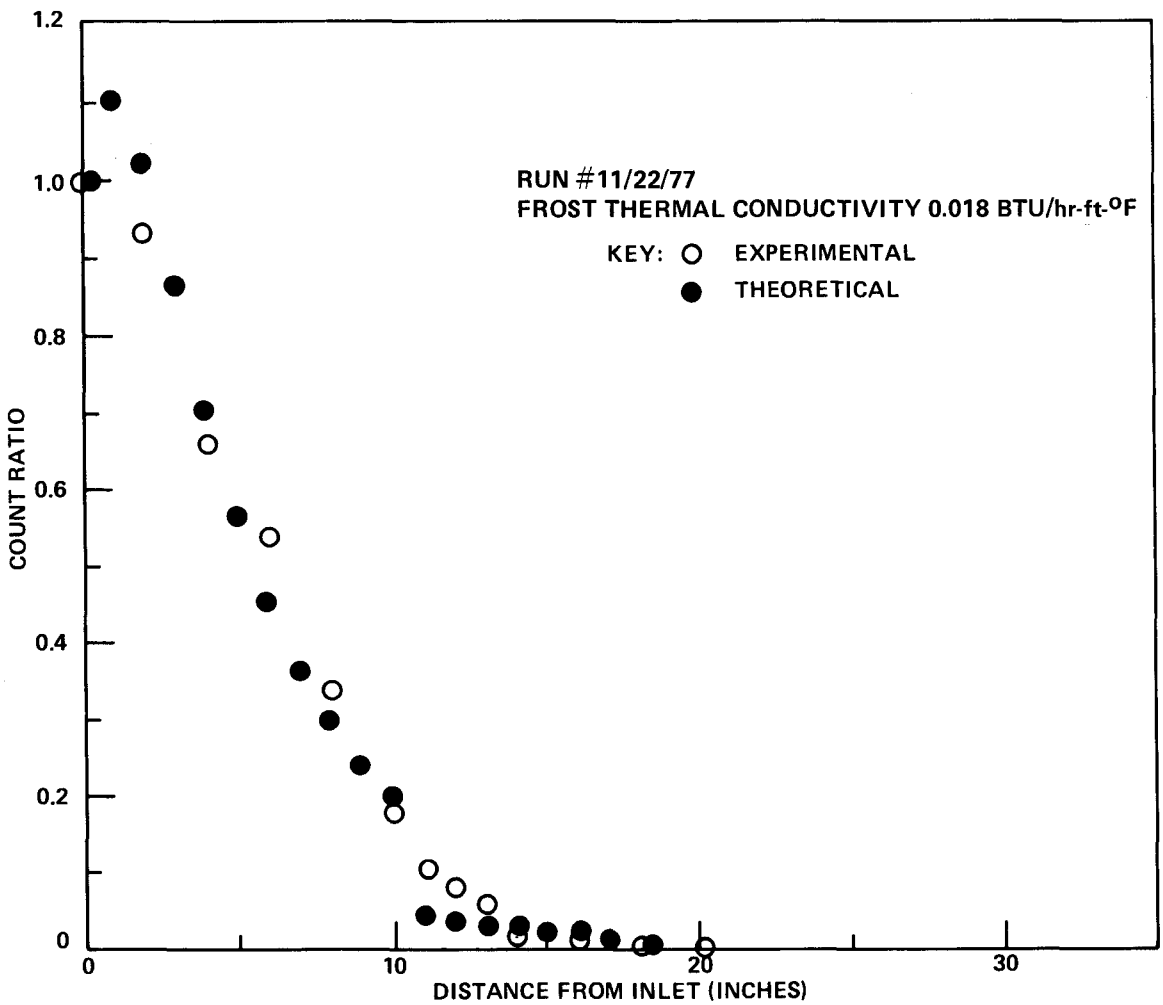

Figure 20

COMPARISON OF EXPERIMENTAL AND THEORETICAL PROFILES FOR RUN 11/22/77 USING INCREASED FROST THERMAL CONDUCTIVITY

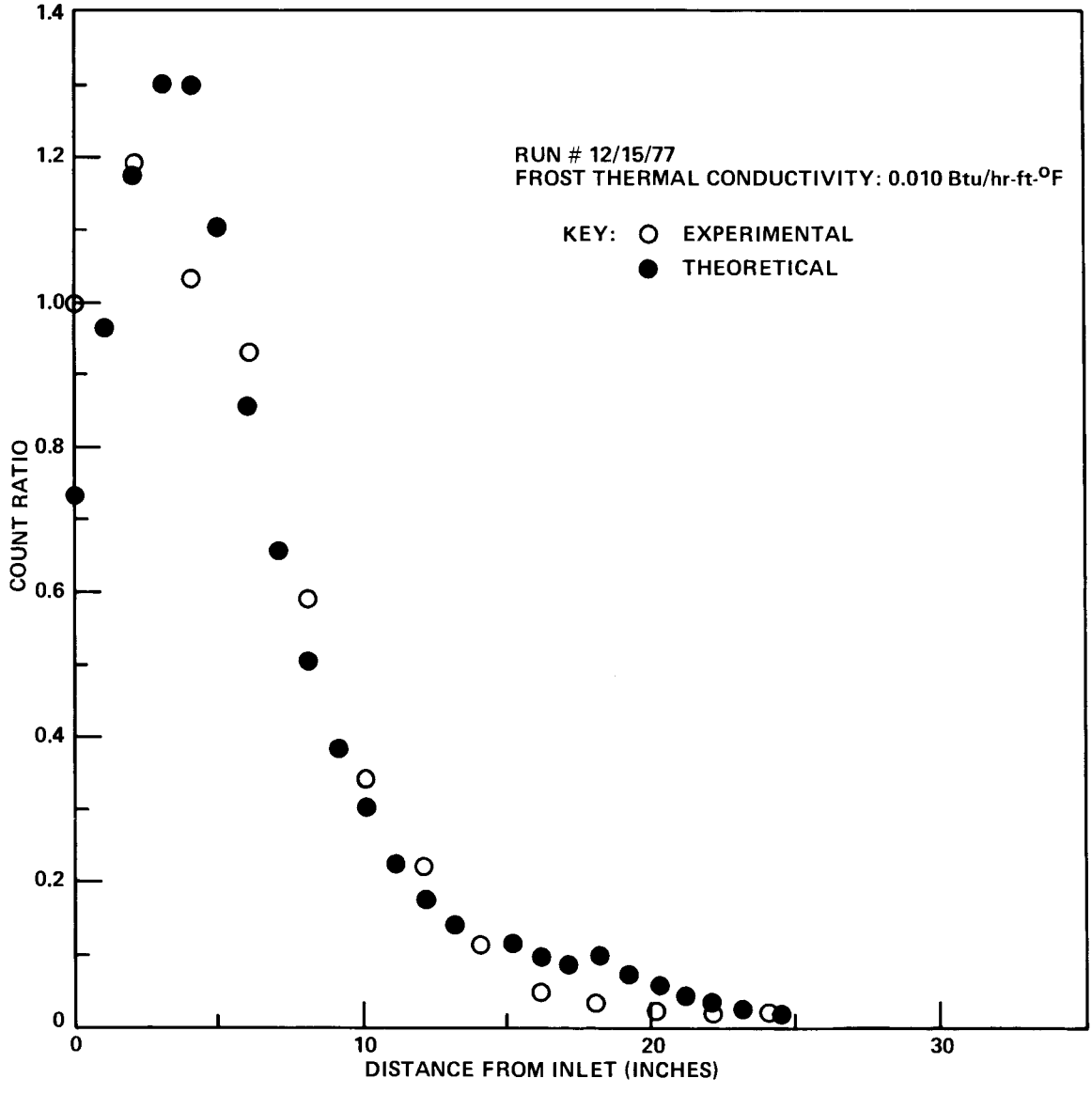

Figure 21

COMPARISON OF EXPERIMENTAL AND THEORETICAL PROFILES FOR RUN 12/15/77 USING INCREASED FROST THERMAL CONDUCTIVITY

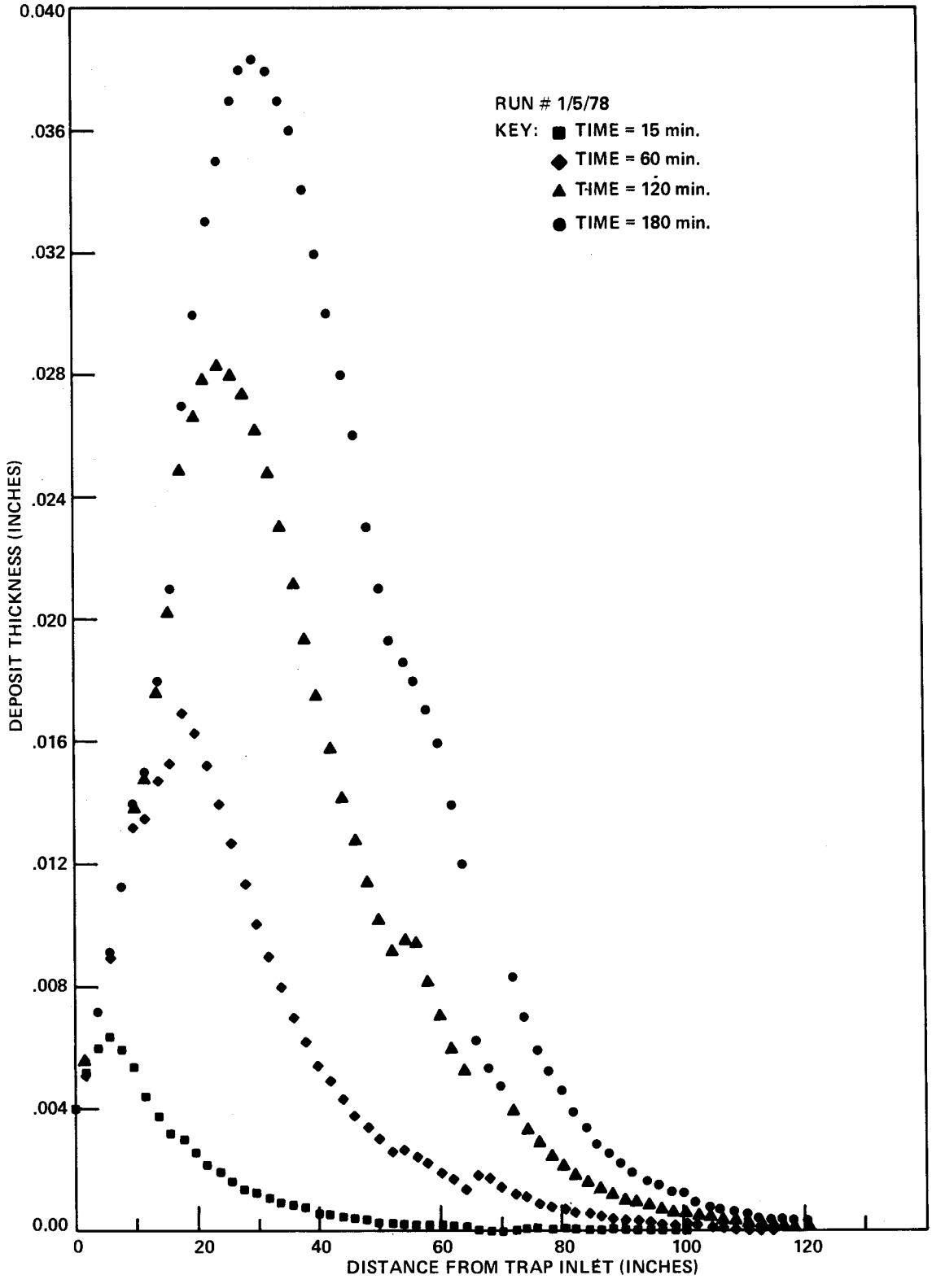

Figure 22

EFFECT OF OPERATING TIME ON SOLIDS BUILDUP PROFILE

II. DISCUSSION OF RESULTS

To be a useful model, the theoretical results should fit the experimentally obtained data within reasonable tolerances, both qualitatively and quantitatively. The following discussion details each experimental/theoretical comparison and attempts to discuss why the model's predictions did or did not agree with the test data.

Run 11/10/77 (Figure 10, Page 68)

This was one of two runs in which the experimentally obtained deposit thickness appeared inconsistent with the model's prediction. Note that, initially, the theoretical profile rises slightly higher than the experimental. The dip observed in both profiles at a distance of 12 to 18 inches is due to the heat inleakage from the initial trap support. Immediately following this heat effect, both profiles increase due to the colder regions found in the trap. The theoretical profile increases, however, for only a few inches, while experimentally, a large deposit was observed for approximately 20 inches before the profile tailed off. This could be due to the temperatures, warmer than predicted by the model, which were found experimentally in the first 20 inches, followed by a sudden 30-degree temperature drop, causing the "snow" to last for an extended period of time. Another possible cause is that the krypton feed gas concentration varied from 2.6% to 6.9% during the experimental run. The model, however, was written to accept in-line

perturbations of this order and the plotted theoretical profile should include any effects caused by such concentration changes. Some of the other tests suggest other possible explanations for this irregularity in the loading profile.

Run 11/15/77 (Figure 11, Page 69)

The flow rate was decreased by a factor of four from the previous run to 0.035 scfm. As expected for such a low flow, the resulting deposit profile indicates that the bulk of the solids are removed near the trap inlet. Theoretical and experimental profiles compare quite favorably for this test case. The only deviation occurs within the first few inches of the trap where, experimentally, krypton deposits were greater than theoretically predicted. This is probably due to inlet effects, some of which are caused by the gas channeling down the first 6 inches of the trap. Notice in the detail drawing of the trap, Figure 5, page 49, that the inlet gas lines are perpendicular to the cold trap. The gas probably uses primarily only two flow channels during this first 6 inches. This reduced flow area causes an increased gas velocity and convective movement. The increased convection enhances the heat transfer, and thus a larger than predicted amount of krypton will freeze out in this region. After the gas flows 6 inches, the initial cut and twist in the finned tube forces the flow to become more evenly distributed throughout the sixteen flow channels. As is seen

in the figure, following the initial entrance effects, the theoretical and experimental profiles agree quite well.

Run 11/22/77 (Figure 12, Page 70, and Figure 20, Page 84)

The flow rate was returned to the base condition of 0.14 scfm; however, the liquid nitrogen temperature was increased to -281°F by raising the pressure of the boiling coolant to 19 psig. As is illustrated in Figure 12, page 70, the model yields a poor representation of the experimental data. Since the trap operating temperature was warmer than previous tests, the frost thermal conductivity and/or frost density should be greater than the values used to obtain Figure 12, page 70, due to the "wetter" krypton solid product.

As indicated earlier in the chapter, accurate values for the density and thermal conductivity of the krypton frost were not known, and values employed in the theoretical analysis were estimated. Since the primary objective of this thesis was to obtain experimental krypton loading profiles and compare those profiles with ones generated by the mathematical model, and since those theoretical profiles were normalized by ratioing count positions and adjusted to make the integral under the theoretical curve equal to the area under the experimental curve, experimental values for the frost density and thermal conductivity could not be individually extracted from the data. A value for the frost density could probably have been obtained by running the trap until the differential pressure transmitter and flow indicators

indicated a plugging condition had occurred. By knowing the total flow area and from the profile scan, the amount of krypton at the plugged position and the total amount in the trap, the frost density could probably be calculated. Because of the size of the experimental apparatus, it would have taken several hundred liters of krypton to plug the equipment. At a cost of $500/100 liters of krypton, this test would have amounted to a major cost with no guarantee of success. Frost density and thermal conductivity studies could be determined much less expensively in bench-scale apparatus.

Although these parameters, frost density and thermal conductivity, do not seem closely related to each other, by examining equations 32 and 33 in Chapter II, it can be readily observed that both variables affect the deposit height, and hence the loading profile, to the extent that it is not easily possible to distinguish effects on the profile caused by changes in one from effects caused by changes in the other. Therefore, for the purpose of this study, the effects of frost density and thermal conductivity on cold trap loading profiles were coupled together, and instead of manipulating both parameters to match the normalized theoretical profile to the experimentally obtained profile, only the frost thermal conductivity was adjusted.

Using a value of 0.018 Btu/hr-ft-°F resulted in the theoretical curve seen in Figure 20, page 84. Obviously, this match between the theoretical profile and experimental

data is much better using this value for thermal conductivity than using the base value of 0.0013. Results from this run support the hypothesis that the frost thermal conductivity or density changes with changing trapping conditions; specifically, the coolant temperature.

Run 12/1/77 (Figure 13, Page 71)

The initial experiment, Run 11/10/77, which exhibited the unusual loading characteristics was repeated. Experimental and theoretical results were similar to the earlier test verifying that something strange was occurring between 20 and 40 inches. Most likely, this effect has to do with thermal instabilities caused by the metal support bracket. Krypton inlet concentrations remained constant at 7.4% during this run, so it can be concluded that the variation in feed observed in Run 11/10/77 was not the cause of the irregular deposit loading.

Run 12/15/77 (Figure 14, Page 72, and Figure 21, Page 85)

The flow was decreased to 0.088 scfm and the krypton concentration increased to 13.5 mole percent. As can be observed in Figure 14, page 72, the match predicted by the base parameters of the model, a frost density of 68.0 lb/ft^3 and a frost thermal conductivity of 0.0013 Btu/hr-ft-°F, is again unacceptable. Since the krypton concentration was nearly twice that of the other runs, it is possible that the frost density and/or frost thermal conductivity might be greater due to an increased solids packing. In Figure 21,

page 85, the experimental data is replotted with a theoretical profile calculated using the increased value of 0.010 Btu/hr-ft-°F for the thermal conductivity of the solid deposit. Entrance effects are again observed initially; however, the overall match is better than with the lower conductivity value.

Run 1/5/78 (Figure 15, Page 73)

The total gas flow was increased to 0.71 scfm. The entrance effect due to the inlet piping situation was again present. It is of interest to note that, with the higher flow, a significant deposit buildup is observed as far as 90 inches from the desublimer inlet. It appears that the high flow, which resulted in a more evenly distributed frost deposit, overshadows the irregular loading effect seen in Runs 11/10/77 and 12/1/77. The consequences of the second 6-inch support bracket beginning 66 inches from the inlet are readily viewed in the figure. Experimentally, the deposit height dipped in this "warm" region, followed by a slight rise downstream of the supports where the temperature again became colder. The theoretical model simulates this effect, as well as the overall run, with excellent agreement.

Run 1/12/78 (Figure 16, Page 74)

The gas flow rate was increased to the highest tested rate of 1.06 scfm. Significant amounts of the krypton deposit were detected over the entire length of the trap. Perturbations in the loading profile due to the inlet effects

and heat conductive metal desublimer supports were observed. The high gas flow again overshadowed the irregular loadings which had been observed in the earlier runs 20 to 40 inches from the inlet. Overall, the model and experimental profiles match with reasonable accuracy for this high gas flow test case.

Run 1/19/78 (Figure 17, Page 75, and Figure 18, Page 76)

The final experimental run was made at the base flow rate of 0.14 scfm; however, the cold trap pressure was reduced to 1.3 atmospheres to determine what effect total trapping pressure had on the proposed model. The resulting experimental profile lends some resemblance to the two previous runs, 11/10/77 and 12/1/77, tested at the same flow rate but higher pressure. Specifically, a larger buildup was again experimentally observed around 20 inches down the trap than that which was theoretically predicted by the model. It can be readily assumed, then, that total trapping pressure does not affect the proposed model as krypton concentration and coolant temperatures do. Due to the ability of the model to predict loading profiles in other areas of the trap for this and other runs, it is suspected that the region of irregular loadings is a result of the physical situation and not a theoretical problem. This hypothesis, though, should be more fully explored.

The point deposit thickness 2 inches from the trap inlet was monitored during this experimental run to obtain a

point deposit buildup versus time relationship. The data are plotted in Figure 18, page 76, along with the profile generated from the model. As per the discussion in Chapter II, the data illustrate the linear buildup in the superheated region of the trap followed by a decreasing buildup rate due to the decreased heat transfer across the accumulating krypton deposit. The experimental and theoretical profiles agree reasonably well for this case.

From the above discussion, it can be justifiably stated that the proposed model can accurately predict the solids buildup profile for the system studied. The most obvious question which arises concerns the relevancy of the work and its practical applications. Since krypton-85 has a half life of more than 10 years, the EPA has decreed that by 1983, 90% of the fission product krypton present in the spent fuel rods will be removed from the fuel reprocessing stack[22]. A well-defined krypton isolation and collection system must be defined prior to that date. This model can aid engineers in designing cold traps for the krypton collection equipment. By simulating several different trap designs and inputting the appropriate physical parameters, designers can use the model to determine optimum operating times, trap size, and plugging or loading situations. It is very important to be able to determine if the trap is sized correctly in order to prevent the cold trap from plugging or releasing krypton before complete loading can occur. Figure 22, page 86, depicts this situation a little more clearly. As the trap is loaded

and time increases, it is observed that, for this case, even though buildups increase rapidly, the effluent concentration of krypton from the trap will increase to significant levels long before trap plugging occurs. This would not be a good operating situation, nor would be the case where plugging occurs near the trap inlet while most of the trap remains unused. For example, should the heat transfer in the trap be sufficiently high and the flow area too small, it is conceivable that a plug near the trap inlet might occur well before total trap loading. Prevention of such misdesigns is the objective of this model. To determine the actual situations and obtain sufficient design data, the relationship of the frost density and frost thermal conductivity to trap operating conditions must be known. For the purpose of this work, however, the values employed in the model showed that the model can simulate krypton desublimation profiles but do not necessarily represent good quantitative values for those parameters.

CHAPTER VI

CONCLUSIONS AND RECOMMENDATIONS

Presented in this chapter are conclusions that can be drawn from the results obtained during this thesis study. Recommendations are also given to define related areas where research and development needs exist.

I. CONCLUSIONS

The following conclusions were derived from the investigation:

1. A theoretical model developed to design uranium hexafluoride cold traps used in volatility processing has been adapted to describe the removal of krypton by cold trapping from a noncondensable carrier gas stream, and the general validity of this model has been verified.

2. The usefulness of the model to predict plugging and loading in the trap is dependent upon obtaining accurate frost density and frost thermal conductivity data.

3. As the gas flow rate was increased, the krypton was observed to travel farther down the length of the trap prior to freezing out of the gas stream.

4. The experimental data indicate that the density and/or thermal conductivity of the frost deposit collected increase as the temperature at which the deposit is frozen out increases. Limitations of the testing apparatus made it

impossible to uncouple these two deposit height parameters and thus determine which changed with increasing temperature.

5. Similarly, as the concentration of the condensable krypton is increased, the data imply that the frost density and/or frost thermal conductivity increase.

6. It does not appear that the frost density or frost thermal conductivity is dependent upon the trapping pressure.

7. The experimental data indicate that, if the frost density and frost thermal conductivity are known, the model can be used as a useful design tool for engineers to design cold traps for use in isolating and collecting radioactive krypton in fuel reprocessing plants.

II. RECOMMENDATIONS

The following recommendations are made to expand the work in the field of desublimation:

1. Uncouple the frost density and/or frost thermal conductivity effects by experimentally obtaining values for these parameters. This might be done by intentionally plugging a known flow area with the solid deposit and, using the appropriate equations presented in Chapter II, back calculating values for these parameters.

2. Expand the applicability of the model by determining the relationships between freeze-out temperature and krypton frost thermal conductivity and/or frost density.

3. Similarly, determine the dependency of the frost density and/or frost thermal conductivity on krypton concentration in the gas stream.

4. Adapt the model to the desublimation of other components such as xenon and carbon dioxide which will be collected with the krypton in fuel reprocessing plants.

5. Since the gas will contain more than one desublimable component in reprocessing applications, expand the model to predict multicomponent situations.

6. If accurate loading profiles are desired, it is recommended that inlet effects be reduced by feeding the gas parallel to the gas flow in the trap instead of perpendicular as was the case in this study.

7. Since "warm spots," which resulted in discontinuous loadings, were encountered due to heat inleakage through the trap supports, it is recommended that any future traps be constructed such that any required heat conducting supports do not come in direct contact with the cold trap.

8. Selective sublimation was observed during the remelt process after the freeze-out step. This may provide a method for higher krypton concentrations for storage and should be more fully explored.

LIST OF REFERENCES

1. Merriman, J. R., et al., *Removal of ^{85}Kr from Reprocessing Plant Off-Gas by Selective Absorption*, Union Carbide Corporation, Nuclear Division, Oak Ridge Gaseous Diffusion Plant, Oak Ridge, Tennessee, November 1972 (K/L-6201).

2. Stephenson, M. J., Eby, R. S., and Huffstetler, V. C., *Selective Absorption Pilot Plant for Decontamination of Fuel Reprocessing Plant Off-Gas*, Union Carbide Corporation, Nuclear Division, Oak Ridge Gaseous Diffusion Plant, Oak Ridge, Tennessee, October 1977 (K-1876).

3. Dunthorn, D. I., *The Design of Batch Desublimers*, Union Carbide Corporation, Nuclear Division, Oak Ridge Gaseous Diffusion Plant, Oak Ridge, Tennessee, September 1968 (K/L-6220).

4. Smiley, S. H., et al, *ORGDP Fuel Reprocessing Studies Summary Progress Report, January Through June 1966*, Union Carbide Corporation, Nuclear Division, Oak Ridge Gaseous Diffusion Plant, Oak Ridge, Tennessee, January 1967 (K-1691).

5. Thompson, W. I., "Theory of Heat and Mass Transfer in Batch Condensation of Solids," Chapter 6, *Engineering Developments in the Gaseous Diffusion Process*, Benedict, M., and Williams, C., Editors, McGraw-Hill Book Company, Inc., New York (1949).

6. Chilton, T. H., and Colburn, A. P., *Industrial and Engineering Chemistry, 26*, p. 1183 (1934).

7. *How to Design Double Pipe Finned Tube Heat Exchangers*, Brown Fintube Company, Tulsa, Oklahoma, Bulletin No. 1000.

8. Colburn, A. P., and Edison, A. G., *Industrial and Engineering Chemistry, 33*, p. 457 (1941).

9. Treybal, R. E., "Simultaneous Mass and Heat Transfer," Chapter 3, *Mass Transfer Operations*, McGraw-Hill Book Company, Inc., New York, 2nd Edition (1968).

10. Olander, D. R., "Design of Direct Contact Cooler-Condensers," *Industrial and Engineering Chemistry*, Vol. *53*, No. 2, p. 121 (1961).

11. Colburn, A. P., and Drew, T. B., "The Condensation of Mixed Vapors," *Transactions of the American Institute of Chemical Engineers*, Volume XXXIII, pp. 197-213 (1937).

12. Mickley, H. S., Sherwood, T. K., and Reed, C. E., "Method of Runge-Kutta," *Applied Mathematics in Chemical Engineering*, McGraw-Hill Book Company, Inc., New York, 2nd Edition, pp. 193-200 (1957).

13. Dorn, W. S., and McCracken, D. D., *Numerical Methods with Fortran IV Case Studies*, John Wiley and Sons, New York, p. 363 (1972).

14. Dorn, W. S., and McCracken, D. D., *Numerical Methods with Fortran IV Case Studies*, John Wiley and Sons, New York, p. 25 (1972).

15. Gardner, R. P., and Ely, R. L., Jr., "Radiotracer Applications to Engineering Processes," Chapter 8, *Radioisotope Measurement Applications in Engineering*, Reinhold Publishing Corporation, New York (1967).

16. Fulman, M. J., and Hulbert, V. G., "Gamma Scanning of Large Towers," *Chemical Engineering Progress*, Vol. *71*, No. 6, pp. 73-77 (June 1975).

17. Burch, W. D., *LMFBR/LWR Fuel Reprocessing Programs Progress Report for Period July 1 to September 30, 1976*, Union Carbide Corporation, Nuclear Division, Oak Ridge National Laboratory, Oak Ridge, Tennessee, November 1976 (ORNL/TM-5668/5660).

18. Burch, W. D., *LMFBR/LWR Fuel Reprocessing Program Progress Report for Period October 1 to December 31, 1976*, Union Carbide Corporation, Nuclear Division, Oak Ridge National Laboratory, Oak Ridge, Tennessee, February 1977 (ORNL/TM-5768/5760).

19. Burch, W. D., *LMFBR/LWR Fuel Reprocessing Program Progress Report for Period January 1 to March 31, 1977*, Union Carbide Corporation, Nuclear Division, Oak Ridge National Laboratory, Oak Ridge, Tennessee, May 1977 (ORNL/TM-5879/5864).

20. Burch, W. D., *LMFBR/LWR Fuel Reprocessing Program Progress Report for Period April 1 to June 30, 1977*, Union Carbide Corporation, Nuclear Division, Oak Ridge National Laboratory, Oak Ridge, Tennessee, August 1977 (ORNL/TM-5993/5987).

21. Washburn, E. W., Editor, *International Critical Tables of Physics, Chemistry, and Technology*, Vol. III, McGraw-Hill Book Company, Inc., New York, p. 102 (1939).

22. *Federal Register*, Vol. *40*, No. 104, Environmental Protection Agency [40 CFR Part 190], Washington, DC, pp. 23420-23425 (May 29, 1975).

23. Freeman, M. P., and Halsey, G. D., Jr., *The Solid Solution Krypton-Xenon from 90 to 120°K, The Vapor Pressure of Argon, Krypton, and Xenon*, The Department of Chemistry, University of Washington, Seattle, Washington (1956).

24. Bromley, L. A., and Wilke, C. R., "Viscosity Behavior of Gases," *Industrial and Engineering Chemistry*, Vol. *43*, No. 7, p. 1641 (July 1951).

25. Sherwood, T. K., Pigford, R. L., and Wilke, C. R., *Mass Transfer*, McGraw-Hill Book Company, Inc., New York, p. 19 (1975).

26. Perry, R. H., and Chilton, C. H., Editors, *Chemical Engineers' Handbook*, 5th Edition, McGraw-Hill Book Company, Inc., New York, p. 4-58 (1973).

27. Perry, R. H., and Chilton, C. H., Editors, *Chemical Engineers' Handbook*, 5th Edition, McGraw-Hill Book Company, Inc., New York, p. 3-215 (1973).

28. McCabe, W. L., and Smith, J. C., *Unit Operations of Chemical Engineering*, Third Edition, McGraw-Hill Book Company, Inc., New York, p. 418 (1976).

29. Perry, R. H., and Chilton, C. H., Editors, *Chemical Engineers' Handbook*, 5th Edition, McGraw-Hill Book Company, Inc., New York, p. 23-39 (1973).

30. Foster, A. R., and Wright, R. L., Jr., *Basic Nuclear Engineering*, Allyn and Bacon, Inc., Boston, Mass., p. 159 (1977).

Blank Page

ACKNOWLEDGMENTS

The author wishes to express his deepest gratitude to his advisor, Dr. D. I. Dunthorn, for his assistance and guidance on this project and to Mrs. M. B. Canterbury for her generous contribution in typing and editing this report. A special thanks go to the program manager, Mr. M. J. Stephenson, for his direction and encouragement, to Mr. J. L. Patton who assisted in the experimental work, and to Mr. C. M. Cummings for his help constructing the equipment. Finally, the author wishes to acknowledge his loving wife who continually gave to him her support throughout the work.

Blank Page

APPENDIX A

EQUATIONS USED TO CALCULATE MODEL PARAMETERS

In the following discussion, the equations for the various physical properties used in the theoretical analysis are presented.

Vapor Pressure Equation for Solid Krypton

$$\ell n\ P_{mmHg}Kr = \frac{-1210.46}{T°K} + 16.5257 \text{ [23]}.$$

In degrees Rankine and atmospheres,

$$P_{atm}Kr = \exp\left(9.89238 - \frac{2178.83}{T°R}\right).$$

Viscosity of Gaseous Mixture

$$\mu_{mix} = \frac{\mu_1}{1 + \frac{X_2}{X_1}\phi_{12}} + \frac{\mu_2}{1 + \frac{X_1}{X_2}\phi_{21}} \text{ [24]},$$

where

$$\phi_{12} = \frac{\left[1 + \left(\frac{\mu_1}{\mu_2}\right)^{1/2}\left(\frac{M_2}{M_1}\right)^{1/4}\right]^2}{\frac{4}{\sqrt{2}}\left[1 + \frac{M_1}{M_2}\right]^{1/2}},$$

$$\phi_{21} = \frac{\left[1 + \left(\frac{\mu_2}{\mu_1}\right)^{1/2}\left(\frac{M_1}{M_2}\right)^{1/4}\right]^2}{\frac{4}{\sqrt{2}}\left[1 + \frac{M_2}{M_1}\right]^{1/2}},$$

$$\mu_{cp} = 0.0026693\left[\frac{1}{r_o^2}\frac{\sqrt{M\varepsilon}}{k}\right] f\left(\frac{kT}{\varepsilon}\right) ,$$

where

k_B = Boltzmann constant, ergs/°K,

T = absolute temperature, °K,

M = molecular weight of gas, g/g-mole,

r_o = collision diameter for low velocity head-on collision, angstroms, and

ε = energy difference between separated molecules and the molecules in the configuration in which they have the maximum energy of attraction, ergs.

For nitrogen,

$$\frac{1}{r_o^2}\frac{\sqrt{M\varepsilon}}{k} = 3.736 \text{ and } \frac{\varepsilon}{k} = 91.4.$$

For krypton,

$$\frac{1}{r_o^2}\frac{\sqrt{M\varepsilon}}{k} = 9.676 \text{ and } \frac{\varepsilon}{k} = 190.$$

Typical values for $f\left(\frac{k_B T}{\varepsilon}\right)$ may be found in the literature[24].

Heat Capacity Equation

At low temperatures, the heat capacity is essentially independent of pressure and temperature and depends only on composition.

$$C_{P_{Kr}} = 0.06 \text{ Btu/lb-°F} = 5.028 \text{ Btu/lb-mole-°F}^{[21]}.$$

$$C_{P_{N_2}} = 0.25 \text{ Btu/lb-°F} = 7.000 \text{ Btu/lb-mole-°F}^{[21]}.$$

$$C_{P_{mix}} = 7.00\ (1 - x) + 5.028\ (x) = 7.00 - 1.972x,$$

where

x = composition of krypton in the gas stream.

Diffusivity

$$D_{AB}, \frac{cm^2}{sec} = \frac{0.001858T^{3/2}\ (\frac{1}{M_A} + \frac{1}{M_B})^{1/2}}{p_T \sigma^2_{AB}\ \Omega_D}\ [25]$$

where

Ω_D = collision integral, $f(\frac{kT}{\varepsilon_{AB}})$,

ε_{AB} = Lennard-Jones force constant for a binary mixture,

$$\frac{\varepsilon_{AB}}{k} = (\frac{\varepsilon_A}{k}\ \frac{\varepsilon_B}{k})^{1/2}, \text{ and}$$

σ_{AB} = Lennard-Jones force constant for a binary mixture,

$$\sigma_{AB} = 1/2(\sigma_A + \sigma_B).$$

Values of the collision integral based on the Lennard-Jones parameter may be found in the literature[25].

$$\sigma_{Kr} = 3.655 \text{ Å}.$$

$$\sigma_{N_2} = 3.790 \text{ Å}.$$

Density of Gaseous Mixture

Density of the gas was obtained from the Ideal Gas Law:

$$PV = nRT \quad [26],$$

$$PV = \frac{m}{M} RT ,$$

$$\frac{m}{V} = \frac{PM}{RT} .$$

Thermal Conductivity of Gaseous Mixture

$$k_{mix} = x(k_{Kr}) + (1 - x)k_{N_2}.$$

Least squares fits were performed on available data[27] to arrive at equations for individual thermal conductivities.

$$k_{N_2} = 0.00004856T°K + 0.000104,$$

$$k_{Kr} = 0.0000196554T°K + 0.0005781.$$

Combining the above three equations yields, in °R,

$$k_{mix} = -1.606 \times 10^{-5}xT°R + 4.7420 \times 10^{-3}x$$

$$+ 2.698 \times 10^{-5}T°R + 1.0410 \times 10^{-3}.$$

Reynolds Number[28]

Equivalent diameter of shell,

$$\text{Shell ID} = \frac{1.939"}{12} = 0.1616 \text{ ft},$$

$$\text{Inner Tube OD} = \frac{0.75"}{12} = 0.0625 \text{ ft}.$$

Cross-sectional area of shell space is

$$\frac{\pi(0.1616^2 - 0.0625^2)}{4} - \frac{16 \times 0.5 \times 0.035}{144} = 0.0155 \text{ ft}^2.$$

The perimeter of the air space is

$$\pi(0.1616) + 1.529 \text{ ft} = 2.037 \text{ ft}.$$

The hydraulic radius, r_h, is

$$\frac{0.0155 \text{ ft}^2}{2.037 \text{ ft}} = 7.61 \times 10^{-3} \text{ ft}.$$

The equivalent diameter, D_e, is

$$4 \times r_h = 4 \times 7.61 \times 10^{-3} = 0.0304 \text{ ft}.$$

$\therefore$ The Reynolds number of the N_2 + Kr mixture is

$$\frac{D_e G}{\mu} = \frac{0.0304 \text{ ft} \times \left[\frac{0.0966 \text{ lbm}}{\text{hr}} \times \frac{28.0 \text{ lb}}{\text{lbm}}\right]}{0.024 \text{ lb/ft-hr} \times 0.0155 \text{ ft}^2}$$

$$+ \frac{\frac{7.23 \times 10^{-3} \text{ lbm } (83.8) \text{ lb}}{\text{hr-lbm}}}{0.024 \text{ lb/ft-hr} \times 0.0155 \text{ ft}} .$$

$$\text{Re} = 270.5.$$

APPENDIX B

FORTRAN PROGRAM FOR SOLUTION OF THE MODEL EQUATIONS

A listing of the computer program is presented in Table VI, along with pertinent information required to process the program on an IBM 360 machine.

Program Input

When the program was originally written by Dunthorn[3] for the design of uranium hexafluoride traps, the program input was set up such that repetitive calculations could be made on similar test runs without requiring certain inputs to be repeatedly read into the machine. Inputs, such as dimensional units for inputs and outputs, as well as trap geometry, may be saved between successive data sets. For these cases, if a variable is "saved," then by leaving a blank space on the data card, the saved variable will retain the value it had on the previous data set. If a value of zero is desired for a saved variable, it is necessary that a value such as 0.001 be specified rather than zero, since a zero value for a saved variable will cause it to retain the value used in the previous data set. This highly unlikely situation would only occur for a temperature value, since other program variables could not have a zero value and still have a useful meaning.

It is possible to initialize certain saved variables prior to reading the first data card by using a DATA

TABLE VI

LISTING OF COMPUTER PROGRAM

```
                    COLD TRAP DESIGN PROGRAM

      IMPLICIT REAL*8 (A-H,O-Z)
      REAL*8 T(501),X(501),B(501),D(501),L(501),ALPH(501),VU(501),
     .       WID(501),TWL(501),TS(501),TW(501),WI(501),XL(501),LLI(500),
     .       LI(500),DI(500),R2(50),R3(50),R5(501),PRES(501),S6(501),
     .       ARA(501),TIN(501),XIN(501),FLOW(501)
      REAL*8 N0,N1,N2,N3,N23,MM,M1,M2,M3,MU1,MU2,MU3,MU,KB,KB0,KB1,KB2,
     .       KS,LB,LB0,LB1,LB2,L1,L2,L3,L4,LENGTH,KB3,OMEGA,
     1      RHOG,PRA,DIF,SCH,TCOR1,TCOR2
      REAL*8 JSCFM/4HSCFM/,JLH/5HLB/HR/,JKH/5HKG/HR/,JKMH/6HKGM/HR/,
     .       JFL/6HLBM/HR/
      REAL TITLE(18)
      INTEGER TYPE,R1(50),R4(50),R6(500),NUM(501)
      LOGICAL SATD,SSAT,DONE,HSPEC
C
C
C                   VARIABLE SPECIFICATIONS
      DATA IN23,ICP,IMU,IK0,ISAT/3HN23,2HCP,2HMU,1HK,2HVP/,
     .     JBLNK,JKGS,JFT,JIN/1H ,2HKG,2HFT,2HIN/,
     .     JCM,JC,JK,JF,JPSI/2HCM,1HC,1HK,1HF,4HPSIA/,
     .     JMM/4HMMHG/,M1,M2,RHOS,KS/352.0,29.0,140.0,0.0,1/,
     .     HSPEC,HCON,SHLDP,JHLDP/.FALSE.,0.67,1.0,2HLB/,
     .     SDIST,JDIST,SCLR,JCLR/1.0,2HFT,12.0,2HIN/,
     .     ST01,ST02,JT0/1.0,-459.69,1HF/,
     .     STI1,STI2,JTI1/1.0,459.69,1HF/,
     .     JPA,SPA,SFL/3HATM,1.0,1.0/,
     .     JR1,SR1,JR2,SR2/2HIN,0.083333,2HIN,0.083333/,
     .     JR3,SR3/4HFRAC,1.0/
      DATA JPS,JM,JPA1/4H  PS,4H  MM,3HATM/
C                   DATA GROUP ONE
    1 READ (5,100,END=69) LX1,LX2,LX3,LX4,(TITLE(I),I=1,18)
  100 FORMAT (2X,4I1,4X,17A4,A2)
      WRITE(6,200) (TITLE(I),I=1,18)
  200 FORMAT (1H1,25X,17A4,A2/1H0,30X,18HPROGRAM PARAMETERS)
C
C                   DATA GROUP TWO
      IF (LX1.LT.1) GO TO 2
      READ(5,101) YT1,YT2,YT3,YT4,YT5,YT6,JT1
  101 FORMAT(6F10.0,I5)
      IF (YT1.GT.0.0) M1 = YT1
      IF (YT2.GT.0.0) M2 = YT2
      IF (YT3.GT.0.0) RHOS = YT3
      IF (YT4.GT.0.0) KS = YT4
      H = YT5
      IF (YT6.GT.0.0) HCON = YT6
      HSPEC = YT5.GT.0.0
    2 WRITE(6,201) M1,M2,RHOS,KS,H,HCON
  201 FORMAT(1H0,6X,2HM1,8X,2HM2,6X,5HRHO-S,7X,3HK-S,7X,1HH,8X,4HHCON/
     .       1H ,3F10.2,3F10.3)
      READ(5,286) TCOR1,TCOR2
  286 FORMAT(2F10.0)
C
C                   DATA GROUP TWO, SECOND PART
      IF %%LX1.LT.1<.OR.%JT1.LT.1<< GO TO 8
      WRITE%6,202<
  202 FORMAT%1H0,15X,38HSPECIFIED PHYSICAL PROPERTY PARAMETERS<
```

TABLE VI (Continued)

```
    3 READ(5,102) JT1,YT1,YT2,YT3,YT4
  102 FORMAT (A4,1X,4F15.0)
      WRITE%6,203< JT1,YT1,YT2,YT3,YT4
  203 FORMAT (1H ,A4,1X,4F20.9)
      IF %JT1.NE.IN23< GO TO 4
      N0 # YT1
      N1 # YT2
      N2 # YT3
      N3 # YT4
      GO TO 3
    4 IF %JT1.NE.ICP< GO TO 5
      C0 # YT1
      C1 # YT2
      C2 # YT3
      C3 # YT4
      GO TO 3
    5 IF %JT1.NE.IMU< GO TO 6
      MU1 # YT1
      MU2 # YT2
      MU3 # YT3
      GO TO 3
    6 IF %JT1.NE.IK0< GO TO 7
      KB0 # YT1
      KB1 # YT2
      KB2 # YT3
      KB3=YT4
      GO TO 3
    7 IF %JT1.NE.ISAT< GO TO 8
      ASAT # YT1
      BSAT # YT2
      CSAT # YT3
C
C                    READ GROUP THREE
    8 IF %LX2.LT.1< GO TO 9
      READ%5,103< JT1,JT2,YT1,JT3,YT2,JT4
      IF %JT1.GT.0< M # JT1
      IF %JT2.GT.0< NTOT # JT2
      IF %YT1.GT.0.0< DTHETA # YT1
      IF %JT3.GT.0< IC # JT3
      IF %YT2.GT.0.0< PRINT # YT2
  103 FORMAT%2I10,2%F10.0,I10<<
    9 WRITE%6,204< M,NTOT,DTHETA,IC,PRINT
  204 FORMAT%1H0,3X,12HX-INCREMENTS,3X,12HT-INCREMENTS,6X,9HTIME STEP,
     .  8X,7HX-PRINT,8X,7HT-PRINT/1H ,2I15,F15.8,I15,F15.8<
C
C                    READ GROUP THREE, PART TWO
      IF %%LX2.LT.1<.OR.%JT4.LT.1<< GO TO 13
      READ(5,104) JT1,JT2,JT3,JT4
  104 FORMAT (10X,4(A4,6X))
      IF %JT1.EQ.JBLNK< GO TO 10
      SHLDP # 1.0
      IF %JT1.EQ.JKGS< SHLDP # 0.45351
      JHLDP # JT1
   10 IF %JT2.EQ.JBLNK< GO TO 11
      SDIST # 1.0
      IF %JT2.EQ.JIN< SDIST # 12.0
      IF %JT2.EQ.JCM< SDIST # 30.48
      JDIST # JT2
   11 IF %JT3.EQ.JBLNK< GO TO 12
      SCLR # 1.0
```

TABLE VI (Continued)

```
      IF %JT3.EQ.JIN< SCLR # 12.0
      IF %JT3.EQ.JCM< SCLR # 30.48
      JCLR # JT3
   12 IF %JT4.EQ.JBLNK< GO TO 13
      STO1 # 1.0
      IF %%JT4.EQ.JC<.OR.%JT4.EQ.JK<< STO1 # 0.5555556
      STO2 # 0.0
      IF %JT4.EQ.JC< STO2 # -273.16
      IF %JT4.EQ.JF< STO2 # -459.69
      JTO # JT4
C
C                    READ GROUP FOUR
   13 IF %LX3.LT.1< GO TO 19
      READ(5,105) JT1,TJ2,TJ3,TJ4
  105 FORMAT%I10,3%A6,4X<<
      CALL WRTZER (TJ2,TJ3,TJ4,8,'(3A6)')
      CALL RDTZER (JT2,JT3,JT4,4,'(3A4)')
      IF %JT2.EQ.JBLNK< GO TO 14
      JTI1 # JT2
      STI1 # 1.0
      IF %%JT2.EQ.JC<.OR.%JT2.EQ.JK<< STI1 # 1.8
      STI2 # 0.0
      IF %JT2.EQ.JC< STI2 # 273.16
      IF %JT2.EQ.JF< STI2 # 459.69
   14 IF %JT3.EQ.JBLNK< GO TC 15
      JPA = JPA1
      SPA # 1.0
      IF (JT3.EQ.JPS) SPA = 0.06805
      IF (JT3.EQ.JPS) JPA = JPSI
      IF (JT3.EQ.JM) SPA = 0.0013158
      IF (JT3.EQ.JM) JPA = JMM
   15 IF %JT4.EQ.JBLNK< GO TC 16
      SFL # 1.0
      JFL = TJ4
      IF (JFL.EQ.JSCFM) SFL = 0.16681
      IF %JFL.EQ.JLH< SFL # 1.0/M2
      IF %JFL.EQ.JKH< SFL # 2.205/M2
      IF %JFL.EQ.JKMH< SFL # 2.205
   16 WRITE%6,205< JTI1,JPA,JFL
  205 FORMAT%1H0,5X,34HFLOW CONDITIONS, TEMPERATURE, DEG ,A1,
     .       12H, PRESSURE, ,A4,8H, FLOW, ,A6/11H  TIME STEP,7X,
     .       7HT-INLET,6X,7HX-INLET,8X,9HFLOW RATE,7X,8HPRESSURE,
     .       7X,6HT-WALL<
      INB # 1
      III # 0
      DO 18 I#1,JT1
      READ%5,106< JT2,YT1,YT2,YT3,YT4,YT5
  106 FORMAT%I5,5F15.0<
      IF %YT1.EQ.0.0< YT1 # TIN%INB</STI1 - STI2
      IF %YT2.EQ.0.0< YT2 # XIN%INB<
      IF %YT3.EQ.0.0< YT3 # FLOW%INB</SFL
      IF %YT4.EQ.0.0< YT4 # PRES%INB</SPA
      IF %YT5.EQ.0.0< YT5 # TWL%INB</STI1 - STI2
      IF %III.EQ.1< INB # INB&1
      III # 1
      WRITE%6,206< INB,YT1,YT2,YT3,YT4,YT5
  206 FORMAT%I10,F15.3,2F15.8,F15.4,F15.3<
      YT1 # %YT1&STI2<*STI1
      YT3 # YT3*SFL
      YT4 # YT4*SPA
```

TABLE VI (Continued)

```
      YT5 # %YT5&STI2<*STI1
      JT2 # JT2&INB-1
      IF %%JT2.GT.NTOT<.OR.%I.EQ.JT1<< JT2 # NTOT
      DO 17 J#INB,JT2
      TIN%J< # YT1
      XIN%J< # YT2
      FLOW%J< # YT3
      PRES%J< # YT4
   17 TWL%J< # YT5
   18 INB # JT2
      GO TO 20
   19 WRITE%6,207<
  207 FORMAT%1H0,10X,34HFLOW CONDITIONS SAME AS LAST CASE.<
C
C                    READ GROUP FIVE
   20 IF %LX4.LT.1< GO TO 25
      READ(5,107) TYPE,ML,DIAM,IBREAK,JT1,JT2,JT3
  107 FORMAT (2I10,F10.0,I10,3(A4,6X))
      IF %%TYPE.NE.1<.AND.%TYPE.NE.2<.AND.%TYPE.NE.3<< TYPE # 4
      IF %JT1.EQ.JBLNK< GO TO 21
      JR1 # JT1
      SR1 # 1.0
      IF %JR1.EQ.JIN< SR1 # 0.0833333
      IF %JR1.EQ.JCM< SR1 # 0.03281
   21 IF %JT2.EQ.JBLNK< GO TO 22
      JR2 # JT2
      SR2 # 1.0
      IF %JT2.EQ.JIN< SR2 # 0.0833333
      IF %JT2.EQ.JCM< SR2 # 0.03281
   22 IF %JT3.EQ.JBLNK< GO TO 23
      JR3 # JT3
      SR3 # 1.0
      IF %JT3.EQ.JIN< SR3 # -6.94444E-3
      IF %JT3.EQ.JCM< SR3 # -1.07638E-3
      IF %JT3.EQ.JFT< SR3 # -1.0
   23 IF %DIAM.NE.0.0< WRITE%6,208< TYPE,DIAM,JR1
  208 FORMAT%1H0,10X,10HTRAP TYPE ,I1,13H DESCRIPTION.,10X,
     .       9HDIAMETER ,F6.3,1X,A2,1H.<
      IF %DIAM.EQ.0.0< WRITE%6,209< TYPE
  209 FORMAT%1H0,10X,10HTRAP TYPE ,I1,13H DESCRIPTION.<
      IF %SR3.GT.0.0< WRITE%6,210< JR1,JR1,JR2
  210 FORMAT%1H ,19X,A2,1H.,12X,A2,1H.,22X,A2,1H.,10X,8HFRACTION<
      IF %SR3.LE.0.0< WRITE%6,211< JR1,JR1,JR2,JR3
  211 FORMAT%1H ,19X,A2,1H.,12X,A2,1H.,22X,A2,1H.,12X,3HSQ ,A2<
      DO 24 I#1,ML
      READ%5,108< R1%I<,R2%I<,R3%I<,R4%I<,R5%I<,S6%I<
  108 FORMAT%I10,2F10.0,I10,2F10.0<
      WRITE%6,212< R1%I<,R2%I<,R3%I<,R4%I<,R5%I<,S6%I<
  212 FORMAT%1H ,I10,2F15.6,I10,2F15.6<
      R2%I< # R2%I<*SR1
      R3%I< # R3%I<*SR1
      R5%I< # R5%I<*SR2
      IF %SR3.LT.0.0< S6%I< # S6%I<*SR3
   24 CONTINUE
      DIAM # DIAM*SR1
   25 CONTINUE
C
C                    PRINT SELECTED TRAP HEADING
      IF %TYPE.EQ.1< WRITE%6,213<
  213 FORMAT%1H0,30X,15HCROSS-FLOW TRAP<
```

TABLE VI (Continued)

```
      IF %TYPE.EQ.2< WRITE%6,214<
  214 FORMAT%1H0,30X,15HRADIAL FIN TRAP<
      IF %TYPE.EQ.3< WRITE%6,215<
  215 FORMAT%1H0,30X,14HEGG-CRATE TRAP<
      IF %TYPE.EQ.4< WRITE%6,216<
  216 FORMAT%1H0,30X,14HFREE-FORM TRAP<
      WRITE%6,217<
  217 FORMAT%1H0,29X,17HDISTANCES IN FEET/1H0,7HSECTION,6X,6HHEIGHT,
     .       9X,5HWIDTH,7X,11HTHIS LENGTH,4X,11HTYPE-LENGTH,3X,
     .       12HTOTAL LENGTH<
      GO TO 30
C
C                   ROUTINES FOR TRAP TYPES
C
C                   CROSS FLOW
   26 R1%I< # R1%I<&1
      X1 # DSQRT%DIAM*DIAM - R3%I<**2<
      W1%I< # %DIAM&X1</2.0
      L1%I< # %DIAM*DIAM*DATAN2%R3%I<,X1<&R3%I<*X1</%2.0*W1%I<<
      D1%I< # R2%I<
      GO TO 32
C
C                   RADIAL FIN
   27 W1%I< # R2%I<
      D1%I< # 1.5708*%2.0*DIAM-R2%I<</FLOAT%R1%I<<
      L1%I< # R3%I<
      GO TO 32
C
C                   EGG-CRATE
   28 W1%I< # R2%I<
      D1%I< # R2%I<
      L1%I< # R3%I<
      GO TO 32
C
C                   FREE FORM
   29 W1%I< # R2%I<
      D1%I< # R3%I<
      L1%I< # R5%I<
      GO TO 32
C
C                   ASSEMBLE TRAP INFORMATION
   30 LENGTH # 0.0
      T1 # 0.0
      J1 # 2
      I # 1
   31 GO TO (26,27,28,29),TYPE
   32 K # R4%I<&J1-1
      LENGTH # LENGTH & FLOAT%K-J1&1<*L1%I<
      LL1%I< # LENGTH-T1
      T1 # LENGTH
      WRITE%6,218< I,D1%I<,W1%I<,L1%I<,LL1%I<,LENGTH
  218 FORMAT%1H ,I6,5F15.6<
      J1 # K&1
      I # I&1
      IF %I.LE.ML< GO TO %26,27,28,29<,TYPE
C
C                   INITIALIZE PROGRAM PARAMETERS
      TIME # 0.0
      ASAT1 # ASAT
      RB # -1.987*BSAT
```

TABLE VI (Continued)

```
      DONE # .FALSE.
      TW1 # TWL%1<
      DELZ1 # LENGTH/FLOAT%M<
      HLDP # 0.0
C
C                    FORM CHANNEL DIMENSIONS AND NUMBER
      J#1
      DO 36 I#1,ML
      K # LLI%I</DELZ1 & 0.5
      IF %I.EQ.ML< K # M-J&1
      J1 # J&K-1
      IF %IBREAK.GT.0< R6%I< # J1&1
      T3 # WI%I<
      T1 # DI%I<
      T2 # T3
      IF %T3.LT.T1< T3#T1
      IF %T2.LT.T1< T1#T2
      T2 # LI%I<
      T5 # -S6%I<
      IF %T5.LT.0.0< T5#-T5*T1*T3*FLOAT%R1%I<<*%1.0&T5<
      T5 # T5/FLOAT%R1%I<<
      DO 35 K#J,J1
      D%K< # T1
      WID%K< # T3
      NUM%K< # R1%I<
      ARA%K< # T5
   35 L%K< # T2
      IF %TYPE.EQ.1< R1%I< # R1%I<-1
   36 J # J1&1
      IF %IBREAK.GT.0< R6%ML<#M&M
      IF %IBREAK.LE.0< R6%1<#M&M
C
C                    FIND AREA OF TRAP APPROXIMATION
      AREA # 0.0
      DO 37 I#1,M
   37 AREA # AREA&2.0*%WID%I<&D%I<<*DELZI*FLOAT%NUM%I<<
      WRITE%6,219< AREA
  219 FORMAT%1H0,20X,14HEFFECTIVE AREA ,F12.6,6H SQ FT<
C
C                    ESTABLISH STARTING PROFILES
      MP1 # M&1
      DO 38 J#2,MP1
      B%J< # 0.0
   38 TS%J< # TW1
      PTHETA # 0.999995*PRINT
      TS%1< # TW1
      B%1< # 0.0
C
C                    START MAIN PROGRAM LOOP, SET BOUNDRY CONDITIONS
      DO 67 I#1,NTOT
      VSCALE # FLOW%I<
      X%1< # XIN%I<
      XSTAR # X%1<
      VT # VSCALE
      ASAT # ASAT1-DLOG%PRES%I<<
      TT # TWL%I<
      T%1< # TIN%I<
      XTJ # DEXP%ASAT&BSAT/%TT&CSAT<<
      HOLDUP # 0.0
      SATD # .FALSE.
```

TABLE VI (Continued)

```
      TSG # 0.0
      DO 39 J=1,370
      TW%J< # TT
   39 VU%J< # VSCALE/FLOAT%NUM%J<<
      DO 988 J=12,18
  988 TW(J) = TW(J)+TCOR1
      DO 989 J=66,72
  989 TW(J) = TW(J)+TCOR2
C
C                    START DISTANCE LOOP
      DO 61 J#1,M
      GO TO 47
C
C                    SUBPROGRAM FOR SINGLE STEP
   40 CMMM # C0&%C2*TT&C1<*XT&C3*TT
      Z1 # C0&C1&%C2&C3<*TT
      CP1 # Z1/M1
      IF %%XT.GE.0.0<.AND.%TT.GE.TST<.AND.%XT.LT.1.0<< GO TO 42
   41 WRITE%6,300<
  300 FORMAT%1H0,34H*****CUMULATIVE ERROR BUILDUP*****<
      WRITE%6,301< I,J,XT,XT1,TT,TST,AREA,V
  301 FORMAT%1H ,5X,1HI,9X,1HJ,13X,2HXT,18X,3HXT1,17X,2HTT,18X,3HTST/
     .       1H ,2I10,4E20.9/1H ,8X,4HAREA,18X,1HV/1H ,2E20.9<
      GO TO 68
   42 XT1 # 1.0-XT
      MM # M1*XT&M2*XT1
      CM # CMMM/MM
      KB=KB0+KB1*XT + KB2*TT + KB3*TT*XT
      MU1=.00043448 + .000202759*TT
      MU2=-.000783719 + .000187594*TT-.000001378*TT**2
      MU=(MU1*XT*M1**0.5+ MU2*(1-XT)*M2**0.5)/(XT* M1**0.5 +XT1*M2**0.5)
      RHOG=MM*PRES(I)/(10.72*TT)*14.7
      PRA=CM*MU/KB
      TEPS=0.00492*TT
      OMEGA=1.06036/TEPS**0.15610 + .19300/DEXP(00.47635*TEPS) +
     11.03587/DEXP(1.52996*TEPS)+1.76474/DEXP(3.89411*TEPS)
      DIF=((0.001032*TT**1.5)*(1.0/M1 + 1.0/M2)**0.5)/(PRES(I)*OMEGA*
     113.891)
      DIF=DIF*3.8706
      SCH=MU/(RHOG*DIF)
      N23=(PRA/SCH)**0.6667
      IF %HSPEC< GO TO 43
      G # V*MM/%XT1*AREA<
      IF %G.LE.0.0< GO TO 41
      H= -1.2587022 - 0.62828111*DLOG(0.0304*G/MU)
      H=HCON*G*CM/(CM*MU/KB)**0.6667*DEXP(H)
   43 LB # RB*%TT/%TT&CSAT<<**2
      A1 # N23*DLOG%EXPTS/XT1<
      AF # Z1/CMMM
      A # AF*A1
      EA = DEXP(A)
      EA1 # EA-1.0
      IF %DABS%A<.LE.1.0E-3< EA1 # A&A*A/2.0
      IF %DABS%A<.GT.1.0E-3< EA2 # 1.0-1.0/EA
      IF %DABS%A<.LE.1.0E-3< EA2 # EA1-A*A
      IF %SATD.OR.%DEXP%ASAT&BSAT/%TT&CSAT<<.LE.XT<< GO TO 46
   44 ALPHA # 0.0
      F1 # -H*XT1*XT1*A1*P*DELZ1/%V*CMMM<
      IF %DABS%EA1<.GT.1.0E-6< GO TO 45
      F2 # -H*%TT-TST<*XT1*P*DELZ1/%V*CMMM<
      GO TO IRS,%50,57,58,59<
   45 F2 # F1*AF*%TT-TST</%XT1*EA1<
      GO TO IRS,%50,57,58,59<
```

TABLE VI (Continued)

```
   46 SATD # .TRUE.
      ZLB # LB/CMMM
      ALPHA # 1.0
      IF %DABS%EA1<.GT.1.0E-6<
     .ALPHA # 1.0 - %ZLB&1.987*TT*TT*XT1/%XT*LB<<//%ZLB&AF*%TT-TST</EA1<
      SATD # ALPHA.GT.0.0
      IF %.NOT.SATD< GO TO 44
      FI # 0.0
      IF %ALPHA.LT.1.0<
     .F1 # -H*XT1*XT1*A1*P*DELZ1/%V*CMMM*%1.0-ALPHA<<
      F2 # BSAT/%DLOG%DABS%XT&F1<<-ASAT<-CSAT-TT
      GO TO IRS,%50,57,58,59<
C
C                     END SUBPROGRAM - START LOOP
   47 XT # X%J<
      X2 # XT
      TT # T%J<
      T2 # TT
      L1 # L%J<
      TST # TS%J<
      IF  %TST.LT.TW%J<< TST # TW%J<
      IF %TST.GT.TT< TST # TT
      EXPTS # 1.0-DEXP%ASAT&BSAT/%TST&CSAT<<
      IF %EXPTS.LT.0.0< GO TO 41
      BT # B%J<
      TEMP # BT&BT
      DT # D%J<-TEMP
      BYPAS # ARA%J<
      IF %DT.GT.0.0< GO TO 49
   48 X%J&1< # X%J<
      T%J&1< # T%J<
      GO TO 60
   49 WIDT # WID%J<-TEMP
      P # 2.0*%WIDT&DT<
      AREA # WIDT*DT
      V # VU%J<*AREA/%AREA&BYPAS<
      IF %XT.LT.XTJ< XT#XTJ
      IF %TT.EQ.TST< EXPTS # 1.0-XT
      ASSIGN 50 TO IRS
      GO TO 40
C
C                     RETURN FROM SUBPROGRAM - GET STEP RESULTS
   50 SK1 # F1
      SL1 # F2
      ALPH%J< # ALPHA
      TSMAX # BSAT/%DLOG%XT<-ASAT<-CSAT
      IF %ALPHA.GE.1.0< GO TO 80
      IF %ALPHA.GT.0.0< GO TO 51
      DBMAX # KS*%TSMAX-TW%J<</%H*%TT-TSMAX<<-BT
      GAMMA # DTHETA*H*A/%RHOS*CP1<
      DB # GAMMA-GAMMA**2/%2.0*DBMAX<&GAMMA**3/%6.0*DBMAX**2<
      IF %DABS%GAMMA/DBMAX<.GT.1.0E-3<
     .         DB #DBMAX*%1.0-DEXP%-GAMMA/DBMAX<<
      B%J< # BT&DB
      GO TO 52
   51 B%J< # B%J<&DTHETA*A*H/%RHOS*CP1*%1.0-ALPHA<<
   52 BT1 # B%J<
      ZLB # LB/Z1
      TWW # TW%J<
      JTST # 1
      TST1 # TST
      TST # TSG
      IF%TSMAX.GT.TT< TSMAX#TT
```

TABLE VI (Continued)

```
      ASSIGN 85 TO JTT
      IF %%TST.LT.TWW<.OR.%TST.GT.TSMAX<<TST#TWW&0.5*%TT-TWW<
   53 W1 # TST&CSAT
      W2 # BSAT/W1
      W8 # ASAT&W2
      W3 = DEXP(W8)
      W4 # W2*W3/W1
      W1 # %1.0-W3<
      IF %W1.GT.0.0< GO TO 54
      TST # TWW&0.9*%TST-TWW<
      GO TO 55
   54 IF %DABS%W8<.LT.1.0E-3< W1 # -W8-W8*W8*0.5
      W9 # W1
      W1 # W1/XT1
      W2 # AF*N23*DLOG%W1<
      IF(W2.EQ.0.0D0)W2=1.0D-08
      W3 # AF*N23*W4/W9
      W7 = DEXP(-W2)
      W4 # 1.0-W7
      IF %DABS%W2<.LT.1.0E-3< W4 # W2-W2*W2/2.0
      W1 # %TT-TST</W4
      W6 # KS*%TST-TWW<-%W1&ZLB<*H*W2*BT1
      GO TO JTT,%85,83<
   85 W5 # KS-%W1&ZLB<*H*W3*BT1&%1.0&W1*W7*W3<*H*W2*BT1/W4
      W5#W6/W5
      W4 # TST-W5
      IF %W4.LT.TWW< W4 # TWW&0.1*%TST-TWW<
      IF%W4.GE.TSMAX<W4#TSMAX-0.1*%TSMAX-TST<
      TST # W4
      IF %DABS%W5<.LT.0.001< GO TO 56
   55 JTST # JTST&1
      IF %JTST.LT.20< GO TO 53
      JTST#1
      ASSIGN 83 TO JTT
      T4#TWW
      T5#TSMAX
   83 IF%W6.LT.0.0< GO TO 81
      T5#TST
      GO TO 82
   81 T4#TST
   82 IF%JTST.GT.19< GO TO 56
      JTST#JTST&1
      TST#0.5*%T4&T5<
      GO TO 53
   80 TST # %TWW&TT<*0.5
   56 TS%J< # TST
      TSG # TST
      TST = TST1
C
C                  CONTINUE SINGLE PASS RUNGE-KUTTA
      TT # T2 & 0.5*F2
      XT # X2 & 0.5*F1
      IF %XT.LT.XTJ< XT # XTJ
      IF %TT.LT.TST< EXPTS # 1.0-XT
      IF %TT.LT.TST< TT # TST
      ASSIGN 57 TO IRS
      GO TO 40
   57 SK2 # F1
      SL2 # F2
      TT # T2&F2*0.5
```

TABLE VI (Continued)

```
      XT # X2&F1*0.5
      IF %XT.LT.XTJ< XT#XTJ
      IF %TT.LT.TST< EXPTS # 1.0-XT
      IF %TT.LT.TST< TT#TST
      ASSIGN 58 TO IRS
      GO TO 40
   58 SK3 # F1
      SL3 # F2
      TT # T2&F2
      XT # X2&F1
      IF %XT.LT.XTJ< XT#XTJ
      IF %TT.LT.TST< EXPTS # 1.0-XT
      IF %TT.LT.TST< TT # TST
      ASSIGN 59 TO IRS
      GO TO 40
   59 XT # %SK1&F1</6.0 & %SK2&SK3</3.0 & X2
      TT # %SL1&F2</6.0 & %SL2&SL3</3.0 & T2
      X%J&1< # XT
      T%J&1< # TT
      IF %BYPAS.LE.0.0< GO TO 60
      X%J&1< #%X%J&1<*AREA&X%J<*BYPAS</%AREA&BYPAS<
      T%J&1< #%T%J&1<*AREA&T%J<*BYPAS</%AREA&BYPAS<
      X2 # DEXP%ASAT&BSAT/%T%J&1<&CSAT<<
      IF %X2.GE.X%J&1<< GO TO 60
      B%J< # B%J< & %X%J&1<-X2<*DTHETA*V**M1/%P*DELZ1**%1.0-X2<**2*RHOS<
      X%J&1< # X2
   60 HCLDUP # HOLDUP & FLOAT%NUM%J<<*RHOS*%%WID%J<-2.0*B%J<<
     .               &D%J<<*B%J<*DELZ1*2.0
   61 CONTINUE
      BIN=B(1)
C                     END OF DISTANCE LOOP - PREPARE OUTPUT
   62 HLDP # HLDP & %VT/%1.0-XSTAR<-VT/%1.0-X%M&1<<<*DTHETA*M1
      IF %I.GT.1< GO TO 75
      TT # %T%1<&TWL%1<<*0.5
      Z1 # C0&C1&%C2&C3<*TT
      LB # RB*%TT/%TT&CSAT<<**2
      XSCL # VT*%X%1</%1.0-X%1<<-X%M</%1.0-X%M<<<*%LB&Z1*%T%1<-TWL%1<<<
      TT # %T%1<&T%M<<*0.5
      Z1 # C0&%C2*TT&C1<*X%M<&C3*TT
      XSCL # XSCL&Z1*VT*%T%1<-T%M<</%1.0-X%M<<
      YSCL # 10.0**%IDINT%DLOG10%XSCL<<-1<
      IXSCL = IDINT(XSCL/YSCL+0.5)
      XSCL = IXSCL*YSCL*1.0000001
      WRITE%6,220< XSCL
  220 FORMAT%1H0,20X,22HAPPROXIMATE HEAT LOAD ,F12.2,7H BTU/HR<
      WRITE(6,319) KB,MU1,MU2,MU,RHOG,PRA,OMEGA,DIF,SCH,N23,H
  319 FORMAT(5(D12.5,3X),/,6(D12.5,3X))
   75 CONTINUE
      DO 70 J#1,M
      IF %%%D%J<-2.0*B%J<<.LE.0.0<.AND.%ARA%J<.LE.0.0<< GO TO 71
   70 CONTINUE
      GO TO 72
   71 PTHETA # 0.0
      HCLDUP # 0.0
      DONE # .TRUE.
   72 CONTINUE
      TIME # TIME & DTHETA
      IF %TIME.LT.PTHETA< GO TO 67
      PTHETA # PTHETA & PRINT
C
```

TABLE VI (Continued)

```
C                    PREPARE PAGE HEADING
      KPAGE # 55
      KPAGE1 # 0
      J2 # 1
      DO 66 J#1,M,IC
      KPAGE # KPAGE&1
      IF %KPAGE.LT.52< GO TC 64
   63 KPAGE1 # KPAGE1&1
      WRITE (6,400) (TITLE(ILIST),ILIST=1,18),KPAGE1,I
  400 FORMAT (1H1,5X,18A4,5X,4HPAGE,I2/1H0,5X,12HTIMESTEP NO.,I5)
      HCLDUP # HOLDUP*SHLDP
      HLDP # HLDP*SHLDP
      IF %KPAGE1.EQ.1< WRITE%6,401< TIME,DTHETA,HOLDUP,JHLDP,HLDP,JHLDP
  401 FORMAT%1H0,5X,5HTIME ,F12.6,4H HR.,10X,9HTIMESTEP ,F12.6,4H HR./
     .    1H0,5X,19HHOLDUP, SOLID BASIS,F12.5,1H ,A2,1H./
     .    1H0,5X,17HHCLDUP, GAS BASIS,F14.5,1H ,A2,1H.<
      HCLDUP # HOLDUP/SHLDP
      HLDP # HLDP/SHLDP
      KPAGE # 1
      IF %KPAGE1.EQ.1< KPAGE # 7
      WRITE%6,402< JDIST,JCLR,JCLR,JTO,JTO
  402 FORMAT(1H0,16X,10HDEPOSITION,39X,7HSURFACE/1H ,5X,8HDISTANCE,3X,
     121HTHICKNESS   CLEARANCE,6X,3HMOL,2X,2(2X,11HTEMPERATURE),4X,
     14HMIST/1H ,8X,A2,1H.,2(9X,A2,1H.),6X,8HFRACTION,2(4X,4HDEG ,A1,
     14X),9HFRACTION,4X,9HDIVISIONS,2X,5HRATIO/1H )
   64 D1 # DELZ1*FLOAT%J-1<*SDIST
C
C                    CHECK BREAK NOTATION
      IF %R6%J2<.GT.J< GO TO 65
      IF %KPAGE.GT.48< GO TO 63
      KPAGE # KPAGE & 3
      WRITE%6,403<
  403 FORMAT%1H ,15%6H------<<
      WRITE%6,404< J2
  404 FORMAT%1H ,25X,9HBREAK NO.,I3<
      J2 # J2 & 1
      WRITE%6,403<
C
C                    PREPARE RESULTS AND PRINT LINE
   65 B1 # B%J<*SCLR
      H1 # %D%J<-2.0*B%J<<*SCLR
      X1 # X%J<
      T1 # T%J<*STO1 & STO2
      T2 # TS%J<*STO1&STO2
      A1 # ALPH%J<
      BR=B(J)/BIN
      WRITE(6,405)D1,B1,H1,X1,T1,T2,A1,NUM(J),BR
  405 FORMAT(1H ,F13.4,2D12.5,F11.6,F11.2,F13.2,F11.4,I10,3X,F10.5)
   66 CONTINUE
      ASAT # ASAT1
      IF %DONE< GO TO 1
   67 CONTINUE
   68 ASAT # ASAT1
      GO TO 1
   69 STOP
      END
```

statement. This would be advantageous if the program is used primarily for an unchanging physical situation.

The input data set for the program consists of five data groups. If any of the last four data groups are not to be changed between data sets, that group or groups may be omitted.

Data Group 1: Control

The first data group consists of one card containing both a title, which will be printed on each page of the output resulting from the data set, and four control markers to indicate which of the other four data groups are included in the data set. If it is not indicated that a particular data group is contained in the set, that group should be left out completely; no blank cards should be inserted in its place.

Card column 3. Either blank or a decimal digit. A nonzero digit indicates that data group 2 is specified in the data set. Zero or blank indicates that the information in data group 2 is the same as for the last data set.

Card column 4. The same type of indicator as above for data group 3.

Card Column 5. The same type of indicator as above for data group 4.

Card column 6. The same type of indicator as above for data group 5.

Card columns 11 through 80. The title, which may be anything the user desires.

Data Group 2: Physical Properties

The first card in this data group contains information about molecular weights, solid properties, and the heat transfer coefficient.

Card columns 1 through 10. The molecular weight of the condensable component in "F" format (without exponent, but with decimal point). This parameter is saved.

Card columns 11 through 20. The molecular weight of the noncondensable component in "F" format. It is a saved parameter.

Card columns 21 through 30. The as-trapped density of the solid deposit in "F" format in lb/ft^3. It is saved.

Card columns 31 through 40. The as-trapped thermal conductivity of the solid deposit in "F" format in Btu/hr-ft-°F. It is saved.

Card columns 41 through 50. If these columns do not contain blanks or zero, the value, in "F" format, will be taken as a constant heat transfer coefficient to be used, in Btu/hr-sq ft-°F. If the columns are blank or zero, the correlation described in the text is used, regardless of what was specified in the previous data set. (If this data group is not read, however, the same convention of constant heat

transfer coefficient or correlation will be used as was used in the previous data set.)

Card columns 51 through 60. The scaling constant, C_n, to be used in the finned surface heat transfer correlation is described elsewhere. This constant should be in "F" format. It is saved. Some influence of fin efficiency may be obtained by using $C_n = C_n \cdot \eta$, where η is the fin efficiency. This effectively multiplies the available heat transfer area by this efficiency.

Card columns 61 through 65. These columns contain a positive integer to indicate that one or more of the gas physical property cards following are being specified. A negative integer, zero or blank, indicates that none of the gas physical property cards are specified.

The second card in this group is to input a temperature rise associated with heat inleakage due to the two mechanical supports on the trap.

Card columns 1 through 10. Input temperature rise, °F, due to first support. This should be in "F" format.

Card columns 11 through 20. Input temperature rise, °F, due to second support. This should be in "F" format.

The specification of gas physical properties is indicated by a positive integer in columns 61 through 65 of the previous card. All gas physical property specifications are in the form of coefficients for correlating equations. These

coefficients must be specified so that, when used in the described forms with mole fractions of condensable, x, and temperatures, T, in degrees Rankine, the value of the physical property will be obtained in the required units. Any of the cards, except for vapor pressure, may be omitted, in which case, the initialized values for the coefficients or those saved from the previous data set will be used. The vapor pressure curve specification must be last, but the others may be in any order. If the vapor pressure equation is not to be changed, a completely blank card may be used in its place. The general format is as follows:

Card columns 1 through 5. The name of the physical property, left justified in the field.

Card columns 6 through 20. The constant, A_0, in "F" format.

Card columns 21 through 35. The constant, A_1, in "F" format.

Card columns 36 through 50. The constant, A_2, in "F" format.

Card columns 51 through 65. The constant, A_3, in "F" format.

The physical properties, names, and equation forms are as follows:

Specific heat of the gas in Btu/lb-mole-°F. The name is CP, and the correlation is of the form

$$CP = A_0 + A_1x + A_2xT + A_3T.$$

Thermal conductivity of the gas in Btu/hr-ft-°F. The name is K, and the correlation is of the form

$$K = A_0 + A_1x + A_2T + A_3xT.$$

Vapor pressure of the condensable in atmospheres. The name is VP, and the correlation is of the form

$$VP = \exp[A_0 + A_1/(T + A_2)].$$

Data Group 3: Increment Specifications

The first card of this group specifies the time and distance increments to be used both in the calculation and for output purposes.

Card columns 1 through 10. The number of distance steps, no more than 500, to be taken to represent the length of the trap in "I" (integer) format. Reasonable accuracy is usually obtained with between 50 and 100 steps, and results are easier to interpret if the number is chosen so that each trap section is represented as an integral number of steps. Accuracy may be checked with a second run using more steps and comparing results. This variable is saved.

Card columns 11 through 20. The number of time steps, no more than 500, in "I" format. Reasonable accuracy and stability are usually obtained with between 50 and 100 steps. This may be checked with a second run using more time steps. This variable is saved.

Card columns 21 through 30. The length of a single time step in hours in "F" format. This variable is saved.

Card columns 31 through 40. An "I" format integer. If 1 is specified, output from the program will list results at each distance increment. If 2, for every other distance increment, etc. This variable is saved.

Card columns 41 through 50. A length of time in hours, "F" format. Intermediate results will be listed as output at intervals of this specified time or close to it if the match with the time step is not exact. The variable is saved and refers to simulated trapping time, not computer time.

Card columns 51 through 60. A positive integer indicates that the next card in this data group is to be specified. A negative integer, zero, or blanks indicate the next card is not supplied.

A second card, specifying the dimensional units for output, may be entered in this data group if columns 51 through 60 of the above card contain a positive integer. The format for this card is as follows:

Card columns 11 through 16. The units in which the trap holdup is to be listed in output. This may be either KG or LB, left justified in the field. It is saved and is initialized to LB.

Card columns 21 through 26. The units in which the distance along the trap is to be listed in output. This may be FT, IN, or CM, left justified in the field. It is saved and is initialized to FT.

Card columns 31 through 36. The units in which the solid deposit thickness and remaining channel clearance are to be listed in output. This may be FT, IN, or CM, left justified in the field. It is saved and is initialized to IN.

Card columns 41 through 46. The units in which the gas temperature is to be listed in output. This may be in R, K, F, or C, left justified in the field. It is saved and is initialized to F.

Data Group 4: Flow Variables

The first card in this group specifies how the flow variable cards are to be interpreted.

Card columns 1 through 10. The number of cards, no more than 500, following this one that are used to specify system flows, pressures, etc.

Card columns 11 through 16. The units in which temperature is given on the following flow variable cards. This may be R, F, K, or C, left justified in the field. This is a saved variable.

Card columns 21 through 26. The units in which pressure is given on the following cards. This may be PSIA, ATM, or MMHG. It is saved.

Card columns 31 through 36. The units in which the noncondensable flow rate is given on the following cards. This may be LBM/HR, SCFM, LB/HR, or KGM/HR. It is saved. (LBM/HR refers to pound-moles per hour and KGM/HR refers to kilogram-moles per hour.)

This data group next contains flow variable cards, the number of which is specified above. The flow variables are all saved as follows: For variables which are not specified on the first of the flow variable cards, values are supplied corresponding to those that were found on the first flow variable card of the previous data set. For variables not specified after the first flow variable card, values are supplied from the previous card and not from the previous set.

Card columns 1 through 5. The number of time steps in "I" format, for which the following conditions are in effect. On the last flow variable card, this number is adjusted to fill in the remaining time steps.

Card columns 6 through 20. The inlet gas temperature, in "F" format, units as specified above. (Temperatures of exactly zero may not be specified; use 0.0001 rather than 0.0.)

Card columns 21 through 35. The inlet mole fraction of condensable in "F" format. Note that the desublimer program assumes that noncondensables are also present. Reliability of the program decreases for inlet mole fractions near one, and the program is not recommended for use with this mole fraction much above 0.9.

Card columns 36 through 50. The flow rate of noncondensable, in "F" format, units as specified above.

Card columns 51 through 65. The trap pressure, absolute, in "F" format, units as specified above.

Card columns 66 through 80. The trap constant coolant temperature, in "F" format, units as specified above. (Temperatures of exactly zero may not be specified. Use 0.0001 rather than 0.0.)

Data Group 5: Trap Specifications

This data group describes the trap design to be tested. With the exception of dimensional unit specifications, none of these variables are saved. One general and three specific trap types are recognized, and the information

is interpreted according to the type. The first card is used for preliminary information.

Card columns 1 through 10. A number, in "I" format, indicating the type of trap, as (1) cross flow, (2) radial fin, (3) egg crate, and (4) free form.

Card columns 11 through 20. The number of following cards (less than 50) used to describe the trap.

Card columns 21 through 30. The diameter of the trap in "F" format, and units as specified. This diameter is ignored for trap types 3 and 4.

Card columns 31 through 40. An integer, in "I" format, greater than zero indicates that break notation is to be used in the output. Numbered dividing lines are printed to indicate passage between various sections of the trap. If a zero or negative integer is given, these markers are omitted.

Card columns 41 through 46. The dimensional units to be used in interpreting the diameter of the trap and the parameters, V_1 and V_2, as described below. This may be FT, IN, or CM, left justified in the field. It is a saved variable.

Card columns 51 through 56. The dimensional units to be used in interpreting the parameter, V_3, as described below. This may be FT, IN, or CM, left justified in the field. It is saved.

Card columns 61 through 66. The dimensional units used to interpret the parameter, A, as described below. This may be FT, CM, IN, or FRACTI, indicating square feet, square centimeters, square inches, or fraction. It is saved.

The remaining cards in the data group are all of the same format, the number of such cards being as specified above.

Card columns 1 through 10. The parameter, I_1, in "I" format.

Card columns 11 through 20. The parameter, V_1, in "F" format.

Card columns 21 through 30. The parameter, V_2, in "F" format.

Card columns 31 through 40. The parameter, I_2, in "I" format.

Card columns 41 through 50. The parameter, V_3, in "F" format.

Card columns 51 through 60. The parameter, A, in "F" format.

The meaning of I_1, V_1, V_2, and V_3 varies with the type of trap. I_2 is always the number of identical trap sections of the type described on the particular card, and A always refers to the amount of "free-flow" area to be put in parallel with the section as described in the procedure; in

the fractional interpretation, it is the fraction of flow area taken up by free-flow. In general, A is specified as zero or just left blank. Figure 23 may be used with the following to determine the meaning of the other parameters for each trap type.

Cross Flow Trap:

I_1 - The number of fins in a baffled section, not counting the baffles.

V_1 - The distance between parallel fins.

V_2 - The distance across a fin.

V_3 - May be left blank.

Radial Fin Trap:

I_1 - The number of radial fins in a section.

V_1 - The length of a fin in the radial direction.

V_2 - The length of a fin in the axial direction.

V_3 - May be left blank.

Egg Crate Trap:

I_1 - The number of equivalent square channels in one egg crate section.

V_1 - The length of a side of an equivalent square channel.

V_2 - The length of the egg crate section in the direction of flow.

V_3 - May be left blank.

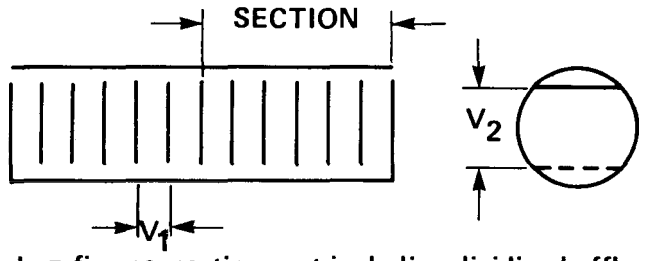

I_1 = fins per section, not including dividing baffles

TRAP TYPE #1 – CROSS FLOW

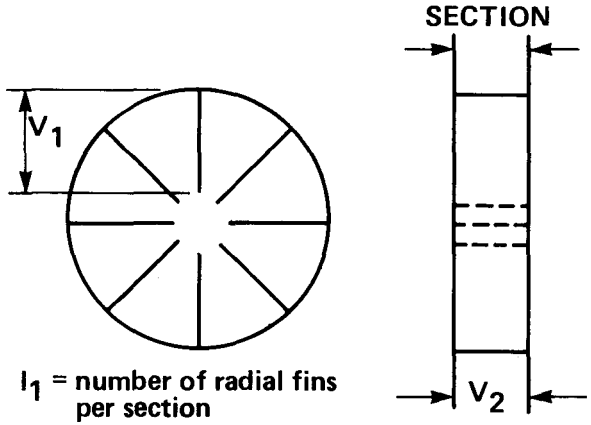

I_1 = number of radial fins per section

TRAP TYPE #2 – RADIAL FIN

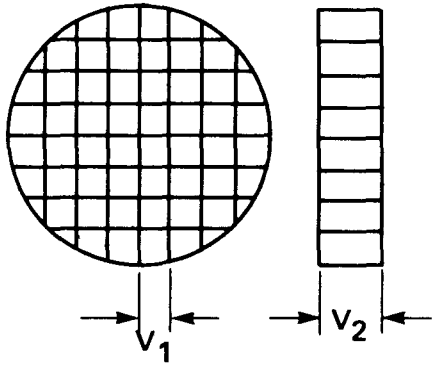

I_1 = number of equivalent square channels

TRAP TYPE #3 – EGG CRATE

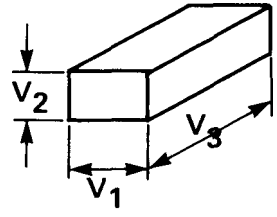

I_1 = number of equivalent rectangular channels

TRAP TYPE #4 – FREE FORM

Figure 23

DESCRIPTION OF TRAP PARAMETERS

Free Form Trap:

I_1 - The number of equivalent rectangular channels in one flow section.

V_1 - The length of one side of the rectangular channel.

V_2 - The length of the other side of the rectangular channel.

V_3 - The length of a channel in the direction of flow.

APPENDIX C

ANALYSIS OF THERMAL STRESS

Presented in this section is a calculation of the expansion and/or contraction of the cold trap due to thermal changes:

Temperature will change from ambient, 80°F, to -320°F or a net change of 400°F.

Thermal expansion coefficient of 304L stainless steel equals 9.6×10^{-6} in./in.-°F[29]. Length of cold trap equals 132 inches.

Total contraction equals (9.6×10^{-6} in./in.-°F) × (132 in.) × (400°F) = 0.51 inch.

The metal bellows installed can flex up to 5/8 inch.

APPENDIX D

SHIELDING THICKNESS REQUIRED FOR BACKGROUND ATTENUATION

This appendix presents the calculation made to determine the thickness of the lead shield necessary to block out the background radiation.

$$\psi(t) = B(\kappa t)\ \psi(0)e^{-\kappa t}\ [30],$$

where $\psi(0)$ and $\psi(t)$ are the radiation flux before and after passage through the shield of thickness t, with a linear attenuation coefficient κ. $B(\kappa t)$ is the buildup factor.

For a shield made of lead blocking out an isotope having a γ energy of 0.5 MeV, $\kappa/\rho = 0.145\ cm^2/g$ (mass attenuation factor),

ρ = density of lead = 0.41 lb/ft^3

$$\kappa = (0.145\ \frac{cm^2}{g})(\frac{1\ in.^2}{6.45\ cm^2})(\frac{454\ g}{lb})(\frac{0.41\ lb}{in.^3}),$$

$$\kappa = 4.18\ in.^{-1}.$$

Using a 2-inch-thick shield, $\kappa t = 8.36$.

The plane collimated buildup factor, $B(\kappa t)$, for $\kappa t = 8.36$ by interpolation is 1.97 [30].

$$\therefore \frac{\psi(t)}{\psi(0)} = B(\kappa t)e^{-\kappa t} = \text{fraction unattenuated.}$$

$$\text{Percent Unattenuated} = (1.97)(e^{-8.36})(100\%) = 0.046\%.$$

Therefore, (1 - 0.046) or 99.54% of the background activity will be attenuated prior to reaching the sodium iodide detector.

Blank Page

DISTRIBUTION

INTERNAL

ORGDP

R. S. Eby (20)
J. R. Merriman
D. S. Napolitan
J. H. Pashley
J. L. Petty, Jr.
R. C. Riepe
M. J. Stephenson (10)
J. R. White
W. J. Wilcox, Jr.
R. A. Winkel
ORGDP Records (RC) (2)

ORNL

J. T. Bell
M. R. Bennett
R. E. Blanco
J. O. Blomeke
W. D. Bond
B. E. Bottenfield
E. C. Bradley
N. C. Bradley
R. E. Brooksbank
K. B. Brown
W. D. Burch
D. O. Campbell
J. M. Chandler
D. A. Costanzo
R. M. Counce
D. J. Crouse
B. F. Crump
J. H. DeVan
J. P. Drago
D. E. Dunning
J. H. Evans
M. J. Feldman
D. E. Ferguson
S. D. Floyd
T. M. Gilliam
J. H. Goode
G. M. Goodwin
N. R. Grant
J. C. Griess
W. S. Groenier
W. R. Hamel
D. C. Hampson

ORNL (Continued)

B. A. Hannaford
W. O. Harms
J. N. Herndon
J. R. Hightower
D. W. Holladay
W. D. Holland
A. R. Irvine
R. T. Jubin
A. D. Kelmers
L. J. King
J. Q. Kirkman
J. A. Klein
R. E. Leuze
B. E. Lewis
B. Lieberman
J. C. Mailen
J. D. McGaugh
L. E. McNeese
S. A. Meachan
R. P. Milford
J. G. Morgan
E. L. Nicholson
E. D. North
A. R. Olsen
F. L. Peishel
J. J. Perona
Herman Postma
R. H. Rainey
A. D. Ryon
W. F. Schaffer, Jr.
C. D. Scott
B. B. Spencer
J. G. Stradley
J. B. Talbot
V. J. Tennery
L. M. Toth
D. B. Trauger
W. E. Unger
J. E. VanCleve
V. C. A. Vaughen
B. L. Vondra
C. D. Watson
B. S. Weil
T. D. Welch
M. E. Whatley
R. G. Wymer

DISTRIBUTION (Continued)

ORNL (Continued)

O. O. Yarbro
E. L. Youngblood
J. Zasler
Central Research Library
ORNL-Y-12 Technical Library
  Document Reference Section
Laboratory Records (5)
Laboratory Records, ORNL
ORNL Patent Office
Nuclear Safety Information Center

Y-12

R. Blumberg
J. D. Jenkins

EXTERNAL

J. L. Crandall, Director, Environmental Sciences Section, E. I. duPont de Nemours & Company, Savannah River Laboratory, Aiken, SC 29801

S. T. Goforth, Savannah River Laboratory, Building 679-G, Savannah River Plant, Aiken, SC 29801

H. J. Groh, Jr., Director, Separations Chemistry & Engineering Section, E. I. duPont de Nemours & Company, Savannah River Laboratory, Aiken, SC 29801

M. L. Hyder, Separations Chemistry & Engineering Section, E. I. duPont de Nemours & Company, Aiken, SC 29801

J. R. Hilley, Director, Nuclear Engineering & Materials Section, E. I. duPont de Nemours & Company, Savannah River Laboratory, Aiken, SC 29801

T. B. Hindman, Jr., Director, Fuel Cycle Project Office, U. S. Energy Research and Development Administration, Savannah River Operations Office, P. Box A, Aiken, SC 29801

C. H. Ice, Director, Savannah River Laboratory, E. I. duPont de Nemours & Company, Aiken, SC 29801

A. S. Jennings, Research Manager, Separations Chemistry & Engineering Laboratory, Aiken, SC 29801

DISTRIBUTION (Continued)

EXTERNAL (Continued)

N. Stetson, Manager, U. S. Energy Research and Development Administration, Savannah River Operations Office, P. O. Box A, Aiken, SC 29801

V. Van Brundt, College of Engineering, University of South Carolina, Columbia, SC 29208

F. S. Waters, Savannah River Plant, E. I. duPont de Nemours & Company, Aiken, SC 29801

Director, Reactor Division, DOE-ORO

Director, Division of Nuclear Fuel Cycle and Production, DOE, Washington, D.C. 20545

Director, Division of Reactor Research and Development, DOE, Washington, D. C. 20545

Research and Technical Support Division, DOE-ORO

Given distribution as shown in TID-4500 under UC-79c, Fuel Recycle Category (Applied)

☆ U.S. GOVERNMENT PRINTING OFFICE: 1977-748-189/245